Tuesday, March 30, 2021
Medway Planning and Economic Development Board
155 Village Street
Medway, MA 02053

Members	Andy Rodenhiser	Bob Tucker	Tom Gay	Matt Hayes	Rich Di Iulio	Jessica Chabot
Attendance	X	X	X	X	X	X

Pursuant to Governor Baker's March 12, 2020 Order Suspending Certain Provisions of the Open Meeting Law, and the Governor's Orders imposing strict limitations on the number of people that may gather inside in one place, no in-person attendance will be permitted at this meeting. Board members will attend the meeting via ZOOM. Meeting access for the public is provided via ZOOM for the required opportunity for public participation in a public hearing. Information for participating via ZOOM is included at the end of this Agenda. Members of the public may also watch the meeting on Medway Cable Access: channel 11 on Comcast Cable, or channel 35 on Verizon Cable; or on Medway Cable's Facebook page @medwaycable.

ALSO PRESENT VIA ZOOM:

- Barbara Saint Andre, Director of Community and Economic Development

There were no Citizen Comments.

PUBLIC HEARING CONTINUATION - ZONING BYLAW AMENDMENTS:

The Board is in receipt of the following documents: (**See Attached)**

- Public Hearing Continuation Notice
- Emails dated 3-23-21 and 3-24-21 from Barbara Saint Andre communicating support for various zoning bylaw amendments from the EDC and the MRA.
- Email dated 3-24-21 from resident Marty Dietrich re: Article 25, rezoning from AR-II to energy Resource.
- Technical information on battery energy storage systems (3 reports provided by Tom Gay)

ARTICLE 25:

The Board was informed that Article 25 has been revised to include a definition for a battery energy storage system and to specify that battery energy storage systems would be allowed only by special permit in the ER zoning district. The Board was informed that since the last meeting

there has been a citizen petition submitted opposing Article 25 and imposing a moratorium for one year.
Member Gay did some extensive research on batter energy storage systems. Through the research, he found that there is a lot of information about how to construct, install, operate and protect these battery storage systems. There is research which outlines how the insurance companies are handling the liability of these facilities. Member Gay has provided the documentation for the Board to review. There has also been information provided which shows that these systems can be installed safely, and properly. Member Gay recommends that the Board take a step back and respect those that signed the petition and place the moratorium in place for this and do the work and research on this and propose it at a later date.

On a motion made by Tom Gay, seconded by Rich Di Iulio, the Board voted by Roll Call to pull Article 25 from the warrant.

Roll Call Vote:

Bob Tucker	aye
Tom Gay	aye
Rich Di Iulio	aye
Andy Rodenhiser	aye
Matt Hayes	aye

Public Comments:

- Resident Mike Fahey – Thanked the Board for pulling this article.
- Select Board Member Dennis Crowley – He wants to listen to the citizens who presented this petition and supports removing this article from the warrant. He would like the Board to have a consultant assist in addressing this.
- Resident Tracy Stewart – Thanked for Board for pulling this article. She also wanted to acknowledge the fact that it is the community who has to figure out what is best for the Town of Medway.

ARTICLE 21 Central Business District:

This Article is to revise Table 1, Schedule of Uses in Section 5.4. This will also delete Section 5.4.1
Special Permit in the Central Business District. There will also be the amending of Section 6.1. Schedule of Dimensional and Density Regulations and Table 2. There is the adding of a new Section 10: Central Business District Development Standards.

Attorney Kenney and Mr. Paul Rao was also present during the zoom call.

There was discussion that there was a clarification of language regarding Section 10.3.C1B. This article was reviewed by Town Counsel and Consultant Brovitz.

Paul Yorkis explained that the MRA voted unanimously to support Article 21 as written.

On a motion made by Rich Di Iulio, seconded by Bob Tucker, the Board voted by Roll Call to recommend Article 21 as written.

Roll Call Vote:

Bob Tucker	**aye**
Tom Gay	**aye**
Rich Di Iulio	**aye**
Andy Rodenhiser	**aye**
Matt Hayes	**aye**

ARTICLE 22 Site Plan Review:

This article is to modify which activities are subject to administrative site plan review. This will be to also add a new Section 3.5.3.A Façade Improvements Review.

On a motion made by Matt Hayes, seconded by Rich Di Iulio, the Board voted by Roll Call to recommend Article 22 as written.

Roll Call Vote:

Bob Tucker	**aye**
Tom Gay	**aye**
Rich Di Iulio	**aye**
Andy Rodenhiser	**aye**
Matt Hayes	**aye**

ARTICLE 23 Solar Electric Installations:

This article is for the adding of a new section with regulations for various typed of solar electric installations.

Public Comments:

Resident Paul Yorkis communicated that he would like to see Section #4 regarding wetlands taken out. He communicated that the Town already has a bylaw and what is proposed in the

article is an extension of the Town's (wetlands) bylaw and this is stricter than bylaw. There has been no significant evidence to support the wetland sections A and B. He also asked if there should be language added which would include "outside of the jurisdiction of the Wetland Protection Act". He also asked if Section B is covered under site plan review.

Barbara Saint Andre communicated that Mr. Yorkis is correct that the language of this proposal is more stringent than the current bylaw. It was recommended that if the Board is planning on making any changes, Subsection B regarding Stormwater should be left in since the Town has a huge issue with stormwater and this section will assist in meeting State requirements. The language included came from model language from the State and language was also taken from other communities. Barbara recommended leaving the language as written in Section 4.

There was a recommendation to keep Section B and discuss eliminating Section A with the Conservation Commission.

On a motion made by Bob Tucker, seconded by Tom Gay, the Board voted by Roll Call to recommend leaving this article as written.

Roll Call Vote:

Bob Tucker	**nay**
Tom Gay	**aye**
Rich Di Iulio	**aye**
Andy Rodenhiser	**aye**
Matt Hayes	**aye**

ARTICLE 24 Flood Plain District:

This article is to amend section 5.6.1 in its entirety in order to comply with the recent changes in State regulatory requirements.

On a motion made by Mike Hayes, seconded by Tom Gay, the Board voted by Roll Call to recommend Article 26 as written.

Roll Call Vote:

Bob Tucker	**aye**
Tom Gay	**aye**
Rich Di Iulio	**aye**
Andy Rodenhiser	**aye**
Matt Hayes	**aye**

ARTICLE 26 Non-Conforming Uses and Structures:

This article is to amend Section 5.5.C.1 to specify that lawfully existing nonconforming structures that are accessory to and on the same lot as nonconforming single-family and two-family structures are afforded the same protections. There article also makes a clarifying amendment to Section 5.5.C.3.b. It also specifies that the special permit criteria in Section 3.4 do not apply to special permit applications under Section 5.5.E Nonconforming Structures Other than One-Family and Two-Family Dwellings.

On a motion made by Mike Hayes, seconded by Rich Di Iulio, the Board voted by Roll Call to recommend Article 26 as written.

Roll Call Vote:

Bob Tucker	**aye**
Tom Gay	**aye**
Rich Di Iulio	**aye**
Andy Rodenhiser	**nay**
Matt Hayes	**aye**

ARTICLE 27 Cottage Cluster Development:

This article is to add a new section to allow for cottage cluster developments by special permit from the Planning and Economic Development Board.

On a motion made by Tom Gay, seconded by Rich Di Iulio, the Board voted by Roll Call to recommend Article 27 as written.

Roll Call Vote:

Bob Tucker	**aye**
Tom Gay	**aye**
Rich Di Iulio	**aye**
Andy Rodenhiser	**aye**
Matt Hayes	**aye**

ARTICLE 28 Digital Advertising Signage for Electric Vehicle Charging Stations:

This article is adding a definition in Section 7.2.6. It also amends of Table 1 Schedule of Uses in Section 5.4 and amends Section 7.2.6. B to allow electric vehicle charging stations with digital advertising signage in certain zoning districts by special permit. It will also amend Section 3.5.3.A.2 to add electric vehicle charging stations with digital advertising to Minor Site Plan Review.

On a motion made by Tom Gay, seconded by Rich Di Iulio, the Board voted by Roll Call to recommend Article 28 as written.

Roll Call Vote:

Bob Tucker	**aye**
Tom Gay	**aye**
Rich Di Iulio	**nay**
Andy Rodenhiser	**aye**
Matt Hayes	**aye**

ARTICLE 29 Accessory Family Dwelling unit:

The article adds a new item 8 in Section 8.2.C with standards for accessory family dwelling units that are located in separate structures.

On a motion made by Matt Hayes, seconded by Rich Di Iulio, the Board voted by Roll Call to recommend Article 29 as written.

Roll Call Vote:

Bob Tucker	**aye**
Tom Gay	**aye**
Rich Di Iulio	**aye**
Andy Rodenhiser	**aye**
Matt Hayes	**aye**

ARTICLE 30 Housekeeping:

The Board was informed that this "housekeeping" article will amend the definitions of "accessory family dwelling unit" and "dwelling" and add a definition of "mixed use building" in Section 2 Definitions. It will also replace the term "parking lot" with the term "parking area" throughout the bylaw due to the previously approved definition of "parking lot". There is also the amending of Section 3.4.H.1 in Special Permits to clarify that the Zoning Board of Appeals serves as the special permit granting authority for all special permit applications under 5.5 Non-Conforming Uses and Structures. There is also the clarification of Section 6.2.F.1 in dimensional requirements.

On a motion made by Rich Di Iulio, seconded by Matt Hayes, the Board voted by Roll Call to recommend Article 30 as written.

Roll Call Vote:

Bob Tucker	**aye**
Tom Gay	**aye**
Rich Di Iulio	**aye**
Andy Rodenhiser	**aye**
Matt Hayes	**aye**

On a motion made by Rich Di Iulio, seconded by Matt Hayes, the Board voted by Roll Call to close the public hearing.

Roll Call Vote:

Bob Tucker	**aye**
Tom Gay	**aye**
Rich Di Iulio	**aye**
Andy Rodenhiser	**aye**
Matt Hayes	**aye**

APPOINTMENTS TO MASTER PLAN COMMITTEE:

The Board is in receipt of a memo from Susy Affleck-Childs recommending two more appointments to the Master Plan Committee – Linda Reynolds as a representative of the Lions Club and Faina Shapiro as a representative of the Medway Business Council. The term of office is through March31, 2023.

On a motion made by Rich Di Iulio, seconded by Bob Tucker, the Board voted by Roll Call to appoint Linda Reynolds and Faina Shapiro to the Medway Master Plan Committee.

Roll Call Vote:

Bob Tucker	**aye**
Tom Gay	**aye**
Rich Di Iulio	**aye**
Andy Rodenhiser	**aye**
Matt Hayes	**aye**

ADJOURN:

On a motion made by Rich Di Iulio, seconded by Bob Tucker, the Board voted by Roll Call to adjourn the meeting.

Roll Call Vote:

Bob Tucker	**aye**
Tom Gay	**aye**
Rich Di Iulio	**aye**
Andy Rodenhiser	**aye**
Matt Hayes	**aye**

The meeting was adjourned at 8:08 p.m.

Respectfully Submitted,
Amy Sutherland
Recording Secretary

Reviewed and edited by,
Susan E. Affleck-Childs
Planning and Economic Development Coordinator

March 30, 2021
Medway Planning & Economic Development Board Meeting

Public Hearing Continuation
Zoning Bylaw Amendments

- Public Hearing Continuation Notice
- Emails dated 3-23-21 and 3-24-21 from Barbara Saint Andre communicating support for various zoning bylaw amendments from the Economic Development Committee and the Redevelopment Authority
- Email dated 3-24-21 from resident Marty Dietrich re: Article 25, rezoning from AR-II to Energy Resource
- Technical information on battery energy storage systems (3 reports provided by Tom Gay)

We have updated the PEDB web page with all of the most recent versions of the proposed amendments. Please view them at: https://www.townofmedway.org/planning-economic-development-board/pages/proposed-zoning-bylaw-amendments-5-10-2021-town-meeting

NOTE - The text for Article 25 has been revised to include a definition for a battery energy storage system and to specify that battery energy storage systems would be allowed only by special permit in the ER zoning district.

Medway Town Hall
155 Village Street
Medway, MA 02053
Phone (508) 533-3291
Fax (508) 321-4987
Email: planningboard@townofmedway.org
www.townofmedway.org

TOWN OF MEDWAY
COMMONWEALTH OF MASSACHUSETTS

PLANNING AND ECONOMIC DEVELOPMENT BOARD

March 24, 2021

NOTICE OF PUBLIC HEARING CONTINUATION
Proposed Amendments to Medway Zoning Bylaw
Tuesday, March 30, 2021 @ 7:00 p.m.

At the March 23, 2021 public hearing to receive public comments on proposed amendments to the Medway Zoning Bylaw and Map, the Planning and Economic Development Board (PEDB) voted to continue the public hearing to Tuesday, March 30, 2021 at 7:00 p.m. The hearing will be held remotely via the ZOOM online platform at: https://us02web.zoom.us/j/84214288229?pwd=QTRlem9yeHY5TCtRZzdnZG16UmdlZz09

The proposed amendments have been prepared for inclusion on the warrant for consideration at the May 10, 2021 Town Meeting. Drafts of the proposed amendments are on file at the offices of the Town Clerk and the Community and Economic Development Department at Medway Town Hall, 155 Village Street, Medway, MA and may be reviewed during regular business hours. The proposed amendments are also posted online at the Planning and Economic Development Board's web page at: https://www.townofmedway.org/planning-economic-development-board/pages/proposed-zoning-bylaw-amendments-5-10-2021-town-meeting

For further information or questions, please contact the Medway Planning office at 508-533-3291.

Interested persons or parties are invited to review the draft proposed amendments, and participate in the public hearing via ZOOM. Written comments are encouraged and may be sent to the Medway Planning and Economic Development Board, 155 Village Street, Medway, MA 02053 or emailed to: planningboard@townofmedway.org. All written comments will be entered into the record during the hearing.

Andy Rodenhiser
Planning & Economic Development Board Chairman

Susan Affleck-Childs

From: Barbara Saint Andre
Sent: Wednesday, March 24, 2021 2:23 PM
To: Andy Rodenhiser; Susan Affleck-Childs
Subject: MRA

Last night, the Medway Redevelopment Authority voted unanimously, 5-0, to support Article 21 of the Town Meeting warrant, the proposed zoning by-law amendments for the Central Business District.

Barbara J. Saint Andre
Director, Community and Economic Development
Town of Medway
155 Village Street
Medway, MA 02053
(508) 321-4918

Susan Affleck-Childs

From: Barbara Saint Andre
Sent: Tuesday, March 23, 2021 4:59 PM
To: Susan Affleck-Childs; Andy Rodenhiser
Cc: Michael Boynton
Subject: ATM Articles 21 and 25

The Economic Development Committee voted at its meeting on March 18th to support Article 21 (Central Business Zoning) and Article 25 (rezoning of land to ER). With respect to Article 25, the Committee members also acknowledged that the neighbors' concerns should be addressed.

The votes were 6-0-0 for both articles (one EDC member was absent from the meeting)

Barbara J. Saint Andre
Director, Community and Economic Development
Town of Medway
155 Village Street
Medway, MA 02053
(508) 321-4918

Susan Affleck-Childs

From: Martin Dietrich <martinwdietrich@gmail.com>
Sent: Wednesday, March 24, 2021 9:01 AM
To: Planning Board; Susan Affleck-Childs; Andy Rodenhiser; Barbara Saint Andre
Cc: John Foresto; Glenn Trindade; dennispcrowley@gmail.com; Michael Fahey; lawrence.ellsworth@comcast.net; tracystewart903@gmail.com
Subject: Thank you and some additional information

Good Morning,

Andy, thank you so much for moderating a robust conversation on warrant article 25 (changing zoning from ARII to ER). I am including all who spoke last night (and whose email I have) to provide some additional information.

One concern that came up was being forced by the EFSB to move forward with this project. I have included an article below that I believe could set a precedent that the EFSB does not have jurisdiction over this type of facility as it is not energy generating (this was brought to the EFSB by the battery storage company). I think we should be cautiously optimistic that this will not be forced upon the town if we do not want it (I believe it is still open).

Additionally, the approval in Carver was mentioned a few times, and if you do some research, it is pretty clear that the Planning Board in Carver wishes they had spent some more time on this issue before approving. I think the approach to require special permitting is a good idea as it will force Able Grid to make sure all of our concerns are addressed and provide deliberate transparency to the project. I also believe that if we leave the zoning as it is, Able Grid can still do its due diligence with the town and after the citizens hear the plans, we can vote to change the zoning then.

Finally, while it has been suggested that we will get a 7-figure tax revenue lift to the town, have we also considered additional funds required to ensure safety, liability, etc. We should make sure that we are not bringing something into the town that will cause us additional liability down the road (for example, turf fields – while they are nice, the economic and environmental impact of maintenance will likely require the town to put in more money than the fields are generating; plus there is nowhere to safely put the old rubber beads/turf carpets when they need to be replaced).

I appreciate your listening to everybody. I have felt that the concept of BESS in Medway at this specific location was being rushed through by the town with very little transparency. I am glad you are digging deeper on how to make sure we approach this with caution and deliberateness.

Thanks again and I hope you have a great week!

https://www.energycleantechcounsel.com/2019/02/04/is-an-energy-storage-system-a-generating-facility/

Thanks,

Marty (he/his)
https://www.linkedin.com/in/martin-dietrich

ELECTRICAL ENERGY STORAGE SYSTEMS

Table of Contents

Page

List of Figures

1.0 SCOPE

This data sheet describes loss prevention recommendations for the design, operation, protection, inspection, maintenance, and testing of electrical energy storage systems (ESS) that use lithium-ion batteries. Energy storage systems can be located in outside enclosures, dedicated buildings or in cutoff rooms within buildings. Energy storage systems can include some or all of the following components: batteries, battery chargers, battery management systems, thermal management and associated enclosures, and auxiliary systems.

This data sheet does not cover the following types of electrical energy storage:

A. Mechanical: pumped hydro storage (PHS); compressed air energy storage (CAES); flywheel energy storage (FES)

B. Electrochemical: flow batteries; sodium sulfide

C. Chemical energy storage: hydrogen; synthetic natural gas (SNG)

D. Electrical storage systems: double-layer capacitors (DLS); superconducting magnetic energy storage

E. Thermal storage systems

This data sheet does not cover non-lithium ion batteries, their associated battery chargers and associated systems related to backup power in UPS systems or DC power for circuit breaker protection, etc. Information related to non-lithium ion batteries used in backup power systems can be found in Data Sheet 5-23, *Emergency and Standby Power Systems*; Data Sheet 5-19, *Switchgear and Circuit Breakers*; and Data Sheet 5-32, *Data Centers*.

1.1 Changes

July 2020. Interim revision. The following changes were made:

A. The scope was updated for clarity.

B. Figure 2.3.1 was corrected to be consistent with 2.3.2.1.

1.2 Hazards

1.2.1 Thermal Runaway

Typically, thermal runaway originates in a cell with an internal short due to internal cell defects, mechanical failures (e.g., vibration or expansion contraction cycles) that can lead to mechanical damage, external heating, overvoltage charging, or failure of the battery management system (or cell controller). Thermal runaway leads to high temperatures and gas buildup, with the potential for an explosive rupture of the battery cell that can lead to fire and/or explosion. To date there is no publicly available test data that confirms the effectiveness of any active fire protection for energy storage systems. Automatic sprinkler protection is recommended to limit fire spread to the surrounding structure, equipment, and building contents.

During a thermal runaway event, the cell produces flammable gas that builds up within the cell enclosure or the room where ESS are installed. Most manufacturers of outdoor enclosures include a specially designed vent that opens and releases the gas. In some cases, this vent can become obstructed or may not open correctly. Hot vented gas, when directed toward adjacent cells, may propagate thermal runaway to those cells. Without prompt action, such as disconnection from the electrical circuit, thermal runaway can cascade from cell to cell, causing much more damage.

1.2.2 Electrical Fire

As with other electrical systems, electrical fires are a concern and can cause property damage and, in severe cases, could initiate a thermal runaway event due to localized overheating.

Unlike lithium batteries, lithium-ion batteries are not water-reactive.

2.0 LOSS PREVENTION RECOMMENDATIONS

2.1 FM Approved Equipment

2.1.1 Use FM Approved equipment, materials, and services whenever they are applicable and available. For a list of products and services that are FM Approved, see the *Approval Guide*, an online resource of FM Approvals.

2.2 Energy Storage System (ESS) Selection

2.2.1 Verify with the manufacturer or integrator that the ESS design, including cell type, battery management system (BMS), etc., is appropriate for the application. Cells/ESS should be selected based on speed of charge/discharge required for the specific end-use.

2.2.2 Establish a management of change procedure to ensure that batteries or BMS components are compatible with modified system requirements or that replacements are appropriate to the existing system requirements.

2.2.3 Do not use refurbished or previously used ESS components, including cells or modules.

2.3 Construction and Location

2.3.1 Location

2.3.1.1 Locate energy storage systems in accordance with one of the following, listed in order of preference:

A. In an enclosure outside and away from critical buildings or equipment in accordance with 2.3.2 (Figure 2.3.1, location 1)

B. In a dedicated building containing only ESS and associated support equipment in accordance with 2.3.3 (Figure 2.3.1, location 2)

C. In a dedicated exterior cutoff room that is accessible for manual firefighting operations and is constructed in accordance with 2.3.4 (Figure 2.3.1, location 3)

D. In a dedicated interior corner cutoff room that is accessible for manual firefighting and is constructed in accordance with 2.3.4 (Figure 2.3.1, location 4)

E. In a dedicated interior cutoff room that is accessible for manual firefighting and is constructed in accordance with 2.3.4 (Figure 2.3.1, location 5)

2.3.2 ESS Enclosures

2.3.2.1 Provide a minimum space separation between ESS enclosures and adjacent buildings or critical site utilities or equipment in accordance with Data Sheet 1-20, *Protection Against Exterior Fire Exposure*, using hazard category 3 for the exposing building occupancy.

2.3.2.2 Provide a minimum space separation of 20 ft (6 m) between adjacent ESS enclosures with noncombustible walls. If the walls are combustible, provide separation between adjacent ESS enclosures in accordance with Data Sheet 1-20.

2.3.2.2.1 If the space separation between ESS enclosures is less than 20 ft (6 m), provide a thermal barrier, rated a minimum 1 hour, on the inside or outside of the enclosure, in accordance with Data Sheet 1-21. See Figure 2.3.2.2.1 for an example of an adequate thermal barrier between adjacent enclosures.

2.3.2.3 Where enclosure vents or other penetrations are provided, ensure they are arranged and directed away from surrounding equipment and buildings.

In a fire, these enclosures may have vents or penetrations that could allow hot gas and products of combustion to escape the enclosure, causing an exposure to adjacent equipment or buildings. Penetrations could include electrical cabling, doors, HVAC units, etc.

2.3.3 Dedicated ESS Building or Enclosure Larger Than 500 ft^2 (46.5 m^2)

Treat any pre-fabricated container or enclosure that is larger than 500 ft^2 (46.5 m^2) as a building.

2.3.3.1 Construct a dedicated ESS building of noncombustible materials.

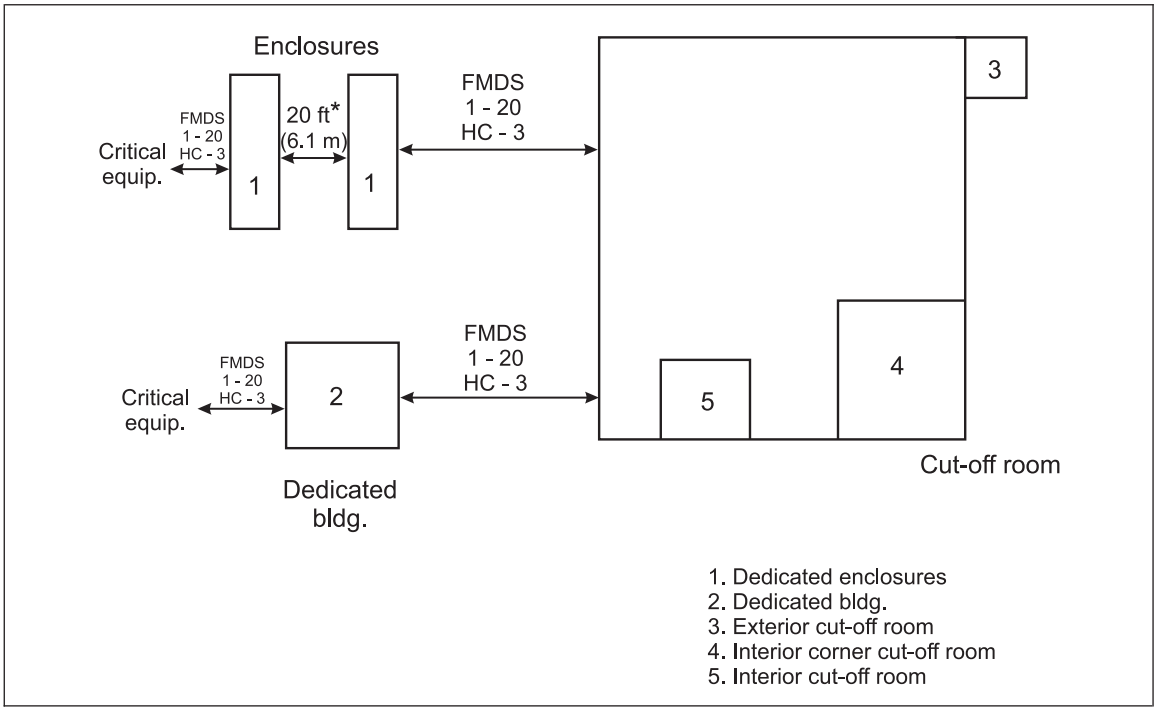

*Fig. 2.3.1. ESS locations by preference (*see 2.3.2.2.1)*

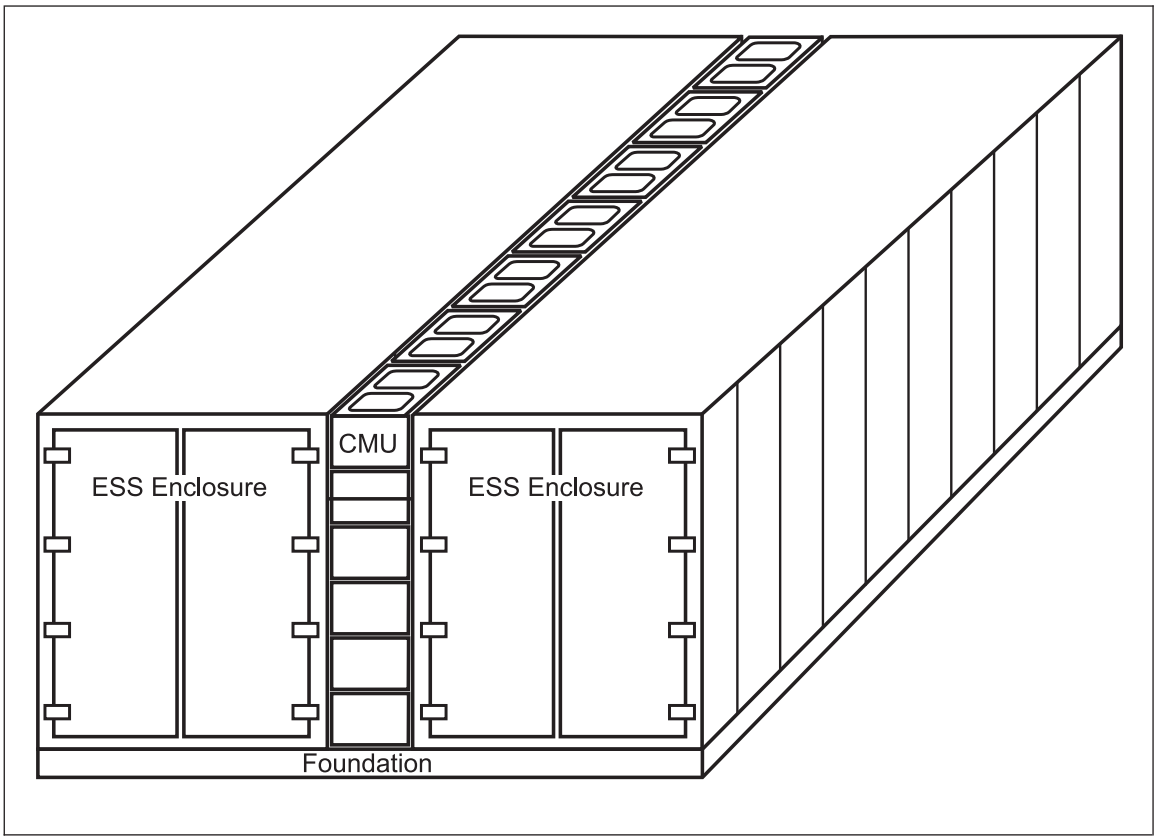

Fig. 2.3.2.2.1. Exterior ESS enclosures with fire barrier

2.3.3.2 Provide a minimum space separation between dedicated ESS buildings and other facility buildings or critical site utilities or equipment in accordance with Data Sheet 1-20 using hazard category 3 for the exposing building occupancy.

2.3.3.3 Provide damage-limiting construction (DLC).

2.3.3.3.1 Design DLC in accordance with Data Sheet 1-44, *Damage-Limiting Construction*, using propane as the representative gas.

2.3.3.4 Install ESS with minimum separation distance in accordance with 2.3.5.

2.3.3.5 Provide mechanical ventilation at a rate of at least 1 cfm/ft^2 (0.3 m^3/min/m^2) of floor area (see 2.5.5).

2.3.3.6 Design HVAC systems to maintain temperatures within operating limits in the event of a single component failure.

2.3.3.6.1 Arrange the HVAC system to alarm to a constantly-attended location or specific operations personnel if any part of the system fails.

2.3.4 ESS Cutoff Rooms

2.3.4.1 For multiple racks installed in a single row or back-to-back, install solid, noncombustible fire barriers between adjacent racks.

2.3.4.2 Provide a minimum 1-hour fire-rated room, floors, walls, and ceiling in accordance with Data Sheet 1-21.

A. Provide FM Approved fire doors with the same room rating.

B. Provide FM Approved fire barriers for all floor, ceiling, and wall penetrations.

2.3.4.3 Install ESS with minimum separation in accordance with 2.3.5.

2.3.4.4 Provide mechanical ventilation in an ESS cutoff room at a rate of at least 1 cfm/ft^2 (0.3 m^3/min/m^2) of floor area. (See 2.5.5)

2.3.4.5 Provide damage-limiting construction.

2.3.4.5.1 Design DLC in accordance with Data Sheet 1-44, *Damage-Limiting Construction*, using propane as the representative gas.

2.3.5 Separation Distances

2.3.5.1 Provide 6 ft (1.8 m) minimum separation from noncombustible materials, noncombustible construction elements, and between the aisle faces of adjacent racks.

2.3.5.2 Provide 9 ft (2.7 m) minimum separation from combustibles and combustible construction elements.

2.4 Protection

2.4.1 Provide automatic sprinkler protection designed to a 0.3 gpm/ft^2 (12 mm/min) over 2500 ft^2 (230 m^2) or the room area, whichever is larger, with an additional allowance of 250 gal/min (946 L/min) for hose streams.

2.4.1.1 Where the sprinkler demand area requires a water supply greater than what is available, provide the following:

A. Install noncombustible floor-to-ceiling partitions with penetrations protected by FM Approved fire stops between adjacent racks perpendicular to the rack door or opening to prevent fire spread. Ensure the partitions extend at least 12 in. (0.3 m) from the face of the rack. See Figure 2.4.1.1. Determine the horizontal distance between thermal barriers based on how many racks can be protected by the available water supply.

B. Install a solid metal partition on the back (non-aisle) of each rack to prevent heat transfer to adjacent racks in the next row. Where the rack design incorporates a solid metal back (no ventilation openings), additional partitions are not needed. (See Figure 2.4.1.1.)

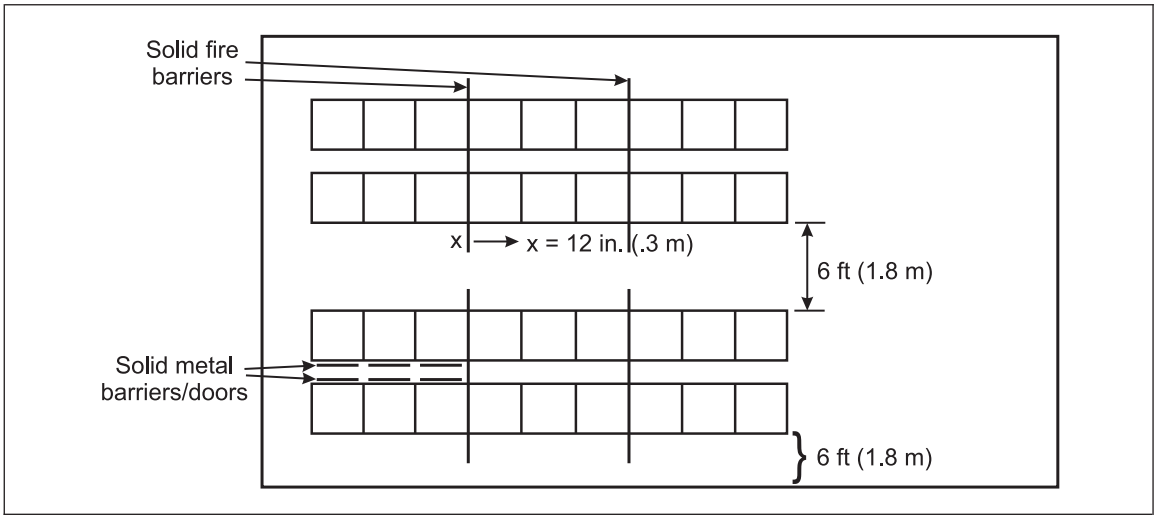

Fig. 2.4.1.1. Thermal barriers to reduce fire risk area

Testing of a 125 kWh ESS utilizing NMC lithium ion batteries demonstrated that the fire growth ultimately exceeded the 2500 ft^2 design area. Therefore, the sprinkler design should be designed for the larger demand area. Video of the sprinkler test can be found on the FM Global YouTube channel: https://youtu.be/HLLXu-2IUpQ

2.4.2 Ensure the water supply is capable of providing sprinkler water and hose stream requirements for the duration of the fire event (see Section 3.2). The expected duration will depend on the number of racks in a single fire area. The fire area is comprised of a row or rows of racks where minimum separation is not provided in accordance with 2.3.5. The duration should be estimated as 45 minutes times the number of adjacent ESS racks.

2.4.3 Provide a smoke detection system within the enclosure, cutoff room, or ESS area designed and installed in accordance with Data Sheet 5-48, *Automatic Fire Detection*.

2.5 Equipment and Processes

2.5.1 Electrical System Protection

2.5.1.1 Perform a system short circuit and protection coordination study to ensure the adequacy of rating and relay settings for existing circuit breakers when the electrical energy storage system adds power to the existing electrical system at a facility. For additional information on short circuit and protection coordination, see Data Sheet 5-20, *Electrical Testing*.

2.5.2 Equipment Protection

2.5.2.1 Provide a disconnect device for maintenance needs or abnormal events for each rack.

2.5.2.2 Provide a method of manual, remote, and local disconnect for the ESS. A remote disconnect should be in an accessible area that is monitored 24/7. A local disconnect should be provided adjacent to the ESS space.

2.5.2.3 Provide temperature monitoring with high alarm for ESS room, building, or enclosure. Have alarms routed to a continuously attended location or specific operations personnel.

2.5.2.4 ESS Rack

2.5.2.4.1 Provide DC ground fault protection for grounded battery systems. For ungrounded battery systems, provide DC ground fault monitoring with alarming function. Have the alarm routed to a constantly-attended location or specific operations personnel.

2.5.2.4.2 Provide overcurrent protection against overload and short-circuit faults.

2.5.2.4.3 Provide overvoltage and under-voltage protection against overcharging and over-discharging.

2.5.3 Battery Management System Safety Functions

2.5.3.1 Provide battery management systems with the following safety functions:

A. High cell temperature trip (cell level): This function isolates the module or battery rack when detecting cell temperatures that exceed limits. A common design is to have modules hard-wired in series within a rack. Therefore, the smallest unit that can be isolated is generally the rack. Where a design accommodates it, isolating a module is acceptable.

B. Thermal runaway trip (cell level): This function trips the entire system when a cell is detected to have entered a thermal runaway condition. In scenarios involving a thermal runaway, this function is the first to activate when thermal runaway conditions are detected.

C. Rack switch fail-to-trip (rack level): This function identifies any failure from the pack switch to trip once a trip command is initiated. The rack switch is also known as the “pack switch.” It is a switch that disconnects a single rack in response to an abnormal condition. The rack switch is shown separately from the “master” level in Figure 2.5.3.1 for clarity. It is generally incorporated into the BMS.

D. Inverter/charger fail-to-trip (supervisor level): This function initiates a trip command to an upstream breaker to isolate the ESS if the inverter/charger fails to respond to a trip command. The “supervisor” control system controls the entire system, including the combination of racks, the environmental support systems, and the charging/discharging status. The supervisor level should isolate the ESS if the inverter/charger fails to trip on an appropriate signal, or if communication is disrupted between the inverter/charger and the supervisor control.

See Figure 2.5.3.1 for explanation of management levels.

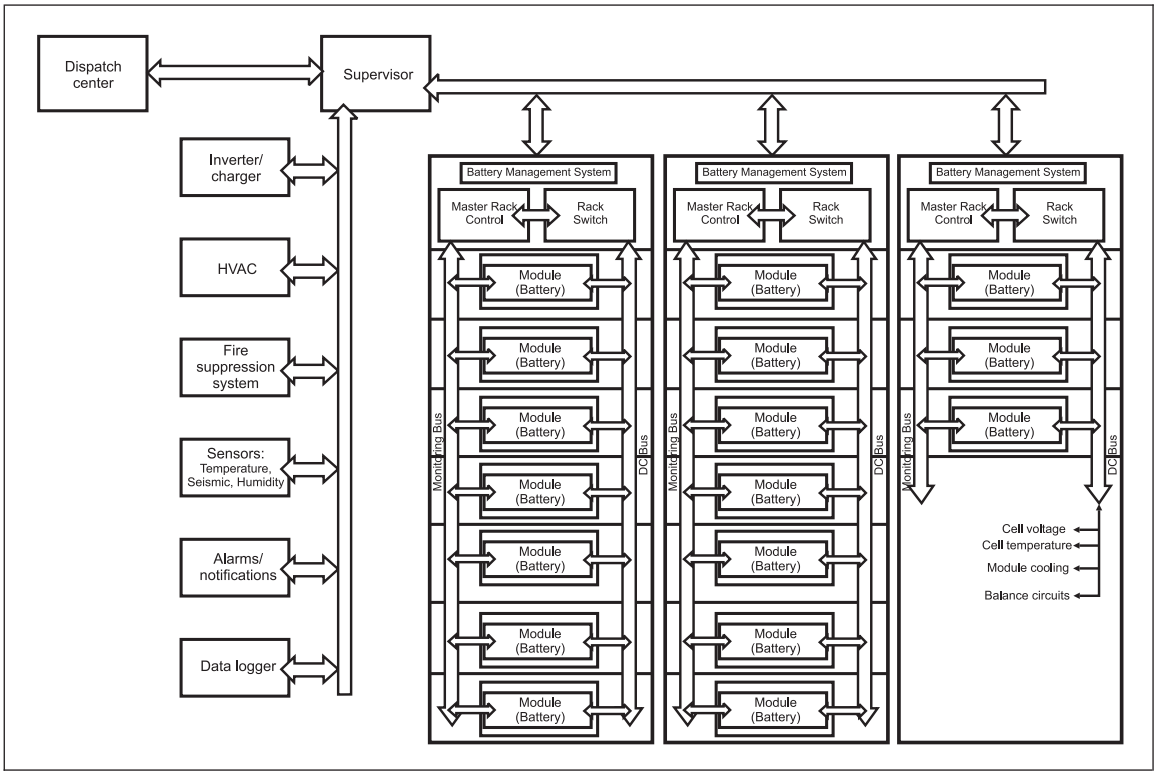

Fig. 2.5.3.1. ESS management levels

2.5.3.2 Online Condition Monitoring

2.5.3.2.1 Provide online condition monitoring systems that will monitor battery room temperature and the following parameters, at a minimum, at the battery module and/or cell level:

- Charging and discharging voltage and current
- Temperature
- Internal ohmic (resistance)
- Capacity
- State of charge (SOC)
- State of health (SOH)
- Alarm or fault log

2.5.3.2.2 Provide online condition monitoring systems with the following features:

A. The ability to transmit data to a constantly-attended location or specific operations personnel

B. The ability to generate alarms when unusual conditions are detected

C. The ability to analyze monitored parameters and generate a summary of the condition of the battery

D. Security to prevent unauthorized changes of critical parameter limits, such as voltage, temperature, and current, which are essential to maintain reliable lithium-ion battery operation.

E. Self-diagnostic capability

2.5.4 Power Conversion Equipment

2.5.4.1 Provide overcurrent protection against overload and short-circuit faults on the AC side.

2.5.4.2 Provide surge arrestors on the AC side for voltage transient “voltage spike” protection. For additional information on voltage transient protection, see Data Sheet 5-11.

2.5.4.3 Provide transformer electrical protection in accordance with Data Sheet 5-4, *Transformers* or 5-20, *Electrical Testing*, as applicable.

2.5.5 Mechanical Ventilation

2.5.5.1 Locate the ventilation system to take suction at or near the ceiling.

2.5.5.2 Install a combustible gas detector that will alarm at the presence of flammable gas (yes/no), shut down the ESS, and cause the switchover to full exhaust of the ventilation system.

2.5.5.2.1 Combustible gas detection in the ventilation system is not needed where combustible gas detection arranged for rack shutdown is provided in each ESS rack as part of the battery management system.

2.5.5.3 Remove exhaust air through a system of blowers, fans, and ductwork terminating outdoors away from air inlets, doorways, and other openings.

2.5.5.4 Construct ductwork of noncombustible materials.

2.5.5.5 Provide make-up air inlets in exterior walls, in a remote location from exhaust outlets to prevent entrainment of exhaust gases.

2.5.5.6 Provide ventilation systems arranged to recirculate air into the room with an FM Approved combustible gas detector arranged to stop recirculation and return to full exhaust when flammable gas is detected in the ductwork.

2.5.5.6.1 Arrange the ventilation system controls to alarm to a constantly-attended location or specific operations personnel.

2.6 Operation and Maintenance

2.6.1 Operation

2.6.1.1 Install, operate, and maintain batteries and battery management systems in accordance with manufacturer's recommendations.

2.6.1.2 As part of commissioning, verify proper operation of all monitoring and protective devices.

A. Inspect the battery system thoroughly for indication of overheating, abnormal vibration, abnormal noise, or malfunction. This should occur daily for a minimum of one week of normal operation.

B. Perform infrared scanning and check battery operating and monitoring parameters to determine if any damage was sustained in shipping and installation.

2.6.2 Equipment Maintenance

2.6.2.1 General

2.6.2.1.1 Perform electrical system inspection and testing of ESS systems in accordance with Data Sheet 5-20.

2.6.2.2 Battery Management System

2.6.2.2.1 Develop and implement a maintenance program for the BMS that includes at least the following:

A. Periodic system self-test to ensure all critical systems are available and operational.

B. Periodic pack switch maintenance. This may involve cycling the switch to ensure mechanical integrity and tightness of cable connections by torqueing to specifications.

C. HVAC maintenance. This may include change of air filters at periodic intervals. These intervals may vary depending on the location of the site. Dusty locations may require more frequent air filter replacement. Other HVAC maintenance items may include coolant check, compressor/heater core check and duct/cable check.

D. Periodic check of spare battery modules to ensure they are maintained in charged state.

E. Periodic tracking of state-of-health (SOH) values, which is the percent of remaining capacity (based on design capacity) in the battery packs.

2.6.2.3 Establish a battery replacement program for aged batteries. Review the battery replacement program regularly and include, at a minimum, the following components:

A. The OEM design life expectancy of the ESS batteries. This will be a number in years that the system is expected to perform adequately. After this point, the batteries should be replaced. This establishes the replacement timeline.

B. Regular monitoring of the ESS SOH, which is the percent of remaining capacity based on design capacity. This information should be available through the BMS, which continuously tracks SOH. Unexpected component malfunctions or failures and operating outside design parameters can age batteries faster than when operating within design limits. The BMS will be able to monitor these unexpected issues and adjust the SOH of the system.

C. Regular review of the replacement program, ensuring there is a method of adjusting the replacement timeline. The plan should allow for adjusting the replacement timeline if feedback from the BMS shows the SOH indicates accelerated aging. The following factors justify earlier replacement:

1. Significant changes or trends in the condition monitoring data that indicate development problems with the battery system

2. Advice from the OEM of design problems that require replacement

3. Operating experience and failure history that indicates the battery should be replaced

4. Exposure to severe operating conditions

D. A method of managing changes. This should consider major changes that affect the life expectancy and replacement timeline of the ESS. Changes could include replacement of the BMS, modifying the thermal management system, and changes in application or operational modes (e.g., modifying the BMS to operate based on an arbitrage mode vs. electric supply capacity).

2.7 Training

2.7.1 Have operation personnel trained by the supplier/manufacturer of the ESS equipment.

2.7.2 Provide other training in accordance with Data Sheet 10-8, *Operators*.

2.8 Human Factors

2.8.1 Housekeeping

2.8.1.1 Do not store combustible material in ESS enclosures, buildings, or cutoff rooms.

2.8.2 Emergency Response and Pre-Incident Planning

2.8.2.1 Develop an emergency response plan to address the potential fire hazards associated with energy storage systems. Refer to Data Sheet 10-2, *Emergency Response*, for general guidelines on establishing and maintaining an emergency response plan.

2.8.2.2 Develop a pre-incident plan with the fire service in accordance with Data Sheet 10-1, *Pre-Incident Planning*. Arrange and prepare the plan with documented procedures to expedite safe entry and emergency response to fires in the battery storage area, including the following:

- Manual disconnection
- Access routes
- Manual fire protection methods
- Manual smoke ventilation (if provided)
- SDS for battery cells

2.8.2.3 Develop a post-incident recovery plan that addresses the potential for reignition of ESS, as well as removal and disposal of damaged equipment.

A fire watch should be present until all potentially damaged ESS equipment containing Li-ion batteries is removed from the area following a fire event. The water supply should be replenished as quickly as feasible.

Fires involving Li-ion batteries are known to reignite. Li-ion batteries involved in or exposed to fires should be adequately cooled to prevent reignition.

The OEM or integrator should provide guidance on decommissioning, removal of damaged equipment, and proper disposal in accordance with local regulations.

2.9 Utilities

2.9.1 In extreme environments, provide an emergency power supply to the HVAC systems. An extreme environment is one that could allow cell-level temperatures to rise or fall outside the normal operating temperature range of 32°F (0°C) to 212°F (100°C) despite BMS control.

2.9.2 Ensure ESS enclosures with common HVAC components, such as a common condensing unit (cooling tower), are designed to shut down the ESS in the event of a component failure.

3.0 SUPPORT FOR RECOMMENDATIONS

3.1 Construction and Location

3.1.1 Space Separation Between Exterior Enclosures

The enclosure, being constructed of steel or other metal, will conduct heat and radiate it away from the enclosure. An uncontrolled fire within one of the enclosures is expected to cause a substantial amount of radiation and conduction through the metal sides of the enclosure and will be able to ignite a fire in adjacent enclosures if not separated by the recommended distance. There are alternative options in lieu of space separation that will minimize the potential for fire spread until the fire service arrives.

3.2 Fire Protection and Minimum Separation Distances for Indoor Installations

Thermal runaway events create a large amount of heat. The heat, coupled with plastic construction components, can lead to a very large fire. Although fire protection may not be practical in exterior installations, it is the best method of cooling a fire involving ESS.

Limited research has been performed on lithium ion-based ESS systems to assess fire propagation characteristics and protection schemes. The report Development of Sprinkler Protection Guidance for Lithium Ion Based Energy Storage Systems, published in June 2019 on the FM Global Website, is the basis for recommendations on fire protection and separation distances from both noncombustible and combustible materials. However, it must be recognized that the research was limited in scope, and the effect of rack design, materials-of-construction, battery specifications and chemistry, and other design features are not well understood. Because of these issues, it does not appear possible to extrapolate the results obtained with the tested lithium iron phosphate (LFP) and Li-nickel manganese cobalt oxide (NMC) systems to other ESS. The recommendations in DS 5-33 represent the current state of knowledge. The data sheet will be updated as additional information is available.

In addition, the National Fire Protection Association (NFPA) recently published the first fire protection standard for ESS, NFPA 855, *Standard for the Installation of Stationary Energy Storage Systems*.

Link to *Development of Sprinkler Protection Guidance for Lithium Ion Based Energy Storage Systems*:

https://www.fmglobal.com/research-and-resources/research-and-testing/research-technical reports

3.3 Gaseous Protection Systems

Generally, gaseous protection systems are not recommended for ESS applications for the following reasons:

A. Efficacy relative to the hazard. As of 2019, there is no evidence that gaseous protection is effective in extinguishing or controlling a fire involving energy storage systems. Gaseous protection systems may inert or interrupt the chemical reaction of the fire, but only for the duration of the hold time. The hold time is generally ten minutes, not long enough to fully extinguish an ESS fire or to prevent thermal runaway from propagating to adjacent modules or racks.

B. Cooling. FM Global research has shown that cooling the surroundings is a critical factor to protecting the structure or surrounding occupancy because there is currently no way to extinguish an ESS fire with sprinklers. Gaseous protection systems do not provide cooling of the ESS or the surrounding occupancy.

C. Limited Discharge. FM Global research has shown that ESS fires can reignite hours after the initial event is believed to be extinguished. As gaseous protection systems can only be discharged once, the subsequent reignition would occur in an unprotected occupancy.

3.4 Electrical

3.4.1 Battery and ESS Aging

Li-ion battery aging depends on several factors, such as number of charge/discharge cycles, depth of discharge, charging/discharging rate, state of charge, calendar time, and operating temperature. The capacity of a li-ion battery will degrade approximately 50% to 80% depending on design and the sizing margin when battery age is close to end-of-life. In addition, the internal resistance value of an aged battery substantially increases from 2 to 3 times initial value at a fixed ampere-hour rate at the cell level, resulting in increased likelihood of thermal runaway.

Industry practice is that the BMS measures the state of health by design to track condition of the batteries due to aging. The state of health is based on actual capacity relative to the initial rated capacity of battery as minimum. It may also take into consideration the internal resistance, total energy throughput, number of cycles, etc. The BMS provides indicator (alarm) for replacement based on the state of health information. In absence of established replacement criteria, consult the OEM for guidance.

4.0 REFERENCES

4.1 FM Global

Data Sheet 1-20, *Protection Against Exterior Fire Exposure*
Data Sheet 1-21, *Fire Resistance of Building Assemblies*
Data Sheet 4-5, *Portable Extinguishers*
Data Sheet 5-4, *Transformers*
Data Sheet 5-19, *Switchgear and Circuit Breakers*
Data Sheet 5-20, *Electrical Testing*
Data Sheet 5-23, *Emergency and Standby Power Systems*
Data Sheet 5-32, *Data Centers and Related Facilities*
Data Sheet 5-48, *Automatic Fire Detection*
Data Sheet 9-0, *Asset Integrity*
Data Sheet 10-1, *Pre-Incident Planning*
Data Sheet 10-2, *Emergency Response*
Data Sheet 10-8, *Operators*

4.2 Other

Institute of Electrical and Electronics Engineers (IEEE). *Guide for the Ventilation and Thermal Management of Batteries for Stationary Applications.* IEEE 1635-2012.

APPENDIX A GLOSSARY OF TERMS

Arbitrage: See electrical energy time-shift.

Black start: Storage systems provide an active reserve of power and energy within the grid and can be used to energize transmission and distribution lines and provide station power to bring power plants online after a catastrophic failure of the grid. The ESS can be used to energize transmission and distribution lines, provide startup power for one or more diesel generators and/or (larger) power plants, and provide a reference frequency.

Battery management system (BMS): The supervisory system that ensures basic functionality of the battery pack while maintaining safe operating conditions and acting appropriately in contingencies. One of the main functions of the BMS is to keep the cells operating within their designed operating parameters to prevent thermal runaway.

Capacity: Specific energy in ampere-hours (Ah). Ah is the discharge current a battery can deliver over time and is a measure of the charge stored in the battery. This can also be measured in kilowatt-hours (kWh) or megawatt-hours (MWh).

Cell: The smallest electrochemical component that can store energy.

Congestion relief: Congestion occurs when available, least-cost energy cannot be delivered to all or some loads because transmission/distribution facilities are not adequate to deliver that energy. Electricity storage can be used to avoid congestion-related costs and charges, especially if the costs become onerous due to significant transmission system congestion. The EES system can be charged when there is no congestion and discharged when congestion occurs.

Demand charge management: Demand charges are based on the highest 15-minute average usage recorded on the meter within a given month. If a facility tends to use a lot of power over short periods, demand charges will comprise a larger part of the utility bill. Demand charge management (similar to electric energy time-shift) involves the implementation of energy storage to reduce the peak demand and reduce costs.

Energy storage system (ESS): Any system through which electrical energy can be stored and reused when needed.

ESS enclosure: An ESS enclosure is a packaged ESS structure of less than 500 ft^2, typically an ISO shipping container or pre-fabricated structure of similar size.

Electrical energy time-shift: Electric energy time-shift involves purchasing inexpensive electric energy, available during periods when prices or system marginal costs are low, to charge the storage system so the

energy can be used or sold at a later time when the price or costs are high. If difference in energy prices is the main driver and energy is stored to compensate for (for example) diurnal energy consumption patterns, this application is often referred to as “arbitrage.”

Electric supply capacity: Depending on the circumstances in a given electric supply system, energy storage could be used to defer and/or reduce the need to buy new central station generation capacity and/or purchasing capacity in the wholesale electricity marketplace. In this application, the EES system supplies part of the peak capacity when the demand is high, thus relieving the generator by limiting the required capacity peak.

LFP: Lithium iron phosphate battery chemistry.

Load following/ramping for renewables: Load following is characterized by power output that typically changes as frequently as every few minutes. The output differs in response to the changing balance between electric supply and load within a specific region or area. The ESS is used to supply (discharge) or absorb (charge) power to compensate for load variations or variations in renewable generation.

Module: A combination of series and parallel connected cells. Modules may also be provided with a smaller version of the BMS to control the cells within and communicate with the system BMS.

NMC: Lithium nickel manganese cobalt oxide battery chemistry.

Power quality: Power quality is a measure of the level of voltage and/or frequency disturbances. Demand fluctuations on a short timescale (few minutes to fraction of a second) can cause power quality issues on the power grid. ESS systems can respond to these short timescale fluctuations to alleviate the effect of the disturbances and provide improved power quality.

Power reliability: The application of energy storage in various operational regimes to improve the overall reliability of power systems. For example, ESS can balance small sections of the grid to achieve a good match between generation and load. Storage devices can provide frequency regulation to maintain the balance between the network’s load and the power generated. The end result is a more reliable power supply for industrial facilities.

Rack: A rack (sometimes called a “pack” or a “string”) consists of multiple modules typically connected in series to develop a high DC voltage that is fed to the inverter/charger. The rack also consists of switching components (circuit breaker, isolator, and contactor) to isolate the rack during a contingency.

Regulation frequency response: Frequency response operation requires the ESS to react to system needs in even shorter time periods (seconds to less than a minute) when there is a sudden loss of a generation unit or a transmission line or sudden energization of a large load. The primary reasons for including regulation in the power system are to maintain the grid frequency and to comply with the North American Electric Reliability Council’s Real Power Balancing Control Performance (BAL001) and Disturbance Control Performance (BAL002) standards.

Retail energy time shift: See electric energy time-shift.

Supplemental reserves: Operation of an electric grid requires reserve capacity that can be called upon when some portion of the normal electric supply resources becomes unavailable unexpectedly. Stored energy reserves are usually charged energy backups that have to be available for discharge when required to ensure grid stability. Other reserves typically fall into spinning and non-spinning categories:

> **Spinning reserve:** The amount of additional capacity that is currently in operation. For example, if a location with a maximum steam generator output of 500 MW is currently operating at 250 MW, there is 250 MW of spinning reserve.
>
> **Non-spinning reserve:** The amount of additional capacity that is not currently in operation and would need to be started in order to provide power output. This is the sum of potential reserve power that is capable of being started and put on the grid. This should not be confused with capacity that is offline and being maintained or otherwise not able to start up and add power to the grid.

State of charge (SOC): The real-time amount of energy stored in the system, compared to the rated capacity. A function of voltage. The SOC could be expressed as a percentage value. This would mean that a fully charged battery would have 100% SOC, and a fully discharged battery would have 0% SOC.

State of health (SOH): A quantitative value (expressed in percentage) depicting the current condition of the battery compared to its condition when new. The SOH is evaluated by the battery management system

(BMS) by monitoring operational variables such as voltage, current, temperature, and internal resistance. Since a battery's performance degrades with time, the SOH value starts at 100% for a new battery and reduces with time. This indication is critical in evaluating and monitoring.

Upgrade deferral: Upgrade deferral involves delaying, and in some cases avoiding entirely, utility investments in system upgrades by using relatively small amounts of storage. Consider a transmission system with peak electric loading that is approaching the system's load-carrying capacity (design rating). In some cases, installing a small amount of energy storage downstream from the nearly overloaded transmission node could defer the need for the upgrade for a few years.

Voltage support: Stable operation of the power grid requires operators to maintain voltage within specified limits. This requires the control of reactive power (VAR) in the grid. Note that no (or low) real power is required from an EES system operating within a voltage/VAr support application, so cycles per year are not appropriate for this application, and storage system size is indicated in reactive power (MVAr) rather than MW.

APPENDIX B DOCUMENT REVISION HISTORY

The purpose of this appendix is to capture the changes that were made to this document each time it was published. Please note that section numbers refer specifically to those in the version published on the date shown (i.e., the section numbers are not always the same from version to version).

July 2020. Interim revision. The following changes were made:

A. The scope was updated for clarity.

B. Figure 2.3.1 was corrected to be consistent with 2.3.2.1.

April 2020. Interim revision. The following substantive changes have been made to the document:

A. Added recommendations for selection of ESS components.

B. Updated location recommendations to reflect current technology.

C. Added recommendations for construction of dedicated buildings.

D. Added recommendations for mechanical ventilation.

E. Added recommendations for separation distance between racks.

F. Added recommendation for water supply duration.

G. Added recommendations for battery management system safety functions.

H. Added recommendations for online condition monitoring.

I. Added recommendation for post-incident fire watch.

J. Expanded support material related to FM Global Research on sprinkler protection and separation distance.

January 2017. This is the first publication of this document.

APPENDIX C REFERENCE INFORMATION

C.1 Introduction

Energy storage has been around for many years in five predominant forms: electrochemical, mechanical, thermal, electrical, and chemical. This data sheet addresses only lithium-ion battery ESS, which is an electrochemical type.

Lithium-ion battery energy storage systems are relatively new, but are quickly becoming the most common type of electromechanical energy storage. These systems offer a method of storing electrical energy that can be used to supplement conventional power generation (e.g., coal and fossil fuels), reduce peak energy demand swings, support high-voltage energy grids, and also support green energy production, such as wind and solar, that are dependent on natural sources and therefore cannot produce power at all times.

Lithium-ion battery (LIB) energy storage systems (ESS) come in a variety of types, sizes, applications, and locations. The use of the technology is continually expanding, becoming more available for a range of energy storage applications, from small residential support systems to large electrical grid systems. LIB ESS consist of many basic components. Cells or batteries are the building blocks of an LIB ESS. Several cells connected together form a module, and several linked modules form a rack or string. Several racks or strings form an energy storage system.

The design of ESS is dependent on the user's voltage, amperage, and power requirements; the system's application; the useful life of the system; and the costs of the system. ESS are designed, manufactured, and assembled by either ESS manufacturers or ESS Integrators. ESS manufacturers manufacture and assemble all components from the cells all the way through to the enclosure as a full package. Integrators will typically purchase batteries and other components and manufacture certain parts and design and assemble the system for their customers. In either case, original equipment manufacturers (OEMs) and integrators use a battery management system (BMS) to control the operation and safety of the ESS, which is critical to prevent abnormal operation. The design and operation of the BMS is proprietary to the OEM or integrator and, at this point, there is limited opportunity to affect its design. The design can include hardware and software components. It is critical to understand all operation and safety functions of the ESS as described within this document.

ESS are typically installed within a building, or outside a building within an enclosure. Exterior installations vary and depend primarily on the size of the system. Small systems may be installed in a NEMA-rated enclosure, while larger systems will be installed within a shipping-type metal container. For very large systems, a stand-alone building may be used to house the ESS.

When installed within a building, ESS are typically located in electrical cabinets within a general space or in a designated room. All the support systems for the ESS are provided by the building support systems or are specifically designed for the room, depending on the needs of the ESS. When installed outside a building, they are provided with thermal management systems (i.e., HVAC) designed for the enclosure. Other auxiliaries are found in both installations: electrical support (e.g., inverters/converters, AC electrical systems including disconnects, voltage/amperage monitors, load monitors, etc.) and fire protection.

C.2 ESS Components

For the purposes of understanding how these systems are built, the following is a description of the components from the cell level to the system level.

C.2.1 Cells

Lithium-ion cells are constructed similar to other battery cells, consisting of an anode, a cathode, electrolyte, insulators, terminals, pressure vent, and a container sometimes called a "case" or "can."

Each cell consists of a cathode and an anode separated by a thin dielectric layer called the "separator." A li-ion cell uses the movement of lithium-ions between positive and negative electrodes for energy storage. Lithium never exists in metallic form, so inherent instability of metallic lithium is mitigated. A typical li-ion cell generates from 3.6 to 4.2 V. Also, the secondary electrolyte interphase layer (SEI), which forms on the anode surfaces, is an ionically conductive and electronically insulating layer. This layer facilitates the working of li-ion technology. Failure of SEI leads to heat generation and thermal runaway.

Li-ion cells include a wide variety of chemistries pertaining to the chemical composition of the anode and cathode that affect the performance and cost. For cathode composition, Li-nickel manganese cobalt oxide (NMC) and Li-nickel cobalt aluminum oxide (NCA) chemistries have known to be very stable at the same time providing high energy density. For anode composition, most popular is partially graphitized carbon. Lithium titanate (LTO) is typically used in high safety applications because it benefits from higher stability. However, LTO cells have approximately 30% lower energy density values compared to other compositions.

The term "cell" is often interchangeable with "battery" when talking about small-format applications. For example, a cylindrical cell with a top positive terminal and bottom negative terminal is used in many applications and called a battery. Cells actually come in a variety of forms. The three most common forms are cylindrical cell, prismatic cell, and pouch cell.

C.2.1.1 Cylindrical Cells

This is the most widely used packaging style for batteries and provides good mechanical stability. Most cylindrical cells feature a pressure-relief mechanism, and the simplest design uses a membrane seal that ruptures under high pressure. Some Li-ion cells connect the pressure relief valve to an electrical fuse that permanently opens the cell if an unsafe pressure builds up. See Figure C.2.1.1.

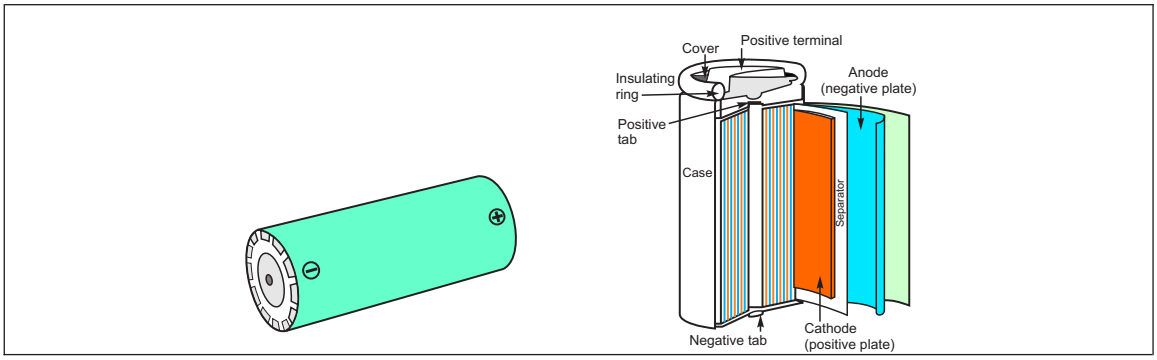

Fig. C.2.1.1. Cylindrical cell form

C.2.1.2 Prismatic Cells

Prismatic cells provide a firm enclosure to the electrochemical cell within. These cells are found in computer tablets and laptops ranging from 800 mAh to 4,000 mAh. No universal format exists and each manufacturer designs its own. Prismatic cells are also available in large formats. Packaged in welded aluminum housings, the cells deliver capacities of from 20 to 50 Ah and are primarily used for ESS applications. See Figure C.2.1.2.

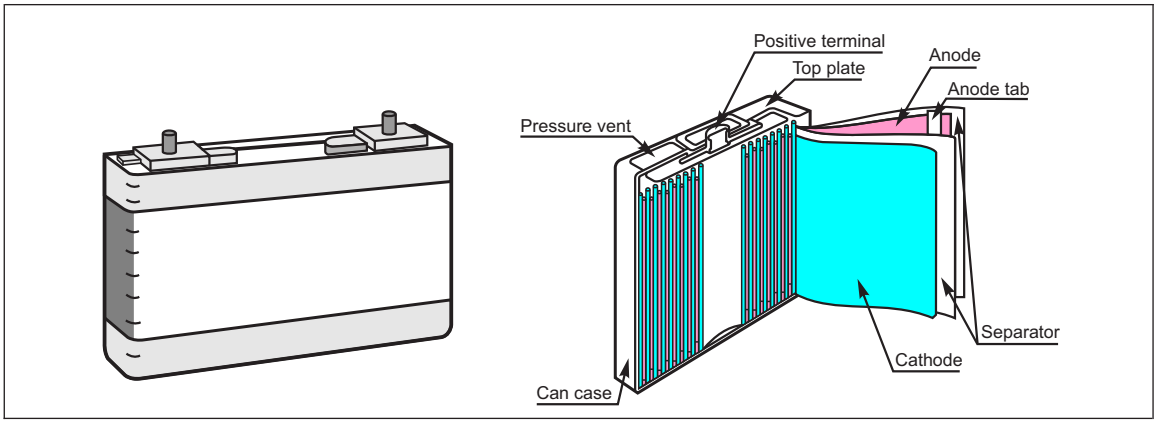

Fig. C.2.1.2. Prismatic cell form

C.2.1.3 Pouch Cells

A pouch cell uses laminated architecture in a bag. The pouch cell makes most efficient use of space. It is light and cost-effective, but exposure to humidity and high temperature can shorten its life. No standardized pouch cells exists; each manufacturer designs its own. The pouch cell is used for similar applications as the prismatic cell. See Figure C.2.1.3.

C.2.2 Modules

The next order of structure is the lithium-ion module or pack. This is an assembly of multiple cells that are electrically arranged in series, parallel, or a combination of both to meet the output voltage and amperage necessary for the installation. See Figure C.2.2(A) and (B).

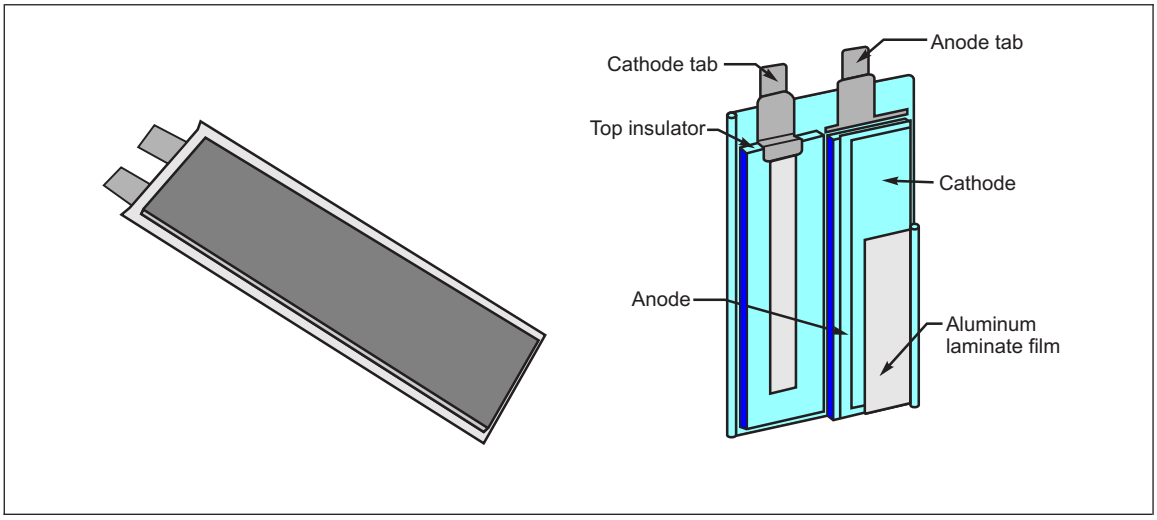

Fig. C.2.1.3. Pouch cell form

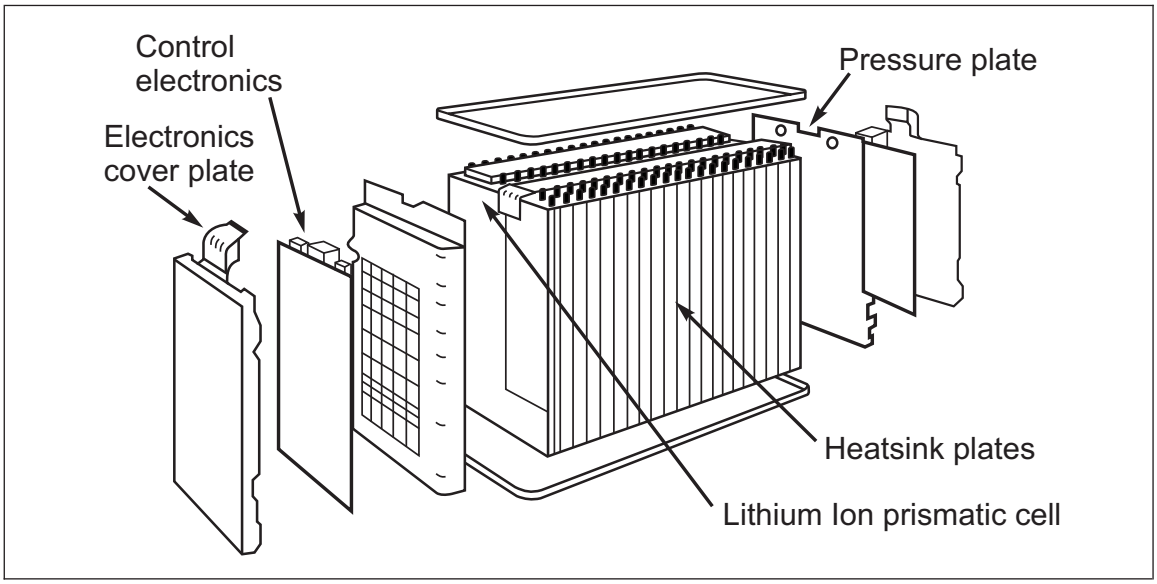

Fig. C.2.2(A). Module configuration

C.2.3 Racks

A rack consists of multiple modules, typically connected in series to develop a high DC voltage that is fed to the inverter/charger. The rack also consists of switching components (circuit breaker, isolator, and contactor) to isolate the rack during a contingency. See Figure C.2.3.

C.2.4 Systems

A large capacity ESS consists of multiple racks connected in parallel and feeding the inverter/charger. The ESS also includes the battery management system (BMS) that controls the batteries' basic functionality, safe operating conditions, and contingency response. An ESS also includes auxiliary systems such as HVAC and fire protection. See Figure C.2.4(A).

Figure C.2.4(B) shows the typical components within an ESS. Most of these components will be standard in every system despite the size or applications. .

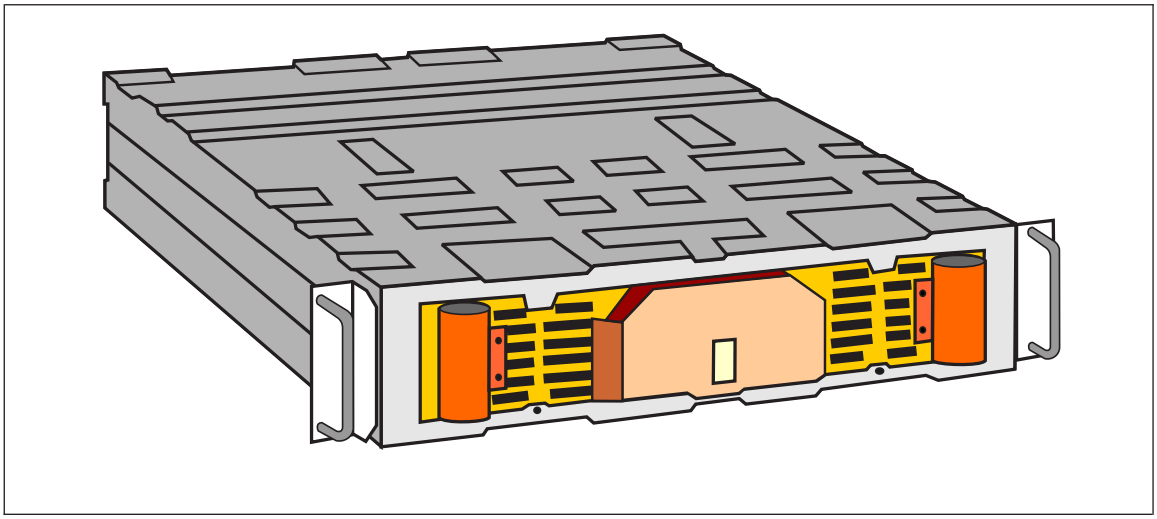

Fig. C.2.2(B). Typical enclosed module

C.3 ESS Applications

ESS applications include bulk energy, transmission, distribution (before meter) and commercial or industrial customer (after meter).

C.3.1 Bulk Energy Services

Bulk electrical energy storage is used to store relatively large amounts of energy in order to make it available (often locally) at another, usually more convenient, time. Applications include the following:

- Electric energy time-shift (arbitrage)
- Electric supply capacity

C.3.2 Ancillary Services

Systems used as ancillary services are used to facilitate and support the electricity grid's ability to provide a continuous flow of electricity and match supply and demand. Providing startup power after a total blackout is also considered an ancillary service. Applications include the following:

- Regulation/frequency response
- Spinning, non-spinning, and supplemental reserves
- Voltage support
- Black start
- Load following/ramping for renewables

C.3.3 Transmission and Distribution Services

Strategically placed electrical energy storage used within a transmission or distribution infrastructure service may act as an energy buffer and thereby defer grid upgrades. Applications include the following:

- Upgrade deferral
- Congestion relief
- Voltage support

C.3.4 Customer Energy Services

EES used within customer energy management is used to provide a customer related service. This can be enhancing the power quality, improving reliability and/or realizing additional profits for a customer. Applications include the following:

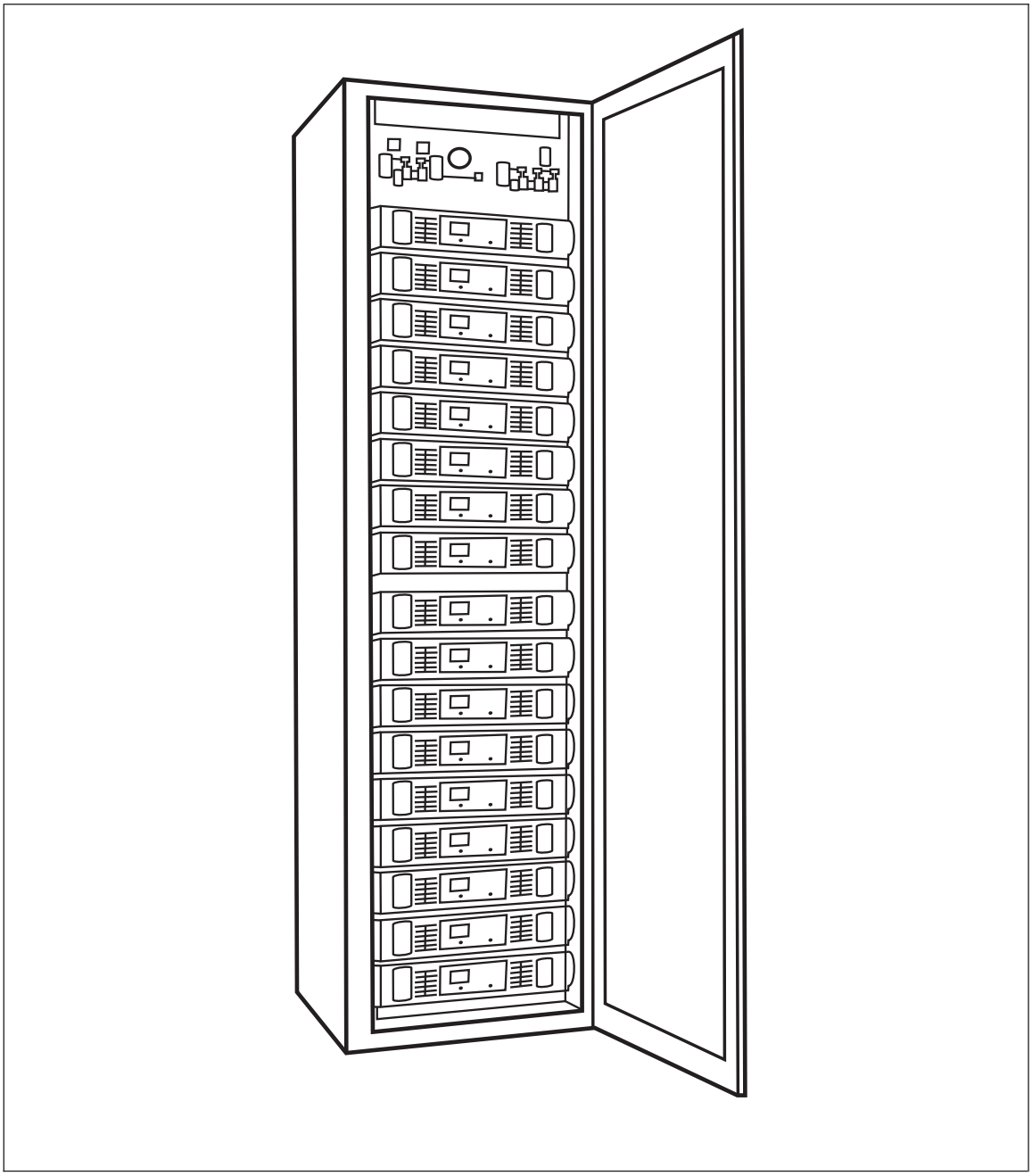

Fig. C.2.3 Typical rack configuration with miltiple modules

- Power quality
- Power reliability
- Retail energy time-shift
- Demand charge management

C.4 Failure Modes

The performance of lithium-ion cells is dependent on both temperature and operating voltage. There is a safe operating window in which these cells can work. This window is a function of cell voltage and temperature. The cell should operate between 32°F (0°C) and 212°F (100°C) while maintaining a voltage from 2 V to 4 V. Should a failure occur and the cell temperature fall below 32°F (0°C), lithium plating will occur during the

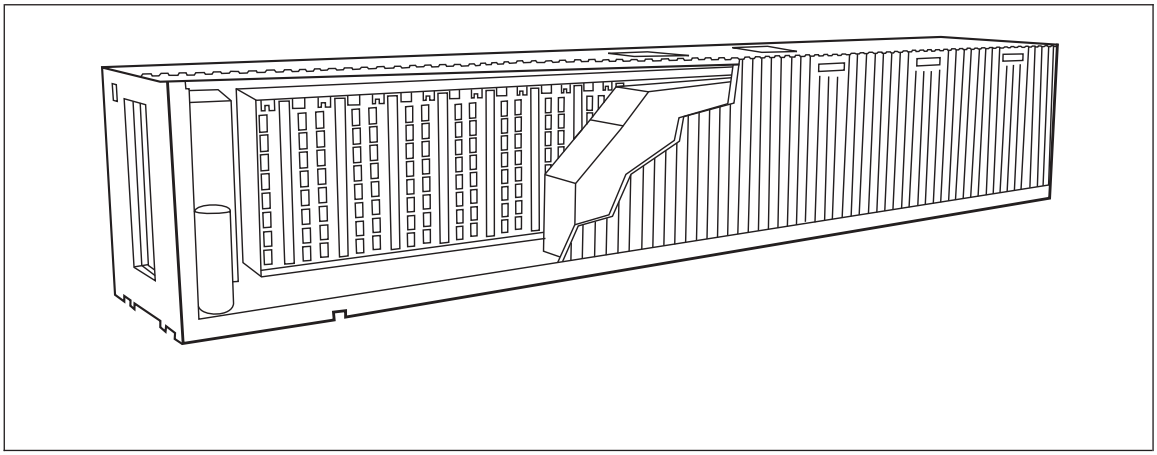

Fig. C.2.4(A). Exterior enclosure with multiple racks

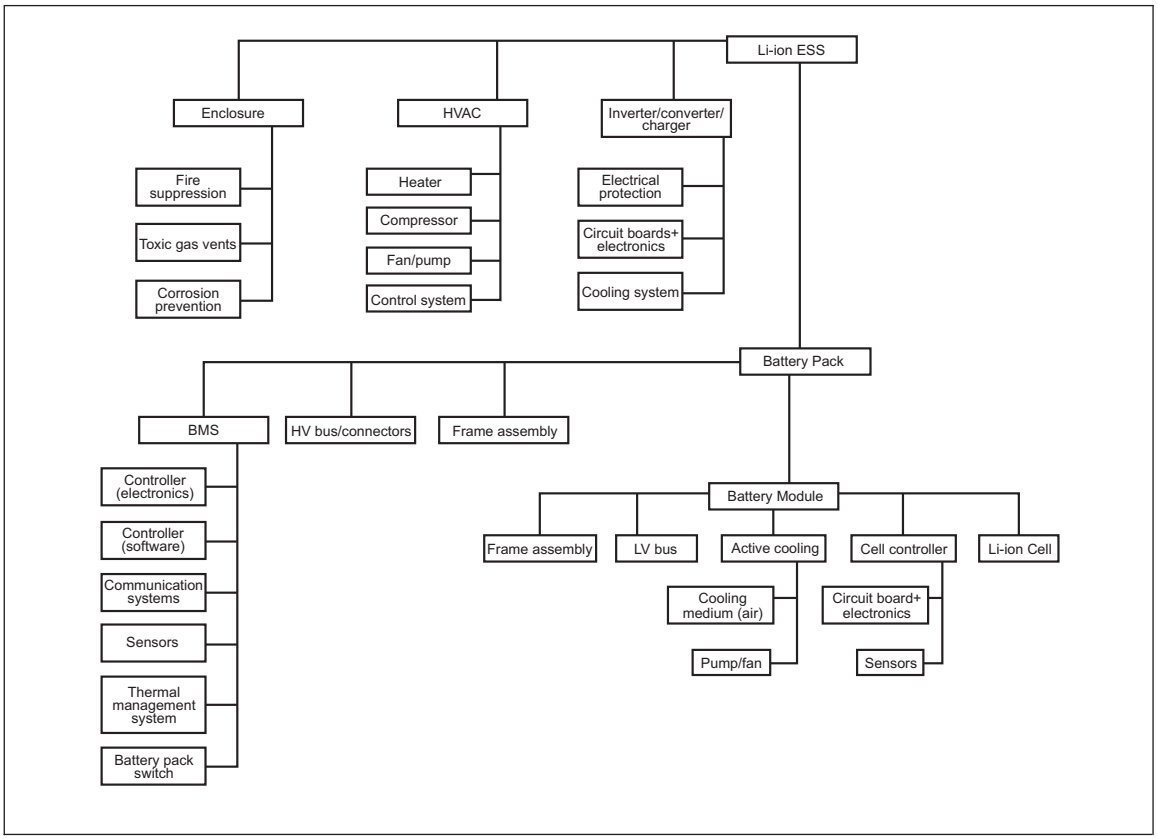

Fig. C.2.4(B). ESS architecture diagram

charging cycle, leading to shorting. Operating above 212°F (100°C) can lead to SEI thermal layer breakdown, and when coupled with operating above 6 V can lead to electrolyte leakage and subsequent vapor ignition. When operating at extreme temperatures (over 392°F [200°C]) the cathode active material will break down, causing even further damage. When operating below 2 V, the copper will dissolve, leading to shorting. When operating above 4 V and between 32°F (0°C) and 212°F (100°C), lithium plating will occur during charging, which will lead to overheating.

This section describes the failure modes for li-ion cells. These failure modes can be split into four broad categories depending on the critical variable triggering the failure: voltage, temperature, mechanical fatigue, and cycling/aging.

C.4.1 Overvoltage

If the charging voltage is increased beyond the recommended upper cell voltage, excessive current could flow, giving rise to two problems:

1. Lithium plating (dentrite growth): Lithium-ions accumulate on the surface of the anode where they are deposited as metallic lithium. This is known as lithium plating. The consequence is an irreversible capacity loss and, since the plating occurs in dendritic form, it can ultimately result in a short circuit between the electrodes. The quantity of lithium available is not sufficient to present a water reactivity hazard and therefore lithium plating is not typically considered a concern for lithium-ion batteries, while dendrite growth is considered a short circuit hazard.

2. Overheating: Excessive current also causes increased Joule heating of the cell, accompanied by an increase in temperature.

C.4.2 Undervoltage/Over-Discharge

Allowing the cell voltage to fall below about 2 V by over-discharging or storage for extended period results in progressive breakdown of the electrode materials.

• Anodes: At low voltage, the anode copper current collector dissolves into the electrolyte. As the voltage is increased (by charging), the copper ions which are dispersed throughout the electrolyte are precipitated as metallic copper wherever they happen to be, not necessarily back on the current collector foil. This is a dangerous situation which can ultimately cause a short circuit between the electrodes.

• Cathodes: Keeping the cells for prolonged periods at voltages below 2 V results in the gradual breakdown of the cathode over many cycles with the release of oxygen by the lithium cobalt oxide and lithium manganese oxide cathodes and a consequent permanent capacity loss. With lithium iron phosphate cells, this can happen over a few cycles.

C.4.3 Low Temperature

The effect of reducing the operating temperature is to reduce the rate at which the active chemicals in the cell are transformed. This translates to a reduction in the current-carrying capacity of the cell, both for charging and discharging. In other words, its power-handling capacity is reduced. The reduced reaction rate slows down and restricts the movement of the lithium-ions. Since the electrodes cannot accommodate the current flow, the result is reduced power and lithium plating of the anode, with irreversible capacity loss.

C.4.4 High Temperature

Operating at high temperatures can result in the destruction of the cell. The Arrhenius effect helps to get more power out of the cell by increasing the reaction rate, but higher currents give rise to higher I2R heat dissipation and thus even higher temperatures. This positive temperature feedback could result in thermal runaway unless heat is removed faster than it is generated.

C.4.5 Thermal Runaway

Several stages are involved in the buildup to thermal runaway, with each one capable of causing more damage than the previous stage.

A. Breakdown of SEI layer. This could be caused by overheating or mechanical impingement or can start at a relatively low temperature of 80|SNC. Once this layer is breached the electrolyte reacts with the carbon anode and leads to electrolytic breakdown and cathode breakdown. These reactions are exothermic and further increases the temperature.

B. Electrolyte breakdown. Heat from anode reaction causes the breakdown of the organic solvents used in the electrolyte releasing flammable hydrocarbon gases (Ethane, Methane and others) but no oxygen. The gas generation due to the breakdown of the electrolyte causes pressure to build up inside the cell. The pressure release vent in the cells are designed to release the gases and relieve internal pressure.

C. Separator melting. At elevated temperature, the polymer separator melts, allowing the short circuits between the electrodes.

D. Cathode breakdown. Heat from the electrolyte breakdown causes breakdown of the metal oxide cathode material releasing oxygen which enables burning of both the electrolyte and the gases inside the cell.

It should be noted that several studies have been undertaken to evaluate the avoidance of thermal runaway by adequate thermal management. This is critical because it forms the basis of mitigation measures against thermal runaway propagation.

C.4.6 Mechanical Fatigue

The electrodes of lithium cells expand and contract during charging and discharging. The cyclic stresses on the electrodes can eventually lead to cracking of the particles making up the electrode, resulting in increased internal impedance as the cell ages. In the worst case, the SEI layer could break down, leading to overheating and immediate cell failure. Alternatively, internal ground fault due to insulation failure between electrodes and enclosure could also cause cell failure.

Similarly, the slow deterioration of the electrolyte each time it is heat cycled could lead to release of small amounts of gases resulting in swelling of the cell and ultimately rupture of the cell casing.

Leakage of enclosure can lead to oxygen/moisture ingress causing electrolyte decomposition. Typically seals and weld failure can cause enclosure failure.

Other mechanical failure modes are drop, puncture, nail penetration, impact, and unsafe operation.

C.4.7 Cycle Life and Role of BMS

As discussed above, the excursions outside of the recommended operating window can cause irreversible capacity loss in the cells and potentially unsafe events if not managed properly. The cumulative effect of such excursions could affect the lifetime of the cell or, in the worst case, cause sudden failure. One of the main functions of the BMS is to keep the cells within their designed operating window. This is typically implemented using safety devices and controlling the operating conditions and environment.

C.5 Fire Protection Technologies

To date there is no publicly available test data that confirms the effectiveness of any active fire protection for energy storage systems, and there are no fire protection systems FM Approved for this application. The ability of active fire protection to stop or prevent Li-ion battery thermal runaway reactions has not been shown. At the same time, some manufacturers are providing active protection systems as an integrated component of the ESS.

RESEARCH FOUNDATION

RESEARCH FOR THE NFPA MISSION

Sprinkler Protection Guidance for Lithium-Ion Based Energy Storage Systems

FINAL REPORT BY:

R. Thomas Long, Jr., P.E., CFEI
Amy M. Misera, CFEI

Exponent, Inc.
Bowie, MD, USA

June 2019

1 Batterymarch Park, Quincy, MA 02169-7417, USA
Email: foundation@nfpa.org | Web: nfpa.org/foundation

FOREWORD

The 2016 Fire Protection Research Foundation project "*Fire Hazard Assessment of Lithium Ion Battery Energy Storage Systems"* identified gaps and research needs to further understand the fire hazards of lithium ion battery energy storage systems. There is currently limited data available on the fire hazard of energy storage systems (ESS) including two full-scale open-air tests from the 2016 Foundation project and a separate project that included intermediate scale fire testing conducted at the module level to evaluate the performance of fire suppressants. The fire protection and fire service communities need guidance on protection requirements for these systems in a building.

The Research Foundation initiated this project to determine sprinkler protection guidance for grid-connected lithium-ion battery based ESS for commercial occupancies. This report includes a summary of the small-scale and large-scale experimental testing undertaken for this project and the resulting protection recommendations.

The Fire Protection Research Foundation expresses gratitude to the report authors R. Thomas Long, Jr., P.E., CFEI, and Amy M. Misera, who are with Exponent, Inc. located in Bowie, MD, USA. The Research Foundation appreciates the guidance provided by the Project Technical Panelists, the funding provided by the Property Insurance Research Group (PIRG), and all others that contributed to this research effort. The Foundation also expresses gratitude to NEC Energy Solutions, Inc. and Retriev Technologies for their donations to support the project.

Special thanks are expressed to FM Global who donated their resources to complete the fire testing. A separate FM Global report containing the results from this experimental effort, as well as additional test results and expanded data analysis, can be found at: https://www.fmglobal.com/research-and-resources/research-and-testing/research-technical-reports.

About the Fire Protection Research Foundation

The Fire Protection Research Foundation plans, manages, and communicates research on a broad range of fire safety issues in collaboration with scientists and laboratories around the world. The Foundation is an affiliate of NFPA.

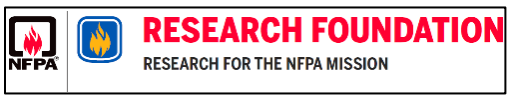

About the National Fire Protection Association (NFPA)

Founded in 1896, NFPA is a global, nonprofit organization devoted to eliminating death, injury, property and economic loss due to fire, electrical and related hazards. The association delivers information and knowledge through more than 300 consensus codes and standards, research, training, education, outreach and advocacy; and by partnering with others who share an interest in furthering the NFPA mission.

All NFPA codes and standards can be viewed online for free.

NFPA's membership totals more than 65,000 individuals around the world.

Keywords: energy storage systems, energy storage, li-ion battery, lithium-ion, ESS, fire hazard of ESS, sprinkler protection of ESS

Report number: FPRF-2019-06-REV

PROJECT TECHNICAL PANEL

Jim Biggins, Global Risk Consultants
Andrew Blum, Fisher Engineering
Tom De Lucia, NEC Energy Solutions
Laurie Florence, UL
Kevin Fok, LG Chem
Jan Gromadzki, Tesla
Kevin Marr, University of Texas
Dirk Long, Renewable Energy Systems (RES)
Celina Mikolajczak, Uber
Erin Minear, Energy Storage Integration Council
Leo Subbarao, FDNY
Nick Warner, Warner Energy Storage Solutions and ESRG
Brian O'Connor, NFPA

PROJECT SPONSORS

Property Insurance Research Group (PIRG):

AIG
CNA Insurance
FM Global
Liberty Mutual Insurance
Tokio Marine America
Travelers Insurance
Verisk
Zurich Insurance Group

Thermal Sciences

Exponent®

Sprinkler Protection Guidance for Lithium-Ion Based Energy Storage Systems

Exponent®

Sprinkler Protection Guidance for Lithium-Ion Based Energy Storage Systems

Prepared for:

Fire Protection Research Foundation
One Batterymarch Park
Quincy, MA 02169

Prepared by:

R. Thomas Long, Jr., P.E., CFEI
Amy M. Misera, CFEI
Exponent, Inc.
17000 Science Drive
Suite 200
Bowie, MD 20715

May 29, 2019

1503637.001 - 7128

Contents

List of Figures

List of Tables

Acronyms and Abbreviations

ESS	Energy Storage System
FPC	Fire Products Collector
FPRF	Fire Protection Research Foundation
HRR	Heat Release Rate
LFP	Lithium Iron Phosphate
NFPA	National Fire Protection Association
LNO/LMO	Lithium Nickel Oxide and Lithium Manganese Oxide
PIRG	Property Insurance Research Group
QR	Quick Response
RTI	Response Time Index
SR	Standard Response

Limitations

At the request of the Fire Protection Research Foundation (FPRF), Exponent has reported on the development of sprinkler protection guidance for lithium-ion based energy storage systems. This report summarizes small- to large-scale free burn fire test and large-scale sprinklered test results from two battery chemistries. The scope of services performed during this assessment of the test data may not adequately address the needs of other users of this report, and any re-use of this report or its findings, conclusions, or recommendations presented herein are at the sole risk of the user.

The tests and any recommendations made are strictly limited to the test conditions included in this report. The combined effects (including, but not limited to) of different energy storage configurations and designs, ceiling heights, protection system design, battery density, state of charge, battery chemistry, and battery type, etc. are yet to be fully understood and may not be inferred from these test results alone.

The findings formulated in this review are based on observations and information available at the time of writing. The findings presented herein are made to a reasonable degree of engineering certainty. If new data becomes available or there are perceived omissions or misstatements in this report, we ask that they be brought to our attention as soon as possible so that we have the opportunity to fully address them.

Executive Summary

This summary report describes the results and fire protection recommendations developed through testing, small- to large-scale free burn tests on lithium-ion battery energy storage systems (ESS). Subsequent large-scale sprinklered tests were conducted to determine performance of water-based fire protection systems. All data, test descriptions, data analysis and figures in this report were graciously provided by FM Global. Exponent has relied on the FM Global testing report, "Development of Sprinkler Protection Guidance for Lithium Ion based Energy Storage Systems" [1] Further details are provided in the FM Global report.

This project was conducted in conjunction with the Property Insurance Research Group (PIRG) and was directed through FPRF. This project is Phase II of a larger project with the goal to develop safe installation practices, fire protection guidance, and appropriate emergency response tactics for ESS. Phase I used literature review and full-scale free burn fire tests to create a fire hazard assessment of ESS in an effort to develop safe installation practices.

All tests were performed on donated battery modules of two different chemistries; lithium iron phosphate (LFP) and lithium nickel oxide (LNO) and lithium manganese oxide (LMO). The predominant difference in the hazard was the battery chemistry and energy density. The small-scale tests were conducted to determine if thermal runaway could be induced. Intermediate-scale testing was conducted to determine the effect of system capacity and thermal exposure. The large-scale tests involved two racks each with 16 modules. The tests were conducted to establish the overall hazard of the ESS. The full-scale sprinklered tests were used to determine the performance of a water-based fire protection system typically found in a commercial occupancy where an ESS could be installed.

All tests showed ignition of a single module was sufficient to produce thermal runaway and allow for fire spread to all modules in a single rack. In all tests, the LNO/LMO modules presented a greater fire hazard than the LFP modules. Due to different battery chemistries and limited understanding of how other factors affect the fire hazard of an ESS, the results of these tests cannot be applied to ESS comprised of modules with a different battery chemistry.

1 Introduction

Lithium-ion batteries and ESS are becoming more common in the world. Unlike other common batteries and energy storage systems, the biggest hazard associated with lithium-ion batteries is the potential for thermal runaway. There have been multiple studies on battery characteristics and cause of thermal runaway of a single battery cell, but there is a lack of research on the subsequent propagation of thermal runaway in adjacent battery cells in a multiple cell module. [2,3]

The research detailed in this report is part of a multi-phase project conducted in conjunction with PIRG and in partnership with the FPRF. The overall project goal is to develop safe installation practices, fire protection guidance, and appropriate emergency response tactics for ESS. The first phase of the project completed in 2016, involved a literature review and gap analysis related to lithium-ion battery ESS and the development and implementation of full-scale free burn fire testing of two 100 kWh ESS's. The literature review and fire test results were used to create a fire hazard assessment of ESS to develop safe installation practices. [4] The goal for this phase of the project was to determine the performance of water-based fire protection systems leading to the development of sprinkler protection guidance for lithium-ion battery ESS.

Separately, tests were conducted at the module level by DNV-GL to evaluate the performance of different fire suppressants such as water, wet chemical, and dry chemical. [5] The tests concluded that water was the most effective fire suppressant. These results were supported by the findings of large-scale testing by FM Global. [6] The recent studies provide confidence that sprinklers can be effective protecting ESS in commercial occupancies, but there is limited real scale data to support sprinkler protection guidance.

This project was directed by FPRF. All resources associated with conducting the tests, as well as compiling the data and results, were generously donated by FM Global. The Foundation expresses gratitude to NEC Energy Solutions, Inc. and Retriev Technologies for their donations to support the project.

2 Existing ESS Sprinkler Protection Guidance Documents

Today there is limited guidance on the installation and protection of ESS in any occupancy. At this point, the ESS protection guidance is for installation of ESS in non-storage buildings, covered in the NFPA 13 Standard for the Installation of Sprinkler Systems [7], and various FM Global documents. Currently, the NFPA 855 Standard for the Installation of Stationary Energy Storage Systems is in the development stage. [8] There is also similar guidance expected to be included in FM Global Property Loss Prevention Data Sheet 5-33, Electrical Energy Storage. [9] The documents listed provide installation and protection guidance for lithium-ion battery based ESS.

3 Battery Description and Test Set Up

The FM Global report focused on the large-scale sprinklered tests to determine performance of water-based fire protection systems leading to the development of sprinkler protection guidance for lithium-ion battery ESS.

3.1 Commodity/Battery Descriptions

Two different types of batteries were donated and used for this project. While it is not possible to test every type of battery, testing two different chemistries provides useful information on how they each react and behave. The two chemistries used were lithium iron phosphate (LFP) and lithium nickel oxide (LNO) and lithium manganese oxide (LMO). Figure 1 below provides more specific information on each battery chemistry tested.

Specification	LFP	LNO/LMO
Battery Description		
Chemistry	Lithium iron phosphate (LFP)	Lithium nickel oxide (LNO) and lithium manganese oxide (LMO)
Capacity (Ah)	20	32.5
Voltage (VDC)	3.3	3.75
Format	Prismatic	Prismatic
Nominal Dimensions, L×W×H (mm [in.])	227 × 161 × 7.25 (8.9 × 6.3 × 0.3)	290 × 216 × 7 (11.5 × 8.5 × 0.3)
Module Description		
Capacity (Ah)	120	130
Voltage (VDC)	42.9	60
Power (kWh)	5.2	7.8
Battery Layout (S= series, P= parallel)	13S6P	16S4P
Battery Quantity (#)	78	64
Nominal Dimensions*, L×W×H [mm (in.)]	700 × 270 × 180 (27.5 × 10.75 × 7)	650 × 320 × 240 (25.5 × 12.75 × 9.5)
Mass, kg (lb)	49 (108)	75 (166)
Rack Description		
Capacity (Ah)	120	130
Voltage (VDC)	686 (16 modules)	960 (16 modules)
Rack Layout (i.e., module configuration)	2 wide × 8 tall	2 wide × 8 tall
Enclosure	Open front, solid sides	Open front, solid sides
Nominal Dimensions, W×D×H [mm (in.)]	660 × 770 × 1,760 (26 × 30.25 × 69.25)	760 × 768 × 2,400 (30 × 30.25 × 94.5)

Figure 1. Battery cell description. Courtesy of FM Global.

Before testing, each battery was balanced within ±200 mV and the modules were charged to at least 95% state-of-charge, such that with the decay rate the modules would be at least 90%

charged at the time of testing. The total combustible load per the modules and racks differed for each type. Figure 2 provides further information on the individual battery chemistries.

Material	LFP Module		LNO/LMO Module	
	Mass	Energy*	Mass	Energy*
	kg (lb)	MJ (BTU×10^3)	kg (lb)	MJ (BTU×10^3)
Electrolyte	2.6 (5.7)	73 ± 7 (69 ± 7)	3.6 (7.9)	100 ± 10 (95 ± 9)
Plastic	4.9 (10.9)	188 ± 19 (178 ± 18)	10 (22.1)	381 ± 38 (361 ± 36)
Electrical Energy†	n/a	18.5 ± 2 (17.5 ± 2)	n/a	28 ± 3 (27 ± 3)
Total [1 Module]	7.5 (16.5)	279 ± 28 (265 ± 26)	13.6 (30.0)	509 ± 51 (482 ± 48)
Rack Total [16 modules]	120 (265)	4,464 ± 446 (4,233 ± 423)	218 (480)	8,142 ± 814 (7,719 ± 772)

*Energy is calculated using a ΔH_c for electrolyte = 28 MJ/kg (12.0 BTU/lb) [20] and unexpanded plastic = 38 MJ/kg (16.3 BTU/lb) [21].
†Electrical energy in MJ calculated from the module power rating as P (kWh) × 3.6 s.

Figure 2. LFP and LNO/LMO battery chemistry mass and energy information. Courtesy of FM Global.

3.2 Test Facility and Set Up

The tests were performed at the FM Global Research campus in West Glocester, Rhode Island. The facility includes multiple indoor test areas equipped with different sized combustion hoods and height adjustable ceilings for sprinklered fire tests.

Thermocouples were attached to the modules in each test to monitor the spread of the fire through the modules and heat flux gauges were used to measure the thermal exposure to other objects. The heat release rate data was measured from the collection of combustion gases to compare the fire development, overall magnitude, and total energy release. For each of the free burn tests, theoretical calculations were performed to predict sprinkler activation for both Quick Response (QR) and Standard Response (SR) sprinklers. The sprinklers used for the prediction calculations had a thermal link activation temperature of 74°C (165°F). The Response Time Index (RTI) for the QR sprinkler was 27.6 $m^{1/2}s^{1/2}$ (50 $ft^{1/2}s^{1/2}$) and 170 $m^{1/2}s^{1/2}$ (309 $ft^{1/2}s^{1/2}$) for the SR sprinkler. Sprinkler operation predictions were calculated for three different ceiling heights; 4.6 m, 6 m, and 7.6 m (15 ft, 20 ft, and 25 ft). For each height, the sprinkler head was located 0.3 m (1 ft) from ceiling, which corresponds with the maximum allowed distance in both NFPA 13 and FM Global Data Sheet 2-0.

4 Small-Scale Free Burn Tests

4.1 Small-Scale Free Burn Test Set Up

For the test, a single module was used with two thermocouples attached on each side of the module. Ignition was achieved with three flat bar heating elements (See Figure 3).

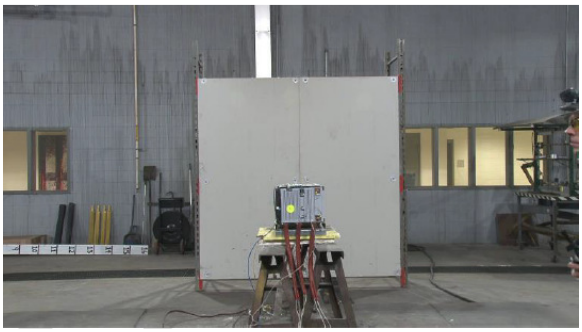

Figure 3. Small-scale free burn test set up. Courtesy of FM Global.

4.2 Small-Scale Free Burn Test Results

The external heating source caused thermal runaway reactions in the batteries for both module chemistries. The time of the observed battery venting was comparable for both chemistries. The LFP module was observed at 2,790 seconds and the LNO/LMO module was 2,820 seconds. For both modules the highest temperature was recorded by the bottom front thermocouple at the time of venting. The LFP module reached 295°C (563°F) and the LNO/LMO module reached 143°C (290°F). An element that was repeated in testing stages was the faster time to ignition in the LFP modules compared to the LNO/LMO modules due to closer contact with the heater and the modules and was not related to the batteries. Similarly, both modules reached peak heat release rate (HRR) around the same time. The LFP peaked at 4,620 seconds and the LNO/LMO peaked at 4,260 seconds. A noticeable difference between the two chemistries occurred in the aftermath of the batteries venting. The sparks from the LNO/LMO module were able to self-ignite the vent gases while the LFP module required a supplemental flame to ignite the vent gases consistently, for all stages of testing sometimes the gases did ignite and sometimes they did not. The HRR data for the LFP module shows a more gradual fire growth and a quicker decay phase, while the LNO/LMO module had almost non-existent fire growth until the time of peak HRR and then had a

longer decay phase. The LFP module reached a peak chemical HRR of 413 kW, while the LNO/LMO module had peak HRR over two times that of the LFP reaching 1,023 kW. Similarly, the total energy produced for the LNO/LMO module was twice as much as the LFP module, 204 MJ and 101 MJ respectively. See Table 1 for a summary of the test results. Full results can be found in the FM Global report.

Table 1. Summary of small-scale free burn testing results. Courtesy of FM Global.

	LFP	**LNO/LMO**
Ignition	2,790 seconds	2,820 seconds
Peak Chemical HRR	413 kW	1,023 kW
Peak Convective HRR	214 kW	450 kW
Total Chemical Energy Release	143 MJ	315 MJ
Total Convective Energy Release	101 MJ	204 MJ
Nominal Fire Duration	600 seconds	1,700 seconds
Burn out (HRR < 100 kW)	4,925 seconds	5,905 seconds

5 Intermediate-Scale Free Burn Tests

The intermediate-scale tests were conducted as a screening tool to evaluate the propensity for involvement of the module exposed to the ignition source and subsequent spread to adjacent modules. The intermediate-scale tests were conducted following the same approach as the small-scale tests.

5.1 Intermediate-Scale Free Burn Test Set up

A single test was performed on each battery chemistry. The test set up included a rack of 6 battery modules and 4 mock modules to record thermal exposure (See Figure 4). To collect the desired information, 23 thermocouples and 4 heat flux gauges were used.

Figure 4. Intermediate-scale free burn test set up. Courtesy of FM Global.

5.2 Intermediate-Scale Free Burn Test Results

Two intermediate-scale free burn tests were conducted following the approach established in the small-scale testing. In both tests, ignition of a single module was sufficient to spread the fire to all modules in the rack. Though the modules in the tests had the same set up, the modules burned differently effecting the time to peak HRR. In addition, the fire in the LFP modules spread vertically over the ignition point before spreading horizontally to the adjacent modules,

resulting in a longer fire duration but lower peak HRR. The fire in the LNO/LMO modules spread horizontally and then vertically, resulting in a shorter fire duration but a higher hazard in terms of fire intensity and thermal exposure. The LFP modules presented sustained flames at 2,970 seconds and reached near peak heat release rate at 7,996 seconds. At the time of peak HRR, the flames extended approximately 0.6 meters (2 ft). Similar to how it spread during the decay phase, the left side of the rack burned out before the right side. The fire lasted for over 9,000 seconds and at time 12,736 seconds a hose was used to manually extinguish the remaining flames. The first observed flames for the LNO/LMO rack occurred at 3,420 seconds with flames visible on the face of the ignition module. The fire reached peak HRR around 7,996 seconds and at that point the flames extended approximately 1.5 m (5 ft). During the decay phase, all modules continued to burn. At time 7,140 seconds the lower modules burned out and all modules were burned out by 7,907 seconds. Although the fire burned out without manual intervention, it was evident that modules contained heat as they maintained an orange glow until time 12,210 seconds. For both tests, the modules reached a peak temperature in the range of 400-600°C (750-1,000°F) and the peak rack temperature for both exceeded 900°C (1,650°F).

Similar to the small-scale results, in the intermediate-scale tests the LNO/LMO modules resulted in higher HRR and total energy compared to the LFP modules. The LNO/LMO module reached a peak chemical HRR of 1,890 KW and a total chemical energy of 2,030 MJ, compared to the LFP modules which reached peak chemical HRR of 500 kW and total chemical energy of 1,152 MJ. The LFP module had an extended growth phase starting around time 3,000 seconds, after the first flames had been observed. The HRR reached a peak of 500 kW around 7,800 seconds. After reaching peak, the HRR had a steady decrease leading to extinguishment at 11,400 seconds. The LNO/LMO modules fire developed differently from the LFP modules. The LNO/LMO modules HRR had a couple peaks and decays until it reached the real peak HRR of 1,890 kW around time 5,520 seconds. After reaching peak HRR, the HRR dropped and fell to under 40 kW by 8,000 seconds. See Table 2 for a summary of the test results. Full results can be found in the FM Global report.

Table 2. Summary of intermediate-scale free burn testing results. Courtesy of FM Global.

	LFP	LNO/LMO
Ignition	2,974 seconds	3,420 seconds
Peak Chemical HRR	500 kW	1,890 kW
Peak Convective HRR	312 kW	1,020 kW
Total Chemical Energy Release	1,152 MJ	2,034 MJ
Total Convective Energy Release	758 MJ	1,435 MJ
Nominal Fire Duration	6,000 seconds	3,300 seconds
Burn out (HRR < 100 kW)	11,600 seconds	7,581 seconds

6 Large-Scale Free Burn Tests

The large-scale free burn tests were conducted with the LFP and LNO/LMO equipment to evaluate the overall fire hazard and performance of sprinkler protection, similar to the previous tests. The two large-scale free burn tests were conducted with full ESS racks located in an indoor open-air environment under a 20-MW fire products collector (FPC). This approach allowed for real-time measurement of the chemical and convective heat release rate from the fire and magnitude of radiant exposure to surrounding objects, which was used to compare the relative hazard of the LFP and LNO/LMO systems.

6.1 Large-Scale Free Burn Test Set up

The large-scale tests included a rack of 16 modules and a mock rack on either side to measure the exposure hazard to adjacent equipment. In addition, faux structural walls were placed 2.7 m (9 ft) away on either side to measure exposure to surrounding objects (See Figure 5). To measure the data, 38 thermocouples and 7 heat flux gauges were used.

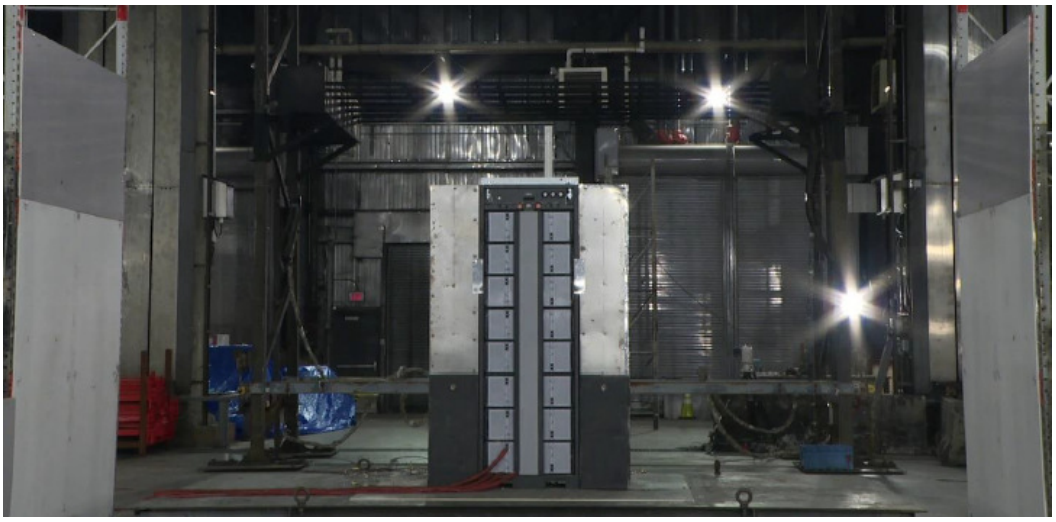

Figure 5. Large-scale free burn test set up. Courtesy of FM Global.

6.2 Large-Scale Free Burn Test Results

Similar to the small- and intermediate-scale tests, the LNO/LMO equipment presented a higher hazard than the LFP equipment in terms of fire intensity and thermal exposure to the surroundings. The LNO/LMO modules exhibited an unusually extended decay phase. The LFP modules exhibited a more traditional decay phase leading to burn out. The LFP modules burned at a nominal temperature range between 400-600°C (750-1,100°F) until the fire self-extinguished. The LNO/LMO modules reached similar temperatures as the LFP module until around 8,000 seconds when the fire transitioned to 'furnace like' combustion within the rack and reached temperatures exceeding 1,000°C (1,800°F). The fire progression through the modules was able to be tracked by monitoring when the thermocouples exceeded the temperature threshold. The thermocouple threshold temperature was set as 66°C (150°F) because it was the highest temperature before the noisy portion of the data on most channels. The noisy portion of the data was believed to occur as a result of leakage current from damaged batteries, more information is available in Section 3.4.2 of the FM Global report. Using this method, it was determined in the LFP modules rack the fire started with the initial module on the bottom left side and spread vertically allowing hot gases to collect and heat the top modules before spreading to the adjacent modules (See Figure 6). The LNO/LMO modules fire spread started with the ignition module and quickly spread vertically up both racks simultaneously (See Figure 7). Considering the size of the fires, the thermal exposure to the surroundings was of interest. Three heat flux gauges were placed 2.7 m (9 ft) away to record near field heat fluxes and a single heat flux gauge was placed 11.6 m (38 ft) away to record far field heat flux values. Heat flux gauge values were used to later to determine the thermal exposure at different separation distances.

Photos of LFP fire development during large-scale free burn test: near time of ignition (left), near time of predicted sprinkler operation (middle), peak heat release rate (right).

Figure 6. LFP fire development during large-scale free burn test. Courtesy of FM Global.

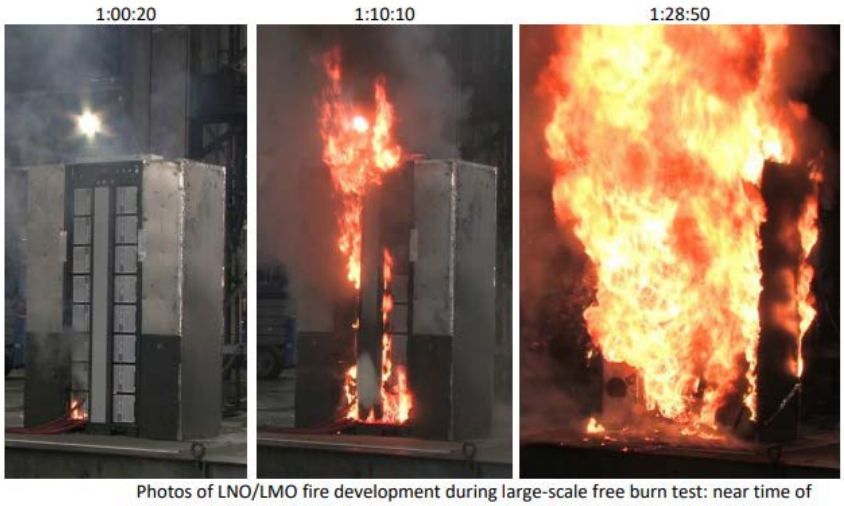

Photos of LNO/LMO fire development during large-scale free burn test: near time of ignition (left), near time of predicted sprinkler operation (middle), peak heat release rate (right).

Figure 7. LNO/LMO fire development during large-scale free burn test. Courtesy of FM Global.

Consistent with the small- and intermediate-scale tests, the LNO/LMO modules presented a significantly higher fire hazard with respect to energy release during the fire. In the full rack tests, the LNO/LMO modules reached a peak chemical HRR of 10,660 kW, which is almost five times higher than the LFP modules which reached a peak HRR of 2,450 kW. The LNO/LMO modules produced 6,390 MJ of total chemical energy, almost doubling the 3,810 MW of total chemical energy produced by the LFP modules. For the LFP module racks, flames were first

observed around 2,280 seconds. After the initial flames, the HRR started to increase reaching the peak chemical HRR between 4,800-5,040 seconds. After reaching the peak, the HRR fell to under 1,000 kW almost instantly and was below 500 kW by 6,000 seconds. During the LNO/ LMO modules test, flames were first observed around 3,500 seconds but the HRR did not register above 500 kW until after 4,200 seconds. From that point, the HRR increased at an accelerated rate reaching the peak of 10,660 kW before 5,400 seconds. Similar to the LFP modules, after reaching the peak the LNO/LMO HRR fell quickly registering under 1,000 kW by 5,880 seconds. Full HRR curves can be seen in Figure 8 and Figure 9. See Table 3 for a summary of the test results. Full results can be found in the FM Global report.

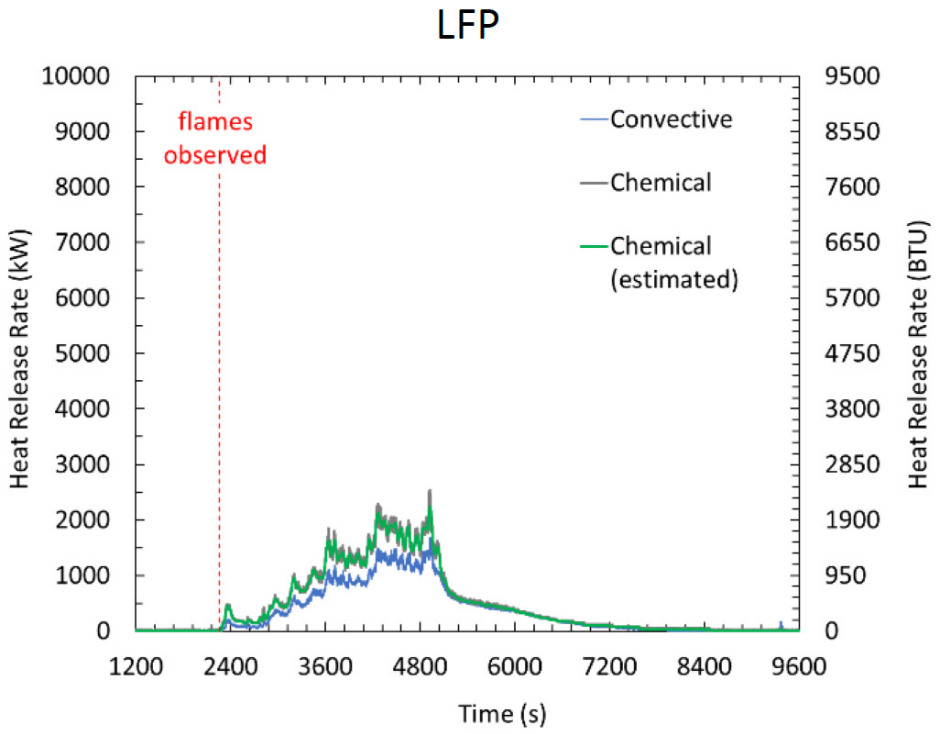

Figure 8. LFP full-scale free burn HRR. Courtesy of FM Global.

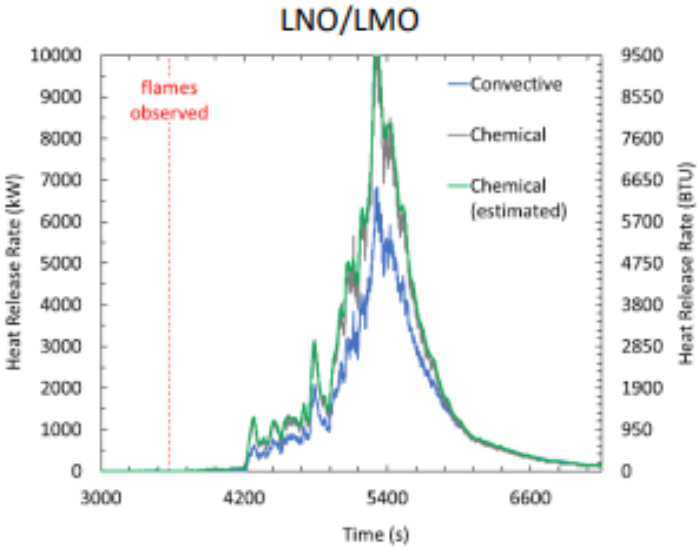

Figure 9. LNO/LMO full-scale free burn HRR. Courtesy of FM Global.

Table 3. Summary of large-scale free burn testing results. Courtesy of FM Global.

	LFP	**LNO/LMO**
Ignition	2,250 seconds	3,565 seconds
Peak Chemical HRR	2,540 kW	10,660 kW
Peak Convective HRR	1,680 kW	6,840 kW
Total Chemical Energy Release	3,810 MJ	6,390 MJ
Total Convective Energy Release	2,770 MJ	4,668 MJ
Nominal Fire Duration	4,750 seconds	3,000 seconds
Burn out (HRR < 100 kW)	7,100 seconds	7,270 seconds

7 Large-Scale Sprinklered Tests

After seeing the results of the large-scale free burn tests and the predicted sprinkler operation, two large-scale sprinklered fire tests were conducted under an unconfined and unobstructed ceiling to represent an ESS installation in a large open area.

7.1 Large-Scale Sprinklered Test Set up

Similar to the large-scale free burn tests, the sprinklered tests had a main rack that included 16 battery modules. In addition, a target rack with 16 battery modules was placed to the left of the main rack to measure fire spread. The modules were placed 0.9 m (3 ft) away from the faux corner and walls. Overall 56 thermocouples, 4 heat flux gauges and 4 radiometers were used to collect data, in addition there were over 180 ceiling level instruments to measure gas temperature, velocity, and sprinkler operation times. Refer to Figure 10 and Figure 11 to see the test set up and placement of data collection equipment. More information can be found in the FM Global report.

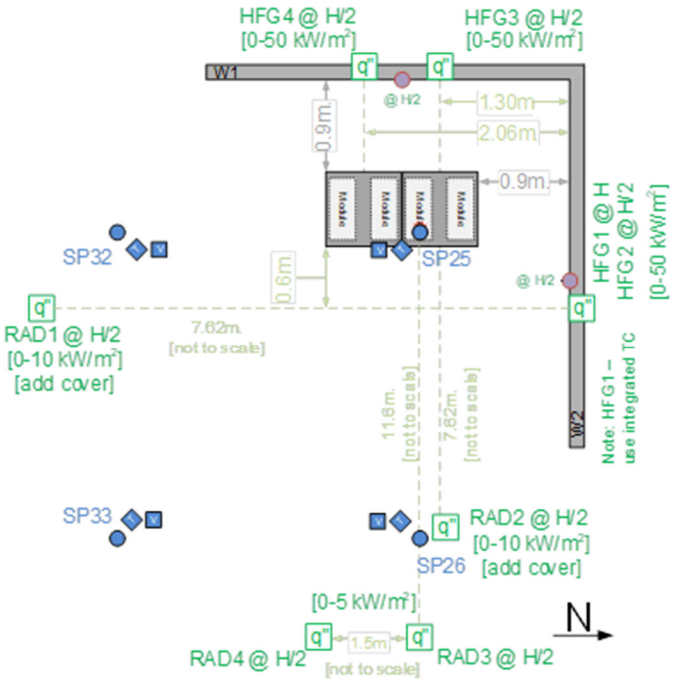

Figure 10. Large-scale sprinklered test set up. Courtesy of FM Global.

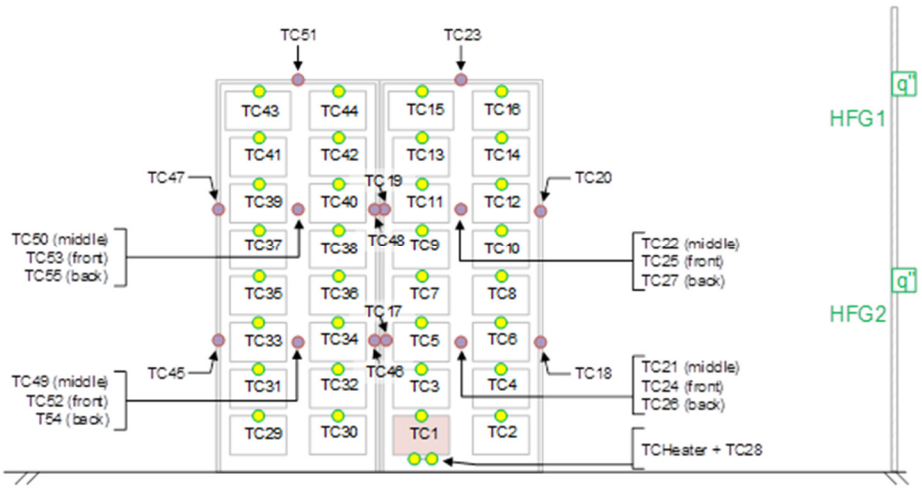

Figure 11. Large-scale sprinklered test set up. Courtesy of FM Global.

7.1.1 Sprinkler layout

For the sprinkler tests, water charged sprinklers were used that matched the qualities used in the sprinkler prediction calculations. The sprinklers used were K81 L/min/bar$^{1/2}$ (K5.6 gpm/psi$^{1/2}$), QR, nominal 74°C (165°F) temperature rated sprinklers. Using a worst case scenario design, the sprinklers were installed with 3 m x 3 m (10 ft x 10 ft) spacing and the sprinkler link was located 0.3 meters (1 ft) below the ceiling. The design area included 49 sprinklers, 4 were active and could produce water if activated, the remaining 45 were used to indicate operation without discharging water.

7.2 Large-Scale Sprinklered Test Results

Both the LFP and LNO/LMO tests show that ceiling-level sprinkler protection can reduce the overall fire intensity but does not adequately cool the modules within the rack to suppress the fire. Within the sprinklered tests, both the module and rack temperatures were recorded and compared. For both the LFP and LNO/LMO module rack tests, the modules were consistent with the other tests recording peak temperatures in the range of 400-600°C (750-1,110°F). Separately, the racks recorded higher temperatures. During the LNO/LMO test, the rack temperatures peaked in the range of 800-900°C (1,470-1,650°F) and the LFP rack exceeded 900°C (1,650°F) in some locations. The lower temperature in the modules could be a result of minimal open space between the modules. Overall, the LFP module was controlled by a single sprinkler and did not

spread to the target racks (See Figure 12). The LNO/LMO modules activated four sprinklers which were unable to prevent the spread and reignition of the target racks after the sprinklers were shut off (See Figure 13).

Photos of LFP sprinklered test during fire development: first sprinkler operation (left) and peak heat release rate (right).

Figure 12. LFP fire development during large-scale sprinklered test. Courtesy of FM Global.

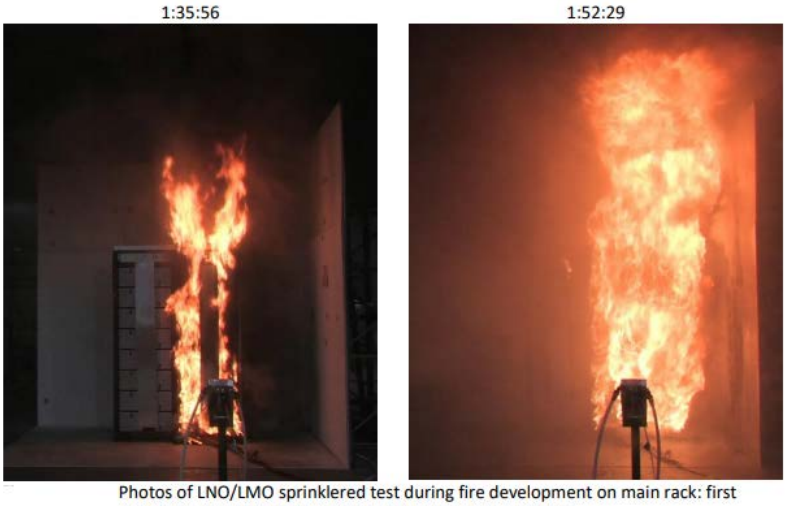

Photos of LNO/LMO sprinklered test during fire development on main rack: first sprinkler operation (left) and peak heat release rate (right).

Figure 13. LNO/LMO fire development during large-scale sprinklered test. Courtesy of FM Global.

In the LFP module rack test, the first flames were observed around 2,400 seconds and a single sprinkler operated at 3,667 seconds. After sprinkler operation, the HRR of the main rack

continued to increase until reaching a peak of 1,880 kW around 5,520 seconds. After reaching the peak, the HRR fell until the instruments failed around 7,200 seconds. The target rack was never involved in the fire and no HRR was recorded from the target racks. Full HRR curves can be seen in Figure 14.

The LNO/LMO modules and fire development behaved differently. The first flames were observed around 5,040 seconds and a single sprinkler activated at time 5,756 seconds, followed by three other active sprinklers and 36 indication sprinklers. The sprinklers were allowed to operate until 9,000 seconds and in that time the HRR of the main rack peaked at 6,690 kW. After the peak, the HRR fell and the sprinklers were turned off once no flames were observed. Once the smoke cleared the lab, small flames were observed in the target rack. Around time 11,160 seconds the HRR of the target rack began to increase and peaked reaching 4,900 kW, once the rack was fully involved the sprinklers were turned back on at 11,520 seconds. After the sprinklers were turned back on, the HRR dropped to around 1,000 kW before increasing to over 4,000 kW. With the use of sprinklers and a manual hose the fire was eventually extinguished. Full HRR curves can be seen in Figure 15.

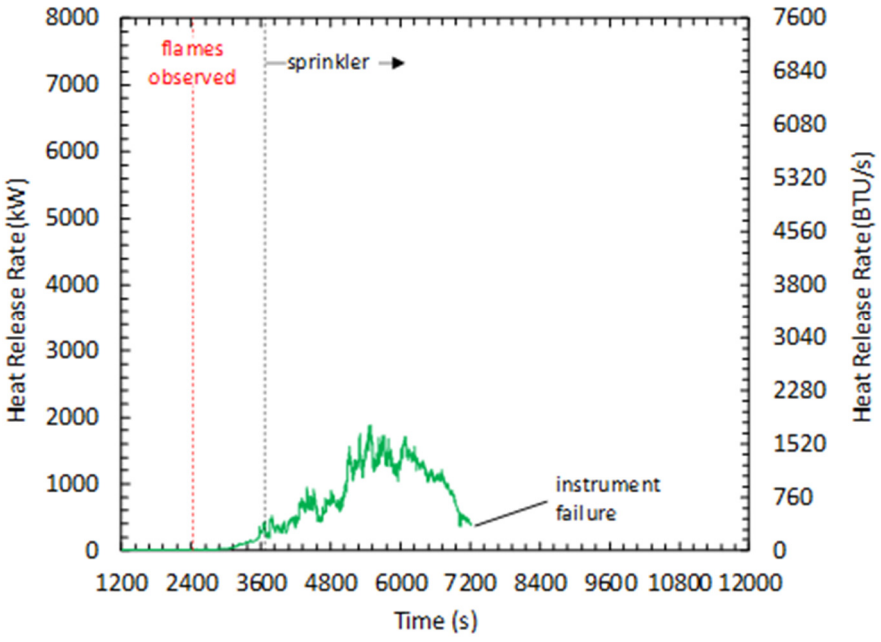

Figure 14. LFP large-scale sprinklered test HRR curve. Courtesy of FM Global.

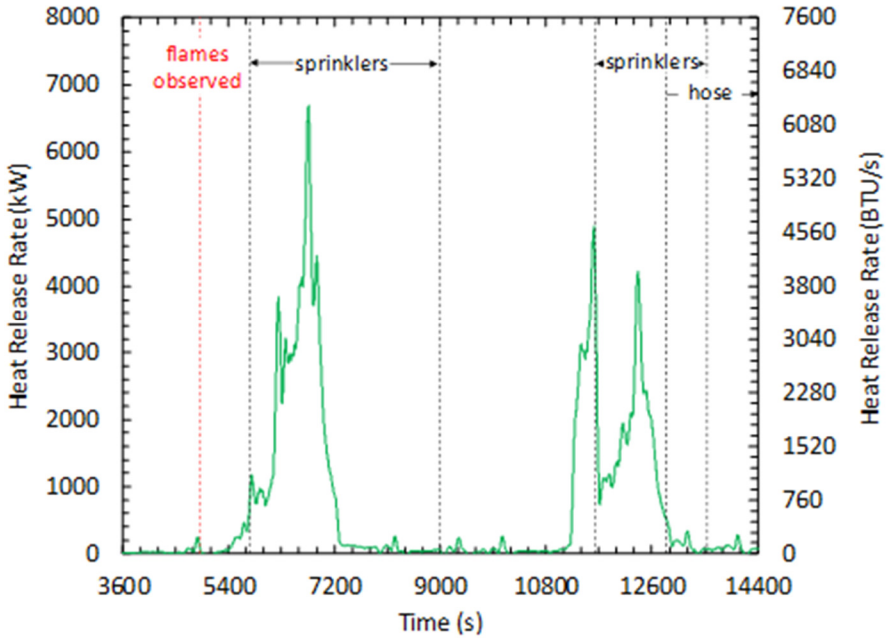

Figure 15. LNO/LMO large-scale sprinklered test HRR curve. Courtesy of FM Global.

7.2.1 Sprinkler Performance

Figure 16 depicts the activation of sprinklers and the time of operation. As mentioned above, during the LFP test a single sprinkler operated at 3,667 seconds and was able to contain the fire to the main rack and stop the spread to the target rack. The LNO/LMO test resulted in the operation of 4 active sprinklers and 36 indicator sprinklers. The first sprinkler in the LNO/LMO test operated at 5,756 seconds. The three other active sprinklers operated between 6,274-6,449 seconds, and the indicator sprinklers operated between 6,245-6,764 seconds. The LNO/LMO fire was able to activate sprinklers on the perimeter of the 230 m^2 (2,500 ft^2) design area which indicates if a fire were to occur in a non-enclosed area it is possible a larger water area would be necessary to control the fire.

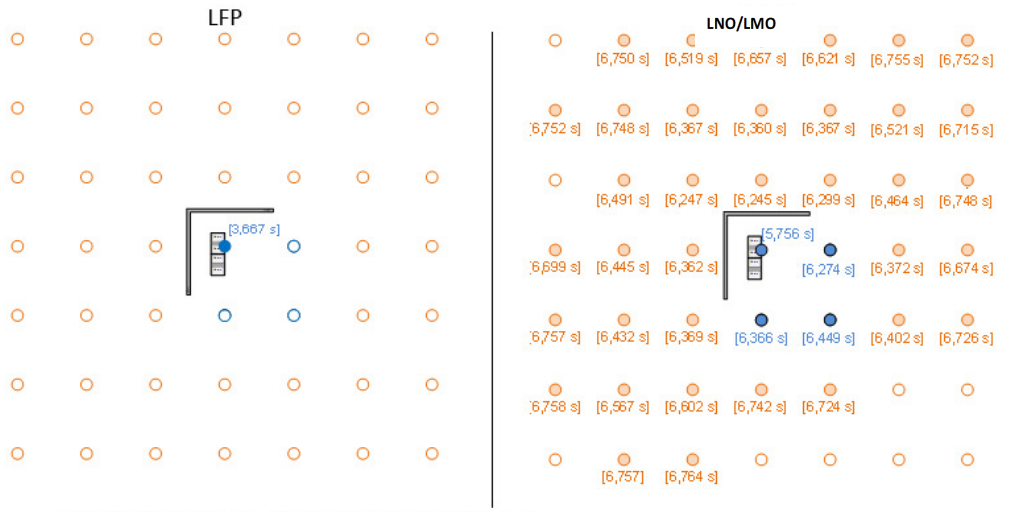

Sprinkler operation overview for LFP (left) and LNO/LMO (right) tests. Sprinklers that operated are shown as solid circles. Blue circles represent active sprinklers that could discharge water and orange circles represent indicator sprinklers that could not.

Figure 16. Sprinkler layout and operation overview for LFP (left) and LNO/LMO (right). Courtesy of FM Global.

8 Applications to Sprinkler Protection Guidance

Large-scale tests have shown sprinklers can control fire spread and reduce the hazard of an ESS fire. For the tests performed, the overall hazard of an ESS fire in a commercial occupancy was assessed by the reduction of fire intensity, potential for damage to the surroundings, and containment of the fire in the origin rack. As seen in the above-mentioned tests, HRR is a suitable way to measure the hazard of an unprotected fire. By using far field heat flux gauge values, it is possible to compare the results from the large-scale free burn and sprinklered tests. The sprinklers made an impact in the HRR of both LFP and LNO/LMO modules as seen in Figure 17. In Figure 17, times were offset to align data for comparison. During the sprinklered test, the LFP modules peak HRR decreased 45% and the LNO/LMO modules peak HRR decreased 34%.

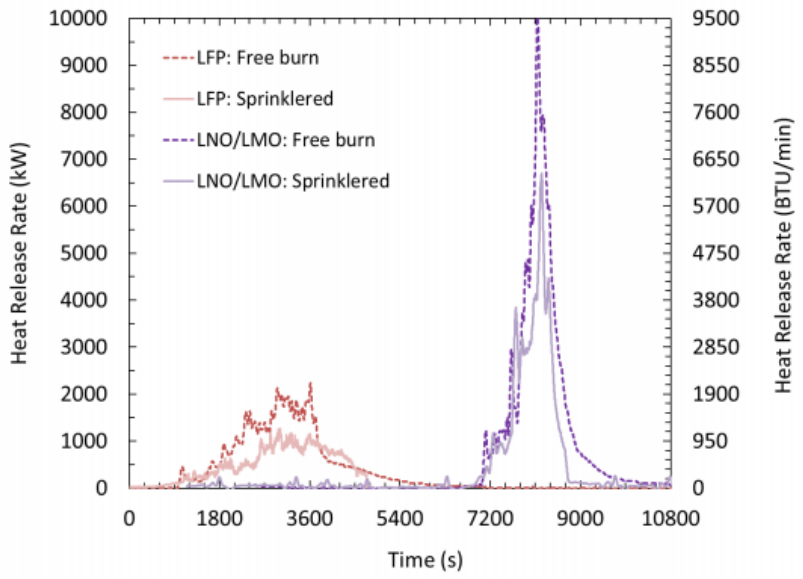

Figure 17. LFP and LNO/LMO free burn and sprinklered HRR comparison. Courtesy of FM Global.

From this data, ceiling sprinkler protection can control an ESS fire, but alone is not sufficient to fully extinguish an ESS fire. One method to aid the sprinkler in ESS protection is the application of physical thermal barriers or clearance space. Separating module racks from each other and from combustible and non-combustible materials can reduce and even prevent fire spread. Looking at the heat flux data from both free burn and sprinklered large-scale tests, the distance thresholds were determined for combustible and non-combustible materials (See Figure

18). Overall the LNO/LMO modules require a larger separation distance, but it is evident that sprinklers make a difference in the distance required.

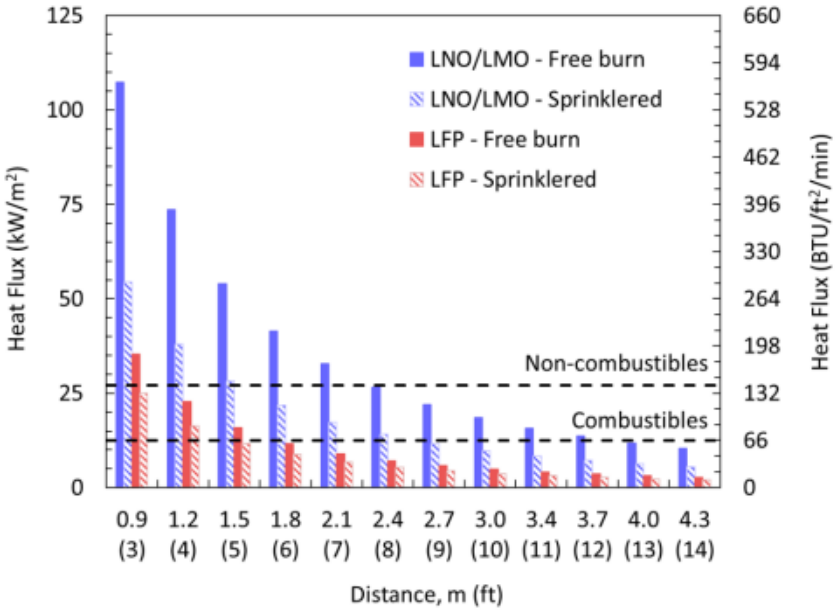

Figure 18. LFP and LNO/LMO free burn and sprinklered threshold comparison. Courtesy of FM Global.

With sprinkler protection, the LFP modules can be located 0.9 m (3 ft) meters from non-combustible materials and 1.5 m (5 ft) from combustible materials. The LNO/LMO modules would have to be located 1.8 m (6 ft) from non-combustible materials and 2.7 m (9 ft) from combustible materials to be considered safely separated. In addition to test data, FM Global Property Loss Data Sheet 1-20 (DS 1-20) Protection Against Exterior Fire Exposure [10] and NFPA 80A Recommended Practice for Protection of Buildings from Exterior Fire Exposures both provide guidance on separation distance and were the sources for the combustible and non-combustible threshold values. [11]

Another factor that was considered during the tests was the effect of ceiling height. If there is not enough distance between the top of a rack and the ceiling it can allow for flame impingement or collection of hot gases at the ceiling. Documents DS 1-20 and NFPA 5000, Building Construction and Safety Code [12] recommend that ceilings in the range of 3 m (10 ft) to 7.6 m (25 ft) should have a 1-hour fire rating. The fire rating on the ceiling can help reduce

and prevent damage, in the same manner thermal barriers such as spray-on foams and fire rated barriers can reduce the damage potential.

In addition to structural factors and surrounding materials, the configuration of the module racks can greatly affect the fire spread and hazard. Configurations can vary greatly, but there are three primary configurations used when multiple racks are stored in the same area (See Figure 19). The configurations include a) separate non-combustible cabinets, b) multiple racks together but separated by non-combustible cabinets, or c) a shared non-combustible cabinet housing multiple racks.

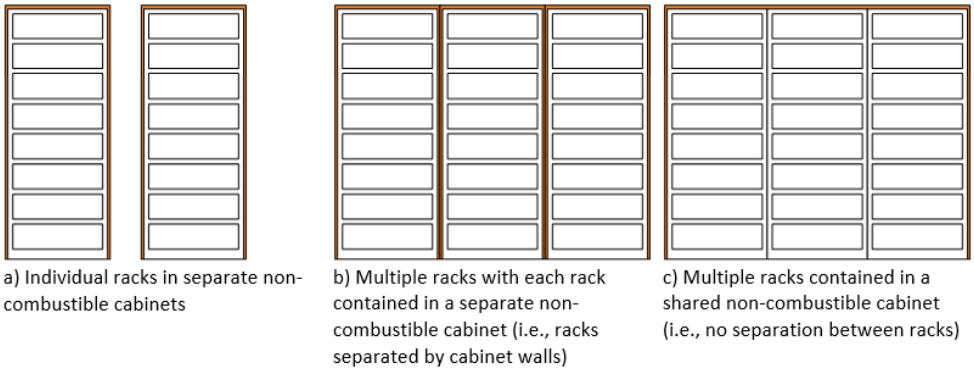

Figure 19. Diagram of three primary rack configurations. Courtesy of FM Global.

The configuration best for a certain ESS depends on which batteries are used. The LFP modules could use both configuration “a” and “b” and disregard the suggested separation distance because the fire did not spread from the origin rack in the sprinklered tests. The LNO/LMO modules could use configuration “a” and “b” as well but would need to adhere to the separation distance requirements to avoid fire spread from one rack to the next. For both LFP and LNO/LMO, multiple rack installations as described in configuration “c” is beyond the scope of this project.

Sprinkler systems can assist with reducing the fire hazard of an ESS if designed properly. Critical factors when designing a sprinkler system include, water demand, the number of sprinklers expected to operate, and the duration of the fire event. The water demand is typically calculated based on the number of sprinklers needed to provide adequate protection during a large-scale fire plus a safety factor of 50%. The large-scale testing performed used the common

criterion of an area of 3 m x 3 m (10 ft x 10 ft) and less than 16 sprinklers operating. In the LFP modules test a single sprinkler operated and the temperature and fire spread were controlled meaning the protection was acceptable. The LNO/LMO module test had multiple sprinklers activate and represented a demand area of over 230 m^2 (2,500 ft^2). The larger demand area and observed fire spread among side-by-side racks deems it reasonable to base the sprinkler demand area on the entire room being protected. For a fire that did not spread to other racks such as with the LFP modules, the time of the fire plus a safety factor can be used as the basis for time of water duration. For the LNO/LMO modules, the observed fire spread makes it necessary to multiply the fire duration of the first rack by the number of adjacent racks in the total configuration.

The design considerations and requirements above can be helpful when developing a fire protection system for an ESS, but the type of battery being stored is important to consider. The batteries tested for this research had similar construction but diverse chemistries which created different results and hazards. Beyond what was tested, the effects of rack design, construction materials, and battery specific features and chemistries are not widely known. A different rack design could reduce or increase the hazard of either battery type. Given the lack of information known, it is not possible to apply the results of the LFP and LNO/LMO battery tests to other batteries or systems that are different. Large-scale testing would be necessary when there is a question on the impact a design change would have on the system hazard.

9 Conclusions

Small- to large-scale free burn tests and a large-scale sprinklered test were conducted on two different types of lithium-ion battery energy storage systems, lithium iron phosphate (LFP) and lithium nickel oxide (LNO) and lithium manganese oxide (LMO). The tests were conducted to evaluate the impact of installation in regard to proximity of combustible and non-combustible material objects and the performance of sprinkler protection common to commercial facilities where ESS are installed.

Every test level showed for both battery chemistries that ignition of a single module was sufficient to involve all modules within the rack tested. Comparing the two battery types, all stages of testing showed the LFP modules presented a lower fire hazard risk than the LNO/ LMO modules. During the LFP test, a single sprinkler operated and was able to control the fire spread to the origin rack. In the LNO/LMO test, multiple sprinklers activated resulting in a demand area of over 230 m^2 (2,500 ft^2), and the fire spread from the origin rack to the target rack.

Based on the experimental results, the following conclusions were made:

1. The ESS comprised of LFP batteries under a 4.6 m (15 ft) ceiling was adequately protected by the target sprinkler protection. The water supply should be based on a minimum 230 m^2 (2,500 ft^2) demand area with a duration of at least 90 minutes. The conclusions are based on a single sprinkler operation controlling the fire to the rack of origin with no involvement of the target rack.

2. The ESS comprised of LNO/LMO batteries under a 4.6 m (15 ft) ceiling can be adequately protected by the target sprinkler protection. However, excessive ceiling sprinklers operated during the test conservatively representing a demand area > 230 m^2 (2,500 ft^2). In addition, fire spread from the origin rack to the adjacent target rack indicating that ESS racks installed side-by-side in a row could eventually be involved in the fire.

3. Large-scale free burn tests as described in Section 6.1 of the FM Global report are recommended to determine adequate space separation distances to prevent fire spread to nearby combustibles or damage to non-combustibles when sprinkler protection is not

provided. Large-scale free burn testing is also necessary whenever there is doubt regarding the potential impact a change in an ESS design feature may have on the system hazard.

4. Large-scale sprinklered tests as described in Section 6.2 of the FM Global report are recommended to determine adequate space separation distances to prevent fire spread to nearby combustibles or damage to non-combustibles, as well as sprinkler protection design including discharge density/area and water supply duration.

Other ESS's representing a hazard outside the above listed conditions, including design features, installation arrangement, and power rating, may require a more robust protection scheme to account for unknowns that can negatively affect protection system effectiveness. Additional large-scale sprinklered fire tests are necessary to establish a protection scheme that can adequately protect buildings and surroundings.

A fire watch should be present until all potentially damaged ESS equipment containing lithium-ion batteries is removed from the area following a fire event. Fires involving lithium-ion batteries are known to reignite. Lithium-ion batteries involved in fires should be adequately cooled in order to prevent reignition. This project has not addressed explosions hazards or any mitigation strategies that may be necessary during an ESS fire event, or firefighting efforts.

The data collected indicates that ESS fires will require lengthy hose stream water durations for final extinguishment. The geometry and installation arrangement of ESS's will affect hose stream water demand and duration potentially beyond/exceeding traditional code requirements for hose streams. At this time, the data does not allow for the further guidance on expected values for water demands for hose streams. While manual firefighting tactics are beyond the scope of the project, firefighting personnel or others considering utilizing manual hose streams on ESS fires should proceed with caution given the concerns associated with off-gassing/ venting and potential explosion hazards, as well as exposure conditions.

10 Recommendations

General protection recommendations for lithium-ion battery based ESS located in commercial occupancies were developed through fire testing. The following recommendations are derived from the results of the specific tests discussed in this report and the FM Global report:

For the tested LFP system:

- Without fire protection, the minimum space separation from any part of the ESS is 1.2 m (4 ft) from non-combustible objects and 1.8 m (6 ft) from combustible objects.
- With sprinkler protection, the minimum space separation from any part of the ESS is 0.9 m (3 ft) from non-combustible objects and 1.5 m (5 ft) from combustible objects. The sprinkler system water supply should be designed for a minimum 230 m^2 (2,500 ft^2) demand area and a duration of at least 90 minutes.

For the tested LNO/LMO system:

- Without fire protection, the minimum space separation from any part of the ESS is 2.4 m (8 ft) from non-combustible objects and 4.0 m (13 ft) from combustible objects.
- With sprinkler protection, the minimum space separation from any part of the ESS is 1.8 m (6 ft) from non-combustible objects and 2.7 m (9 ft) from combustible objects. The sprinkler system water supply should be designed for the total room area where the ESS is located, and the water supply should be calculated as 45 minutes times the number of adjacent racks.

11 Possible Future Work

The following possible future work is suggested to further understand protection requirements for Energy Storage Systems:

- Investigate and provide guidance on the effectiveness of different thermal barriers installed between adjacent ESS racks to reduce the risk of fire spread.
- Determine the fire hazard and sprinkler protection criteria for ESS multiple rack installations.
- Conduct additional sprinklered fire testing to reduce the sprinkler demand, area, water duration, and separation distances.
- Conduct additional sprinklered fire testing to evaluate the design of rack enclosures, materials of construction, and its effect on fire development and effectiveness of sprinkler protection.
- Conduct additional sprinklered fire testing to evaluate the relationship between fire hazard and variables such as battery or module design, including chemistries, capacities, and/or format.
- Conduct full-scale testing to evaluate durations and flows associated with hose stream use as well as potential hazards for firefighting personnel utilizing manual hose streams as well as any potential environmental concerns associated with water runoff.
- Consider testing with sprinklers protecting the modules in a configuration as in “in rack sprinkler protection” for rack storage.

12 Acknowledgements

The authors would like to thank Benjamin Ditch and the entire FM Global Research campus crew for their significant efforts in setting up, instrumenting, and conducting the fire and sprinkler tests and providing access to the data and analysis gathered during the testing.

The Foundation expresses gratitude to NEC Energy Solutions, Inc. and Retriev Technologies for their donations to support the project.

11 References

[1] B. Ditch, D. Zeng, “Development of Sprinkler Protection Guidance for Lithium Ion based Energy Storage Systems” FM Global Technical Report March 2019.

[2] J. Lamb, C. J. Orendorff, L. A. Steele, and S. W. Spangler, "Failure propagation in multi-cell lithium ion batteries," Journal of Power Sources, vol. 283, pp. 517-523, June 2015. DOI: 10.1016/j.jpowsour.2014.10.081.

[3] H. Webster. (May, 2012, accessed 12-13-2018) Full Scale Battery Fire Test Plan Update. presentation. [Online]. https://www.fire.tc.faa.gov/pdf/systems/May12Meeting/Webster-0512-FullScaleBatteryTestPlanUpdate.pdf.

[4] A. Blum and R. T. Long, "Hazard Assessment of Lithium Ion Battery Storage Systems," Final Report prepared for Fire Protection Research Foundation February, 2016.

[5] DNV-GL, "Considerations for ESS Fire Safety," Consolidated Edison New York, NY, Final Report OAPUS301WIKO(PP151895), Rev. #, 2017.

[6] B. Ditch, "Development of Protection Recommendations for Li-ion Battery Bulk Storage: Sprinklered Fire Test," FM Global, Technical Report 3053291, 2016.

[7] National Fire Protection Association Standard 13, Standard for the Installation of Sprinkler Systems, 2010.

[8] National Fire Protection Association Standard 855, Standard for the Installation of Stationary Energy Storage Systems, Proposed Standard, anticipate issuance in 2019.

[9] FM Global Property Loss Prevention Data Sheets 5-33, Electrical Energy Storage, January 2017.

[10] FM Global Property Loss Prevention Data Sheets 1-20, Protection Against Exterior Fire Exposure, Interim Revision, October 2016.

[11] National Fire Protection Association Standard 80A, Recommended Practice for Protection of Buildings from Exterior Fire Exposures, 2017.

[12] National Fire Protection Association Code 5000, Building Construction and Safety Code, 2018.

RESEARCH TECHNICAL REPORT

Development of Protection Recommendations for Li-ion Battery Bulk Storage: Sprinklered Fire Test

Development of Protection Recommendations for Li-ion Battery Bulk Storage: Sprinklered Fire Test

Prepared by

Benjamin Ditch

October 2016

FM Global
1151 Boston-Providence Turnpike
Norwood, MA 02062

PROJECT ID 0003053291

Disclaimer

The research presented in this report, including any findings and conclusions, is for informational purposes only. Any references to specific products, manufacturers, or contractors do not constitute a recommendation, evaluation or endorsement by Factory Mutual Insurance Company (FM Global) of such products, manufacturers or contractors. FM Global does not address life, safety, or health issues. The recipient of this report must make the decision whether to take any action. FM Global undertakes no duty to any party by providing this report or performing the activities on which it is based. FM Global makes no warranty, express or implied, with respect to any product or process referenced in this report. FM Global assumes no liability by or through the use of any information in this report.

Executive Summary

A project was conducted to determine fire protection guidance for warehouse storage of cartoned Li-ion batteries. The methodology for this project consisted of a comparison of the free-burn flammability characteristics of a large-format polymer pouch Li-ion battery to FM Global standard commodities and previously tested small-format Li-ion batteries in a rack storage array. A large-scale fire test then assessed the performance of ceiling-level sprinkler protection. The goal of the experimental approach was to maximize the application of the successful large-scale fire test result. For example, adequate sprinkler protection established in a large-scale test may be applied to all Li-ion batteries that are shown in the reduced-commodity evaluation to pose a hazard less than or equal to that of the battery used in the large-scale test.

A supplemental task involved assessing the impact of internal ignition within a pallet load of batteries versus the external ignition typically used in large-scale fire testing. An assessment of the effectiveness of sprinkler water at suppressing a fire at a later stage of battery involvement than could be achieved in the large-scale test was also conducted. Both of these tasks reinforce the sprinkler protection guidance resulting from the successful large-scale fire test.

This project was conducted in partnership with the Property Insurance Research Group (PIRG) and in collaboration with the Fire Protection Research Foundation (FPRF). The previous two phases of the project included a use and hazard assessment report[i] and a series of reduced-commodity fire tests comparing the flammability characteristics of several Li-ion batteries and FM Global standard cartoned commodities[ii, iii]. These tests showed that bulk storage of small-format Li-ion batteries (*i.e.*, 2.6 Ah) exhibits similar fire growth leading to first sprinkler operation as cartoned commodities. Further, it was determined that the time required for involvement of Li-ion batteries in a fully developed fire is on the order of five minutes. These conclusions provided the basis for sprinkler protection recommendations for small-format Li-ion batteries in bulk storage, with the goal of suppressing the fire before the anticipated time of involvement of Li-ion batteries. The current project evaluated ceiling-only sprinkler protection based on large-scale sprinklered fire test experience of cartoned Li-ion batteries.

The Li-ion battery available for this project was a 20 Ah, 3.3 V, polymer pouch battery with lithium iron phosphate ($LiFePO_4$) chemistry. The battery dimensions were 160 mm × 230 mm × 7.25 mm (6 in. × 9 in. × 1/3 in.) and the state-of-charge (SOC) was nominally 50%. Packaging consisted of corrugated containerboard cartons, where each carton contained 20 batteries separated by 10 levels of nested

[i] C. Mikolajczak, M. Kahn, K. White, and R. Long, "Lithium-Ion Batteries Hazard and Use Assessment," Report prepared for the Fire Protection Research Foundation, June 2011.

[ii] B. Ditch and J. de Vries, "Flammability Characterization of Lithium-ion Batteries in Bulk Storage," FM Global Technical Report, March 2013.

[iii] R. Thomas Long Jr., R. T. Long Jr., J. Sutula, and M. Kahn, "Li-ion Batteries Hazard and Use Assessment Phase IIB: Flammability Characterization of Li-ion Batteries for Storage Protection," Report prepared for the Fire Protection Research Foundation, 2013.

plastic dividers. This packaging and battery layout was consistent with the previously tested small-format Li-ion polymer batteries[ii, iii].

All test evaluations were conduct by FM Global at the FM Global Research Campus in Rhode Island, USA. The report findings are only valid under the following conditions:

- Storage height up to 4.6 m (15 ft)
- Ceiling height up to 12.2 m (40 ft)
- Bulk-packaged 20 Ah polymer pouch batteries in corrugated board cartons with heavy plastic dividers at nominally 50% state-of-charge (SOC).

The flammability characteristics of the selected 20 Ah Li-ion polymer pouch battery were compared to those of FM Global's standard commodities and previously tested small-format Li-ion batteries[iv,v]. This test, referred to as "reduced-commodity," was used to estimate the fire hazard present at the time of first sprinkler operation in a sprinklered warehouse fire scenario. Measurements focused on the fire development of each commodity and the time of battery involvement for the Li-ion products during a free-burn rack storage fire test. Based on the result of the test presented in this report, and building upon Reference[ii], the following conclusions can be made:

- The cartoned 20 Ah large-format battery used in the present study represented a higher hazard than the previously tested 2.6 Ah small-format batteries (cylindrical and polymer pouch). This conclusion is based on the following test results indicating that the large-format battery contributed to the overall fire severity closer to the predicted time of sprinkler operation than the small-format batteries:
    - The predicted time of sprinkler operation was similar for all cartoned Li-ion batteries and FM Global standard commodities included in this project. This result supports the assumption that for three-tier-high, open-frame racks, the carton packaging dominates the fire development leading to first sprinkler operation.
    - Under free-burn conditions, the 20 Ah Li-ion polymer pouch battery used in this project contributed to the overall severity of the rack storage 2 min 30 s (150 s) after igntion, versus 5 minutes for the previously tested 2.6 Ah cylindrical and polymer pouch batteries in Phase 2.
- The product packaging, e.g., corrugated board containers and dividers, was identified as a key factor driving the hazard in Li-ion batteries in storage. While the corrugated board cartons were

[iv] B. Ditch and J. de Vries, "Flammability Characterization of Lithium-ion Batteries in Bulk Storage," Technical Report, March, 2013. Available at www.fmglobal.com/researchreports.

[v] R. T. Long Jr., J. A. Sutula, M. J. Kahn, "Lithium Ion Batteries Hazard and Use Assessment Phase IIB - Flammability Characterization of Li-ion Batteries for Storage Protection," Fire Protection Research Foundation Report, 2013.

shown to dominate the initial fire growth, the plastic content within the cartons was shown to be a driving factor in the overall commodity hazard, in particular:

- Cartoned batteries containing significant quantities of plastics exhibited a similar rapid increase in the released energy due to plastics involvement early in the fire development.
  - For the large-format 20 Ah Li-ion polymer pouch batteries used in this project, the heavy plastic dividers contributed to the overall severity of the fire before involvement of the batteries.
  - For the power tool packs, tested in Phase 2[vi], the heavy plastic case of the battery pack dominated the fire hazard and there was no observable contribution from the batteries.
- Cartoned batteries containing minimal plastics (*e.g.,* the small-format Li-ion cylindrical and polymer batteries tested in Phase 2) exhibited a slower increase in energy release and a delay in the battery involvement due to heating of the batteries. In this case the plastic dividers represented a lesser combustible load than the heavy plastic dividers used for the 20 Ah polymer pouch battery.

Caution should be taken when extending the results of the testing presented in this report beyond the specific combination of packaging and battery listed. Changes in the components of the packaging can significantly impact the flammability characteristics of cartoned Li-ion batteries. One key aspect of the packaging driving the fire hazard is the divider used to separate the batteries within the cartons. Potential divider materials represent a wide range of fire properties and include liner board, fiber board, thin or heavy plastic, and expanded foam[vii]. Even for the same battery, changing the liner material can significantly impact the fire hazard. Changes in the Li-ion battery can also have a similar effect on the overall hazard of the cartoned product. For instance, high SOC has been shown to increase the likelihood and severity of thermal runaway[viii]. The quantity of electrolyte, which is the main combustible source, is a function of the battery capacity and can also vary with the battery format (e.g., cylindrical or polymer pouch). Thus even for the same packaging, changes in the battery can impact the fire hazard. A new flammability assessment should be conducted when potentially significant changes to the cartoned product are encountered.

The performance of ceiling-level sprinkler protection was then assessed with a large-scale sprinklered fire test of the large-format 20 Ah polymer pouch batteries. The test was conducted using a three-tier-

[vi] B. Ditch and J. de Vries, "Flammability Characterization of Lithium-ion Batteries in Bulk Storage," Technical Report, March, 2013. Available at www.fmglobal.com/researchreports.

[vii] M.M. Khan, A. Tewarson, and M. Chaos, "Combustion Characteristics of Materials and Generation of Fire Products," in *SFPE Handbook of Fire Protection Engineering*, P. DiNenno, Ed. Quincy, Massachusetts, New York: Springer, 2016, ch. Section 3, Chapter 4, pp. 1143-1232.

[viii] P. Ribiere, S. Grugeon, M. Morcrette, S. Boyanov, S. Laruelle, and G. Marlair, "Investigation on the Fire-Induced Hazards of Li-ion Battery Cells by Fire Calorimetry," *Energy and Environmental Science*, vol. 5, pp. 5271-5280, 2012. DOI: 10.1039/clee02218k.

high rack-storage array, which represents storage up to 4.6 m (15 ft) high. Protection was provided by quick-response, pendent sprinklers, having a 74°C (165°F) rated link with a K-factor of 320 L/min/bar$^{1/2}$ (22.4 gpm/psi$^{1/2}$) under a 12.2 m (40 ft) ceiling. In accordance with the established evaluation criteria, the following conclusions can be made:

- Storage up to 4.6 m (15 ft) under ceiling heights up to 12.2 m (40 ft) was adequately protected by a fire protection system comprised of pendent sprinklers having a K-factor of 320 L/min/bar^{½} (22.4 gpm/psi^{½}), with a nominal 74°C (165°F) temperature rating and a nominal RTI of 27.6 m^{½}s^{½} (50 ft^{½}s^{½}), installed on 3.0 m × 3.0 m (10 ft × 10 ft) spacing at an operating pressure of 2.4 bar (35 psig). This conclusion is based on one sprinkler operation extinguishing a large-scale test fire without manual intervention.

- Protection guidance established from the large-scale fire test can be reasonably applied to the small-format (i.e., 2.6 Ah cylindrical and polymer pouch) Li-ion batteries previously tested for this project. This conclusion is based on the results of the reduced-commodity test indicating that the cartoned large-format battery used in this project represented a higher hazard in the reduced-commodity test than the previously tested small-format batteries.

Three supplemental evaluations were then included to reinforce the sprinkler protection guidance resulting from the successful large-scale fire test. The first evaluation assessed the likelihood and impact of ignition resulting from thermal runaway of one or more batteries within a carton. The effectiveness of sprinkler water at suppressing a fire at a later stage of battery involvement than was achieved in the large-scale test was then conducted. Finally, literature data were reviewed to compare the minimum water application rate needed to prevent flame spread along the carton packaging versus the sprinkler protection used in the large-scale test. Based on the results of the tests presented in this report, the following conclusions can be made:

- For all small- and large-format Li-ion batteries used in this project, the development of a rack storage fire leading to sprinkler operation should be similar for both an ignition scenario where the fire initiates inside or outside of the carton. This conclusion is based on the following test results:

    - Thermal runaway of the 20 Ah polymer pouch battery used in this project did not result in battery-to-battery propagation within the carton. Experimental data have shown that thermal runaway of up to three batteries simultaneously within a single carton did not propagate to the adjacent batteries within the same carton.

    - There is not sufficient air within a carton to support combustion of a single 20 Ah polymer pouch battery. Thus, the fire propagation primarily occurs outside of the carton. In addition, review of literature data has shown that battery-to-battery

propagation following thermal runaway of small-format cylindrical batteries occurs after the carton has breached[ix].

- Once an external fire is present, flame propagation along the carton material will dominate the fire development leading to sprinkler operation and will occur before the batteries contribute to the overall fire severity.

- The sprinkler system used in the large-scale fire test was sufficient to protect against a fire where the Li-ion batteries were contributing more to the overall fire severity than occurred in the large-scale test. This conclusion is based on the following analysis:
  - Intermediate-scale testing, designed to delay the application of protection water until the batteries were contributing to the overall fire, confirmed the adequacy of sprinkler protection guidance resulting from the successful large-scale fire test.
  - In addition, review of literature data provided in Reference [x] has shown that a lower sprinkler discharge rate than used in the large-scale fire test can also control or suppress fire development along corrugated board cartons.

The best protection recommendations based on current knowledge, for each Li-ion battery included in this project, are summarized below. All ceiling-level sprinkler protection should be installed in accordance with FM Global Property Loss Prevention Data Sheet 2-0 (DS 2-0), *Installation Guidelines for Automatic Sprinklers*, January 2014. The protection recommendations are:

- Li-ion polymer pouch batteries (*i.e.*, capacity up to 20 Ah at ≤ 50% SOC) and Li-ion cylindrical batteries (*i.e.,* capacity up to 2.6 Ah at ≤ 50% SOC):
  - For a single unconfined pallet load of batteries stored on the floor to a maximum of 1.5 m (5 ft) high, protect as an HC-3 occupancy per FM Global Property Loss Prevention Data Sheet 3-26, *Fire Protection Water Demand for Nonstorage Sprinklered Properties*, July 2011. Additionally, maintain a minimum of 3.0 m (10 ft) separation between adjacent combustibles.
  - For batteries stored solid pile, palletized, or in racks up to 4.6 m (15 ft) under a ceiling up to 12.2 m (40 ft) high, protect with quick-response, pendent, sprinklers with a 165°F (74°C) nominal temperature rating. Protection options include:
    - K320 L/min/bar$^{1/2}$ sprinklers @ 2.4 bar (K22.4 @ 35 psi). The water flow demand should allow for 12 sprinkler operations.

[ix] H. Webster, "Flammability Assessment of Bulk-Packed, Rechargeable Lithium-Ion Cells in Transport Category Aircraft," U.S. Department of Transportation Federal Aviation Administration, DOT/FAA/AR-06/38, September 2006.

[x] S. Thumuluru and Y. Xin, "An Experimental Study of Pre-Wetting on Fire Propagation in Parallel Panels," in *Proceedings of the 13th International Fire Science and Engineering Conference (INTERFLAM 2015)*, Windsor, UK, 2013, pp. 317-326.

        - K360 L/min/bar$^{1/2}$ sprinklers @ 2.4 bar (K25.2 @ 35 psi). The water flow demand should allow for 12 sprinkler operations

    - For batteries stored higher than 4.6 m (15 ft) or ceiling heights greater than 12.2 m (40 ft), store batteries in racks and protect with Scheme A per Section D.2.2.1 of FM Global Property Loss Prevention Data Sheet 7-29, *Ignitable Liquid Storage in Portable Containers*, April 2012 (DS 7-29).

- Li-ion power tool packs (*i.e.,* comprised of 18650-format cylindrical batteries with a total pack capacity up to 26 Ah at ≤ 50% SOC):

    - Protect in-process storage of power tool packs as an HC-3 occupancy per FM Global Property Loss Prevention Data Sheet 3-26, *Fire Protection Water Demand for Nonstorage Sprinklered Properties*, July 2011. Limit in-process storage area to 19 m^2 (200 ft^2) and one pallet high. Additionally, maintain a minimum of 2.4 m (8 ft) separation between adjacent combustibles.

    - For power tool packs stored up to 4.6 m (15 ft) high under a ceiling up to 12.2 m (40 ft), protect as FM Global standard cartoned unexpanded plastic (CUP) commodity per FM Global Property Loss Prevention Data Sheet 8-9, *Storage of Class 1, 2, 3, 4 and Plastic Commodities*, FM Global, July 2011.

    - For power tool packs stored higher than 4.6 m (15 ft) or ceiling heights greater than 12.2 m (40 ft), store batteries in racks and protect with Scheme A per Section D.2.2.1 of DS 7-29.

Storage beyond the above listed conditions, including battery characteristics (*e.g.*, SOC, quantity of electrolyte, and format) and packaging components (e.g., cartons and dividers), requires a more robust protection scheme to account for several unknowns that can negatively affect protection effectiveness. Fire Protection Scheme A combines in-rack automatic sprinklers (IRAS) and horizontal barriers for protection of high-hazard commodities, such as rack storage of ignitable liquids or level 3 aerosols. Complete specifications and drawings can be found in Section D.2.2.1 of DS 7-29. Similar specifications can be found in Section E.2 of FM Global Property Loss Prevention Data Sheet 7-31, *Storage of Aerosol Products*, January 2012. This system design is expected to provide the highest level of protection required for storage of the Li-ion batteries tested in this project and can be applied to array configurations beyond the scope of this project.

Abstract

Protection recommendations for warehouse storage of cartoned Li-ion batteries have been developed through fire testing and comparison to analogous commodities with similar hazard characteristics. A unique approach was developed that incorporated four different fire test evaluations, ranging from small- to large-scale, with the goal of extending the application of a successful large-scale fire test to additional types of Li-ion batteries. A reduced-commodity test evaluated the flammability characteristics of large-format, 20 Ah Li-ion polymer batteries, compared to FM Global's standard commodities and previously tested small-format Li-ion batteries. The performance of ceiling-level sprinkler protection was then assessed with a large-scale sprinklered fire test of the large-format 20 Ah polymer pouch batteries. Two supplemental tasks reinforced the sprinkler protection guidance resulting from the large-scale fire test. The impact of internal ignition within a pallet load of batteries versus the external ignition typically used in large-scale fire testing was assessed through small-scale testing. Finally, the effectiveness of sprinkler water at suppressing a fire at a later stage of battery involvement than could be achieved in the large-scale test was assessed through intermediate-scale testing. Where applicable, best protection recommendations based on current knowledge have been provided.

Acknowledgements

The author thanks Mr. R. Chmura, Mr. J. Chaffee, Mr. M. Skidmore and the entire FM Global Research Campus crew for their efforts in conducting the fire tests. There were several testing phases included in this project that utilized the talented personnel of many laboratories. The diligent oversight of project safety and hazardous material disposal by Mrs. J. Pitocco ensured personnel safety throughout this project.

The author greatly acknowledges the discussion and input from the FM Global Engineering Standards group. Their expertise in loss prevention allowed for definitive protection recommendations, improving the practical application of this work.

The author further thanks Ms. Kathleen Almand, of the Fire Protection Research Foundation, and the members of the Property Insurance Research Group for their insightful discussions. In addition, the funding provided by PIRG members and other sponsors for the procurement of Lithium-ion batteries and disposal services was essential to the economic feasibility of this project.

Finally, the author would like to thank Ms. Denise Staplins for processing this report.

Table of Contents

List of Figures

List of Tables

1. **Introduction**

Fire protection guidance for warehouse storage of lithium ion (Li-ion) batteries presently remains a relatively unexplored topic within the fire protection community. At the same time, demand for Li-ion batteries continues to grow for applications such as electric and hybrid electric vehicles, consumer electronics, and energy storage systems. This is highlighted by a 2013 report that forecasted the global Li-ion battery market will increase from US$11.7 billion in 2012 to US$33.1 billion by 2019 [1]. As manufacturing capacity grows to meet the new global demand, so too will the volume of batteries stored in warehouses.

The fire hazards inherent to Li-ion battery technology are well documented in many overview documents [2, 3, 4, 5] and through experimental studies [6, 7, 8, 9, 10, 11, 12, 13]. The unique potential for thermal runaway reactions to spread a fire differentiates Li-ion batteries from typical ordinary combustible materials found in warehouse storage. As a result, neither *FM Global Property Loss Prevention Data Sheets* nor National Fire Protection Association Standard 13, "Standard for the Installation of Sprinkler Systems," [14] currently contain specific, research based, sprinkler installation recommendations or requirements for Li-ion battery storage. Consequently, the existing approach for sprinkler protection often relies on designs for high-hazard commodities, *e.g.,* automatic in-rack sprinklers [15].

This report describes part of a multi-phase project conducted in conjunction with the Property Insurance Research Group (PIRG) and in collaboration the Fire Protection Research Foundation (FPRF). The previous two phases of the project included a use and hazard assessment report [16] and a series of reduced-commodity fire tests comparing the flammability characteristics of several Li-ion batteries and FM Global standard cartoned commodities [17, 15]. These tests showed that bulk storage of small-format Li-ion batteries exhibits similar fire growth leading to first sprinkler operation as cartoned commodities. Further, it was determined that the time required for involvement for Li-ion batteries in a fully developed fire is on the order of five minutes. These conclusions provided the basis for developing sprinkler protection recommendations for small-format Li-ion batteries in bulk storage, with the goal of suppressing the fire before the anticipated time of involvement of the batteries. The current project evaluates ceiling-only sprinkler protection based on large-scale sprinklered fire test experience of Li-ion batteries.

A consultancy company, Exponent Inc., was retained by FPRF to provide a detailed description of the batteries and prepare a summary report of the project findings [18].

FM Global donated the resources associated with conducting the research program, including storage and cleanup of the Li-ion batteries. The batteries used in the test were donated by a private supplier. Disposal and recycling services were donated by a waste management company specializing in disposal of Li-ion batteries. The balance of the costs, which included program management services, was supplied by PIRG.

2. Experimental Program

The methodology for this project consisted of a comparison of the free-burn flammability characteristics of the available large-format Li-ion polymer pouch battery to FM Global standard commodities and previously tested small-format Li-ion batteries in a rack-storage array. A large-scale fire test then assessed the performance of ceiling-level sprinkler protection. The goal of this experimental approach was to maximize the application of the successful large-scale fire test result. For example, adequate sprinkler protection established in a large-scale test may be applied to all Li-ion batteries that are shown in the reduced-commodity evaluation to pose a hazard less than or equal to that of the battery used in the large-scale test.

A supplemental task for this project involved assessing the impact of internal ignition within a pallet load of batteries versus the external ignition typically used in large-scale fire testing. A separate task assessed the effectiveness of sprinkler water at suppressing a fire at a later stage of battery involvement than can be achieved in the large-scale test. Both of these tasks reinforced the adequacy of sprinkler protection guidance resulting from the successful large-scale fire test.

2.1 Test Facility

Testing for this program was primarily conducted in the Large Burn Laboratory located in the Fire Technology Laboratory at the FM Global Research Campus in West Glocester, Rhode Island, USA. Figure 2-1 is a plan view of the LBL showing the north movable ceiling, the south movable ceiling, and the 20-MW Fire Products Collector (FPC).

The 20-MW FPC, used for the reduced-commodity test described in Section 3, consists of an 11 m (36 ft) diameter inlet that tapers down to a 3.0 m (10 ft) diameter duct. The inlet to the 20-MW FPC is at an elevation of 11.3 m (37 ft). Gas concentration, velocity, temperature, and moisture measurements are made within the FPC duct. Beyond the measurement location, the exhaust duct connects to a wet electrostatic precipitator (WESP) prior to the gases venting to the atmosphere. The air exhaust rate was set to 71 m^3/s (150,000 ft^3/min).

The north movable ceiling, used for the large-scale fire test described in Section 4, is smooth, flat, and horizontal. The ceiling measures 24.4 m x 24.4 m (80 ft x 80 ft) and is adjustable for heights above the floor ranging from 3.0 m to 18.3 m (10 ft to 60 ft). The air emission control system (AECS) exhaust ducting consists of four extraction points, located at the lab ceiling, that merge into a single duct with a cross sectional area of 6.1 m^2 (66 ft^2). Gas concentration, velocity, temperature, and moisture measurements are made downstream of the manifold. Beyond the measurement location, the exhaust duct connects to a wet electrostatic precipitator (WESP) prior to the gases venting to the atmosphere. The air exhaust rate was to 94 m^3/s (200,000 ft^3/min).

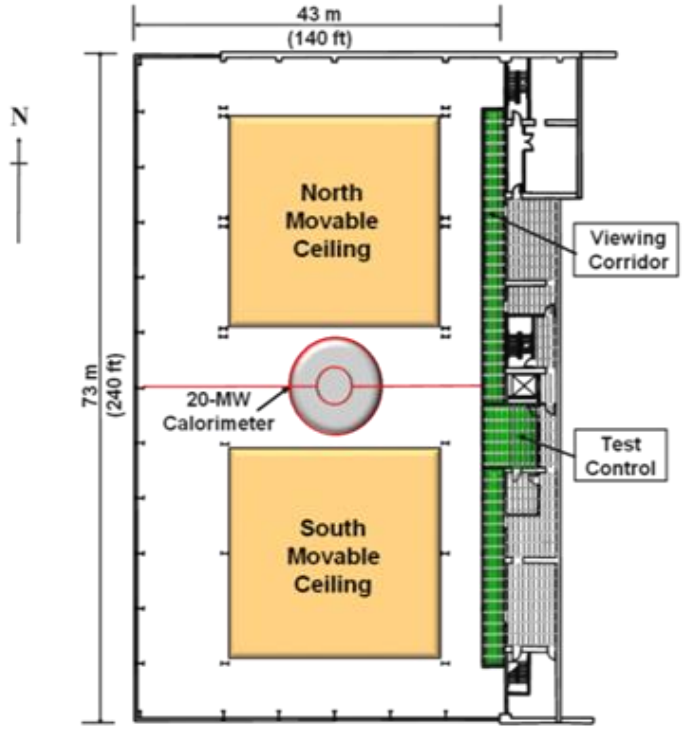

Figure 2-1: Illustration of FM Global Large Burn Laboratory test locations.

2.2 Li-ion Battery Test Commodity

The Li-ion battery available for this project was a 20 Ah polymer pouch battery and the specifications are shown in Table 2-1. The battery is constructed by stacking alternating layers of electrodes, which are then enclosed in foil pouches with heat-sealed seams, Figure 2-2.

It is important to note that the 20 Ah battery used in this project contained approximately 7% electrolyte per total mass of the battery. This represents a similar combustible loading compared to the smaller capacity Li-ion batteries (*i.e.*, 2.6 Ah) used in the previous study, which contained approximately 5% electrolyte for the cylindrical battery and 8% for the polymer pouch battery [15]. The listed state-of-charge is consistent with the typical storage condition for each battery.

The packaging, as received from the supplier, consisted of a 430 mm × 330 mm × 150 mm (16.75 in. x 12.81 in. x 5.75 in.) corrugated containerboard carton. Each carton contained 20 batteries separated by nested polystyrene plastic dividers, Figure 2-3. This packaging and the battery layout is consistent with the previously tested small-format Li-ion polymer batteries [15].

The pallet load design consisted of 56 cartons arranged among seven levels of eight cartons each for a total of 1,120 batteries per pallet load, Figure 2-4. Consistent with the pallet design received from the supplier, the cartons are arranged in a "doughnut shape," resulting in an open area at the center of pallet. The orientation of the cartons alternated each level for stack stability and to ensure consistency in the battery layout on all sides of the pallet load. The overall dimensions of the pallet load were 1,080 mm x 1,080 mm x 1,020 mm tall (42.5 in. x 42.5 in x 40.25 in.).

Table 2-1: Lithium-ion battery specifications. *[courtesy of Exponent, Inc.]*

Specification	Value
Voltage	3.3 V
Capacity	20 Ah
Dimensions	7.25 mm x 160 mm x 227 mm (0.3 in. x 6.3 in. x 8.9 in.)
Mass	490 g (1.1 lb)
Chemistry	Lithium iron phosphate ($LiFePO_4$)
Approximate Electrolyte Mass	34 g (0.08 lb)
Approximate State-of-Charge	50%

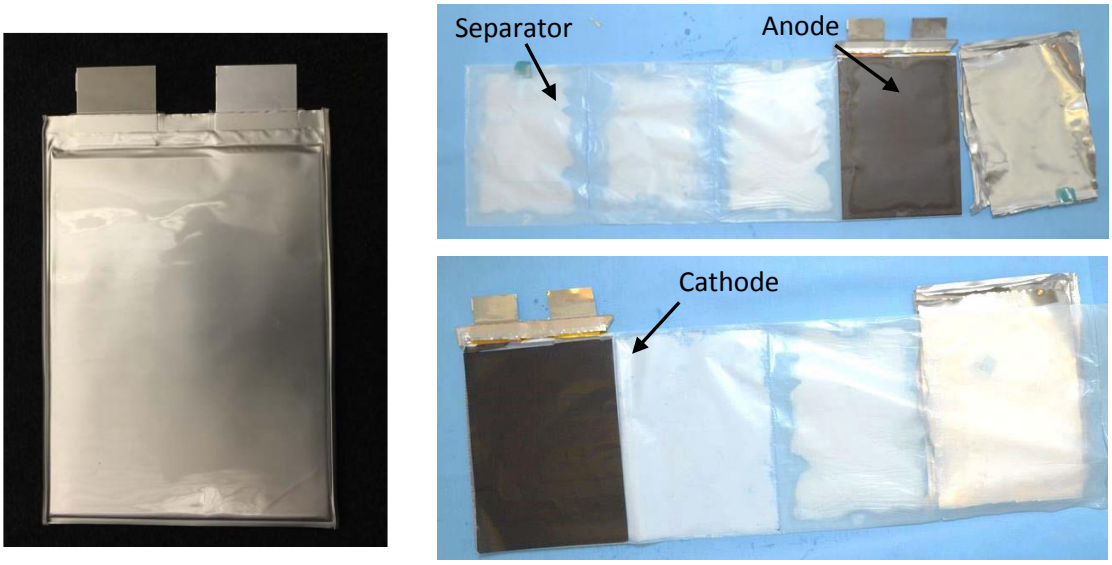

Figure 2-2: Li-ion polymer pouch battery; outside foil pouch shown on left, internal components shown on right. *(images courtesy of Exponent, Inc.)*

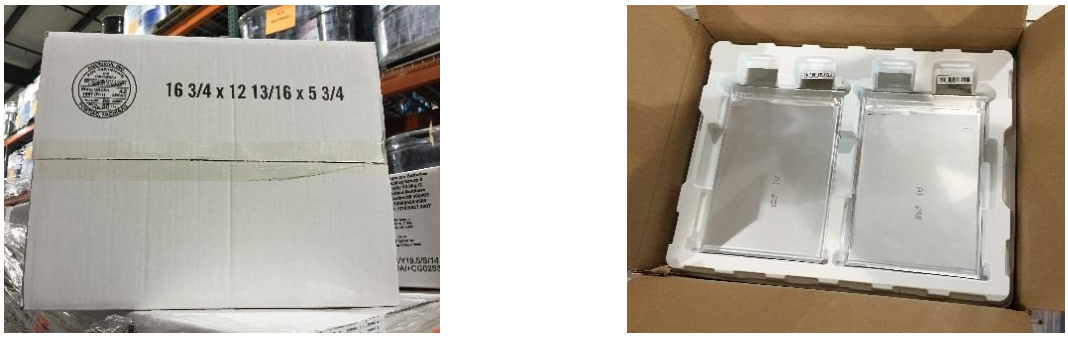

Figure 2-3: Packaging images; individual carton shown on left and top view of packaging shown on right.

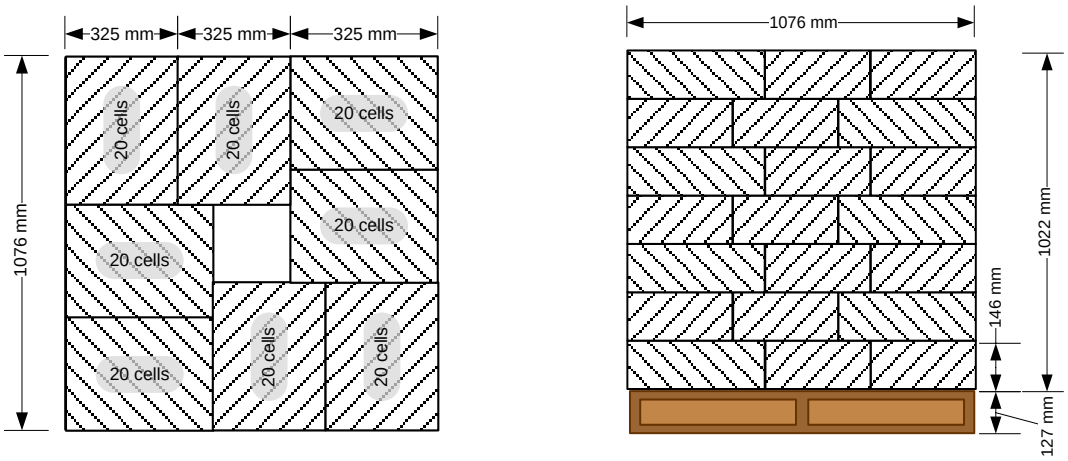

Plan View Elevation View

Figure 2-4: Li-ion polymer pouch battery pallet layout; top view shown on left and elevation view shown on right.

As shown in Table 2-2, the combustible loading per carton of batteries is 86 ± 3.5 MJ. When supported on an FM Global standard wood pallet, the combustible weight of the commodity is approximately 177 kg (390 lb); of this total the cartoned Li-ion battery commodity is 155 kg (340 lb) and the pallet 22 kg (50 lb). The total chemical energy per pallet load is nominally 5,105 ± 117 MJ, based on the above masses and the heat of combustion for each material listed in Section 2.3.

Table 2-2: Combustible load per carton of batteries.

Component	Individual Weight (kg)	Quantity per Carton (ea)	Weight per Carton (kg)	Energy* (MJ)
Carton	0.6	1	0.6	8.3 ± 0.2
Plastic Divider	0.15	10	1.5	58.3 ± 1.5
Electrolyte	0.35	20	0.7	19.6 ± 2.0
		Total:	2.8	86 ± 3.7

* Heat of combustion and uncertainty values are listed in Section 2.3.

2.3 Heats of Combustion

Table 2-3 contains average chemical heat of combustion values for each component of the test commodities. These are average values for each material type and up to 5% variance can be expected with the exception of the Li-ion battery electrolyte. The heat of combustion value for diethyl carbonate (DEC) was used as a representative estimate for electrolyte as it has been shown to be similar to other organic carbonate solvents typically found in Li-ion battery electrolyte [9]. The exact composition of the Li-ion battery electrolytes is unknown, therefore a variance of ±10% was assumed.

Table 2-3: Heat of combustions for test commodities.

Material	Chemical Heat of Combustion, kJ/g (BTU/lb)	Representative Material	Reference
Wood pallet	12.4 ± 0.3 (5,300 ± 130)	Red oak	[19]
Corrugated and paper board	14.4 ± 0.4 (6,200 ± 170)	Newspaper	[19]
Unexpanded plastic	27.5 ± 0.7 (11,800 ± 300)	Polystyrene	[19]
Electrolyte	20.9 ± 2 (9,000 ± 860)	Diethyl carbonate	[20]

2.4 Carton Combustion Parameters and Moisture Content

FM Global carefully controls the material properties of the corrugated board cartons used for construction of all standard cartoned commodities. Testing of the flammability characteristics is conducted with the fire propagation apparatus (FPA) [21]. Among the measurements are the thermal response parameter (TRP)[i] and time to ignition under different heat flux exposures [22]. Measurements for the carton material from the Li-ion batteries were within the benchmark values for the carton material used for FM Global's Class 2 standard commodity. Therefore, all commodities included in this

[i] TRP is a quantification of the ignition resistance of a material and relates the time to ignition to the net heat flux.

evaluation were expected to have a similar initial fire growth rate, before involvement of material contained within the cartons.

In addition, the commodity moisture content of the outer cartons was controlled to within 6.0% ± 2% on a dry basis for each test.

3. **Reduced-Commodity Test**

This section presents the results of the reduced-commodity fire test conducted to evaluate the relative flammability characteristics of the large-format 20 Ah Li-ion polymer pouch battery compared to FM Global's standard commodities and previously tested small-format Li-ion batteries [15].

3.1 Test Configuration

3.1.1 Overview

The test configuration was designed to capture the fire growth characteristics leading to sprinkler operation in a warehouse storage scenario. As shown in Figure 3-1, the array consisted of a three-tier-high, open-frame, single-row steel rack with overall dimensions of approximately 2.4 m long × 1.2 m wide × 4.3 m tall (8 ft × 3.25 ft × 14 ft). This array size was used to represent rack storage up to 4.6 m (15 ft), assuming nominally 1.5 m (5 ft) per tier.

The bottom tier of the array consisted of a non-combustible product (metal liner) supported on a wood pallet. The non-combustible product was constructed to maintain the FM Global standard 1.07 m × 1.07 m × 1.07 m (42 in. × 42 in. × 42 in.) commodity dimensions and representative airflow around the commodity. The upper two tiers consisted of pallets loads of cartoned Li-ion batteries also stacked to maintain the standard FM Global pallet load dimensions.

A summary of the pallet load design can be found in Section 2.2. The total chemical energy of the entire reduced-commodity test array is 21,000 ± 480 MJ, *i.e.,* four pallet loads of commodity plus two additional wood pallets under the first-tier non-combustible product (5,105 x 4 + 278 x 2 ≈ 21,000 MJ).

It should be noted that the pallet design for previous reduced-commodity testing only had test commodity lining the ignition flue of the test array [15]. The increased availability of test commodity for this project allowed for the entire pallet load to be comprised of cartoned Li-ion batteries. Increasing the quantity of batteries allows for greater lateral spread, thus longer duration for sprinkler operation predictions. No impact on the time of battery involvement is expected because battery involvement is predominantly due to the thermal exposure at the ignition flue, which does not change with additional commodity. Comparisons of peak heat release rate between tests should be avoided due to the discrepancy in quantity.

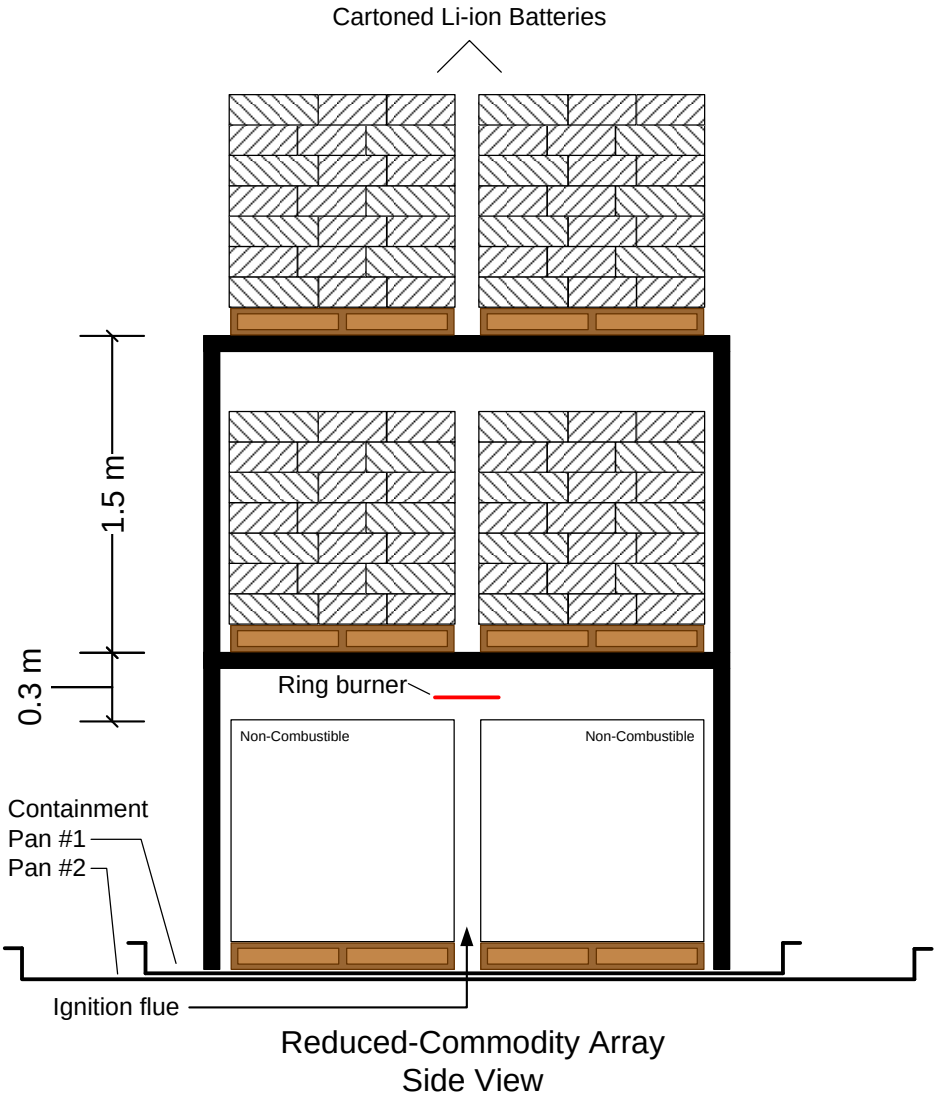

Figure 3-1: Elevation view of reduced-commodity test rack.

3.1.2 Ignition

Ignition was achieved with a 0.33 m (13 in.) diameter propane ring burner centered in the transverse flue 0.15 m (6 in.) below the second-tier test commodity, Figure 3-2. Propane was supplied at a rate of 30 L/min (1.06 ft^3/min), resulting in a nominal 45 kW (chemical) heat release rate, calculated as

$$\dot{q}_{C3H8} = \dot{v} \times \rho \times \Delta H_c.$$

Here $\dot{v}$ is the volume flow in m^3/s, ρ is the density of propane at 20°C (68°F) and 101.3 kPa (1 atm) with a value of 1.88 kg/m^3 (0.12 lb/ft^3), and ΔH_c is the net heat of complete combustion of propane with a value of 46.0 kJ/g.

All fire size estimates in this report include the contribution from the propane ring burner ignition source, which was constant for the test duration. The minimum measurable burner contribution was estimated as 20 kW (convective).

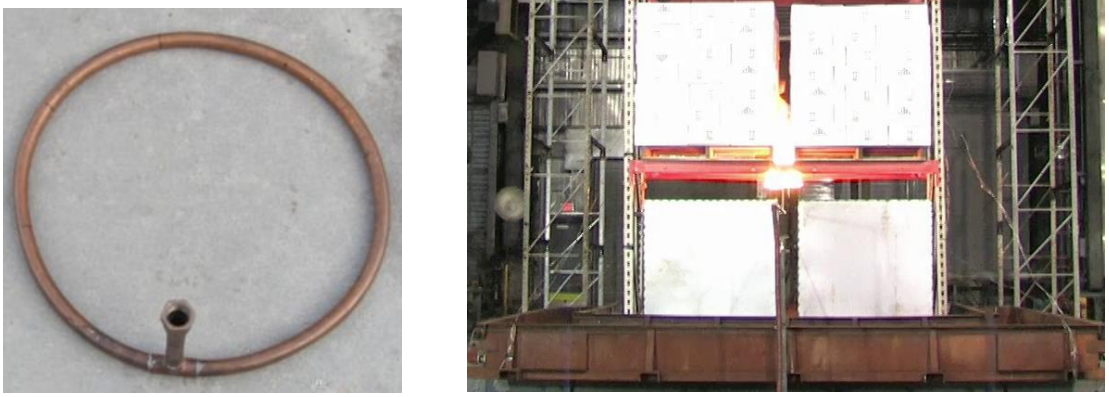

Figure 3-2: Propane ring burner (left) within the rack and fire size within rack (right).

3.2 Documentation and Instrumentation

Documentation for each test included video, still photography, and pertinent measurements necessary to evaluate product performance. All instrumentation was calibrated in accordance with ISO 17025 [23]. The following instrumentation was installed within the laboratory space and the exhaust duct for the 20-MW FPC:

- Environmental conditions, including relative humidity, dry-bulb temperature, and wet-bulb temperature of the air inside and outside of the lab, were measured just prior to each test as well as continually during each test with Vaisala HMT337 humidity and temperature transmitters. Units are located within the laboratory space at four points surrounding the test array and at one outdoor location near the air inlet to the laboratory.
- Convective flow within the FPC duct was measured with a Type K, bare-bead, 6.4 mm (0.252 in.) sheathed, chromel-alumel thermocouple and an impact tube averaging ring.
- Combustion gases within the FPC duct were measured with non-dispersive infrared (NDIR) CO and CO_2 gas analyzers to calculate the generation of carbon monoxide and carbon dioxide; a paramagnetic O_2 analyzer to measure depletion of oxygen; a flame ionization detector (FID) total hydrocarbon (THC) analyzer to measure the release of volatile organic compounds (VOC) as equivalent methane.
- A flow meter and metering valves monitored and controlled the propane flow to the ring burner.
- Twelve thermocouples were used to monitor internal heating of the commodity during the fire test. Each thermocouple was a Type K, grounded junction, 1.6 mm (0.625 in.) diameter, sheathed, chromel-alumel thermocouple. As shown in Figure 3-3, the thermocouples were located 150 mm (6 in.) in from the ignition flue between the third and fourth level of cartons on

both the second- and third-tier commodity. Horizontally, thermocouples were located at the midpoint of the pallet load and 150 mm (6 in.) from the outer edges.

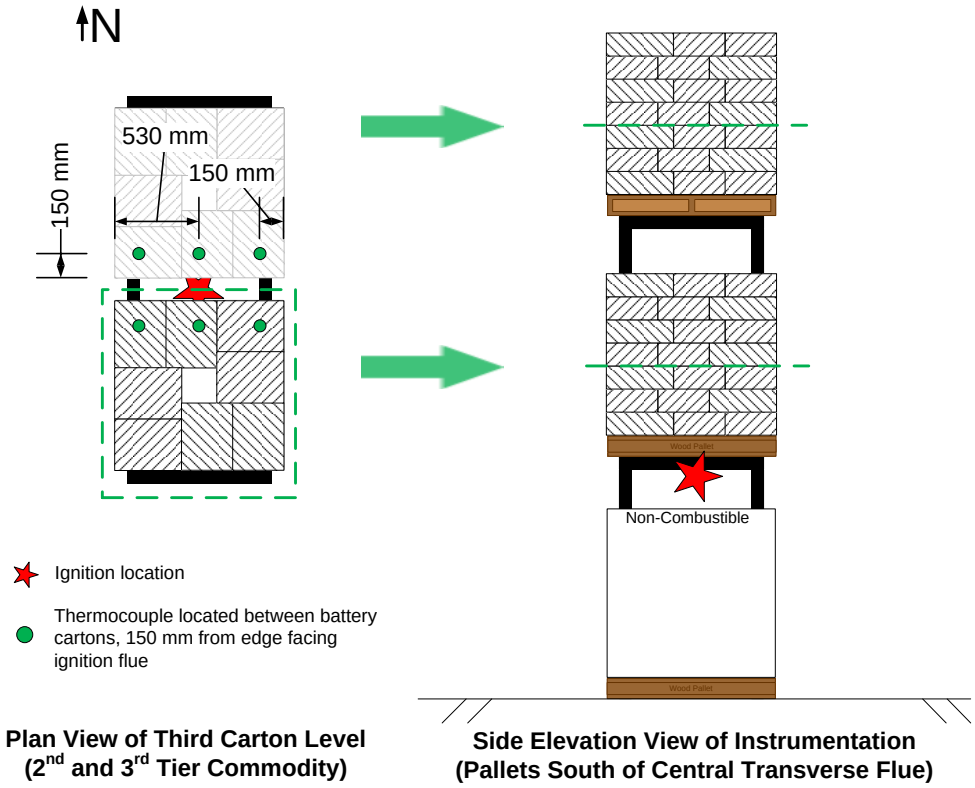

Figure 3-3: Thermocouple locations used during the reduced-commodity test.

The video data included two high-definition video cameras set at floor level, one high-definition camera elevated above the floor, and two infrared cameras (FLIR® T650sc long-wave IR (LWIR) and Bullard® T4MAX) for observation of the fire. A schematic of camera locations is shown in Figure 3-4.

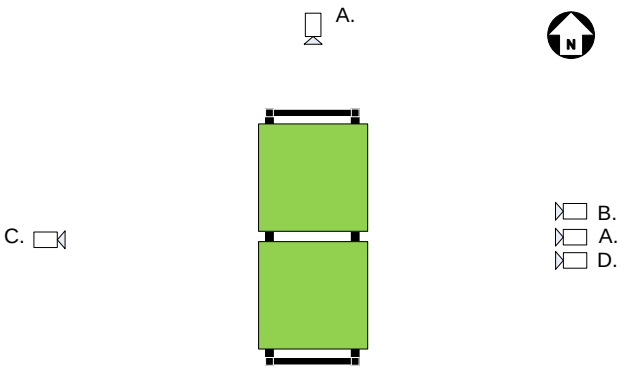

Figure 3-4: Plan view schematic of camera locations (not to scale).

3.3 Test Results

3.3.1 Heat Release Rate

The convective heat release rates, determined from the temperature rise of the gas flow in the FPC, is shown in Figure 3-5. Previous data from small-format Li-ion batteries and FM Global standard cartoned commodities are included as reference. To simplify the comparison, the time of each test has been slightly offset to align with the initial fire growth period of the 20 Ah polymer pouch battery. The data series for CUP and Class 2 commodities, and Li-ion battery packs, are truncated when the test material was largely consumed.

A close-up of the convective heat release rates is provided in Figure 3-6 to highlight the change in fire development that occurs once the cartons are breached and the contents become involved. The commodities are grouped based on their fire development, where materials that exhibit a fire development similar to CUP commodity are shown in the left figure and those similar to Class 2 commodity are shown in the right figure.

The 20 Ah polymer pouch battery exhibited a steady increase in the initial growth until a nominal peak value of 700 kW (convective) was achieved at 1 min (60 s). A delay in the fire growth was then observed as a temporary plateau in the heat release curve until 1 min 15 s (75 s). The fire intensity steadily increased to a value of 2,500 kW at 2 min 30 s (150 s) before exhibiting another temporary plateau until 3 min 10 s (190 s). The fire then increased to a value of 5,300 kW by 5 min 40 s (340 s) before a prolonged plateau until 9 min 30 s (570 s). Though not shown on Figure 3-5, the heat release rate increased to a maximum of 8,750 kW at 10 min 4 s (604 s), followed by a dip in the heat release until 13 min (780 s), before steadily declining as the combustible material was consumed. An estimated 10,300 ± 1,030 MJ (9,800 ± 980 BTU$\times 10^3$) of convective energy was released during the data collection portion (7,200 s total) of this test.

It should be noted that the convective heat release rate was used for this evaluation because it is relevant to determine sprinkler activation and the chemical heat release of a Li-ion battery cannot be accurately measured. The vent gases and combustion products of a Li-ion battery contain significant percentages of CO_2 and O_2 formed from the thermal degradation processes (pyrolysis rather than combustion) of the organic carbonates in the electrolyte. This form of CO_2 and O_2 production does not involve the same energy release of typical combustion processes and may lead to an over-prediction of the chemical heat release rate from carbon dioxide and oxygen consumption calorimetry [15].

Qualitatively, all commodities shown in Figure 3-5 exhibited a similar initial fire development as the flames spread vertically along the corrugated board cartons that lined the fuel space above ignition. After the initial fire development, the 20 Ah polymer pouch batteries exhibit an increased fire hazard compared to the small-format cylindrical and polymer Li-ion batteries, in terms of fire growth rate. The fire growth trend, however, is consistent with that of the power tool packs until the limited quantity of battery packs was consumed. Quantified values of fire growth rate leading to sprinkler operation can be found in Table 3-1.

Note: In Figure 3-5, “cylindrical” refers to the 18650 form factor batteries with a capacity of 2.6 Ah at 3.7 V; battery packs contained ten 18650 cylindrical batteries in a robust plastic casing. All small-format batteries were at a nominal 50% state-of-charge, consistent with their normal storage condition [15].

As highlighted in Figure 3-6, the 20 Ah polymer pouch batteries exhibit a fire growth similar to CUP commodity. It was previously established that the plateau in the heat release rate for CUP commodity occurred as the flames penetrated the cartons and the plastic cups stored within became involved in the fire [15]. For the 20 Ah polymer pouch batteries the subsequent increase in the heat release rate indicates involvement of the batteries and is further discussed in Section 3-5. In the case of the power tool packs, the heavy plastic cases of the battery pack dominated the fire hazard and there was no observable contribution from the batteries before the product was consumed.

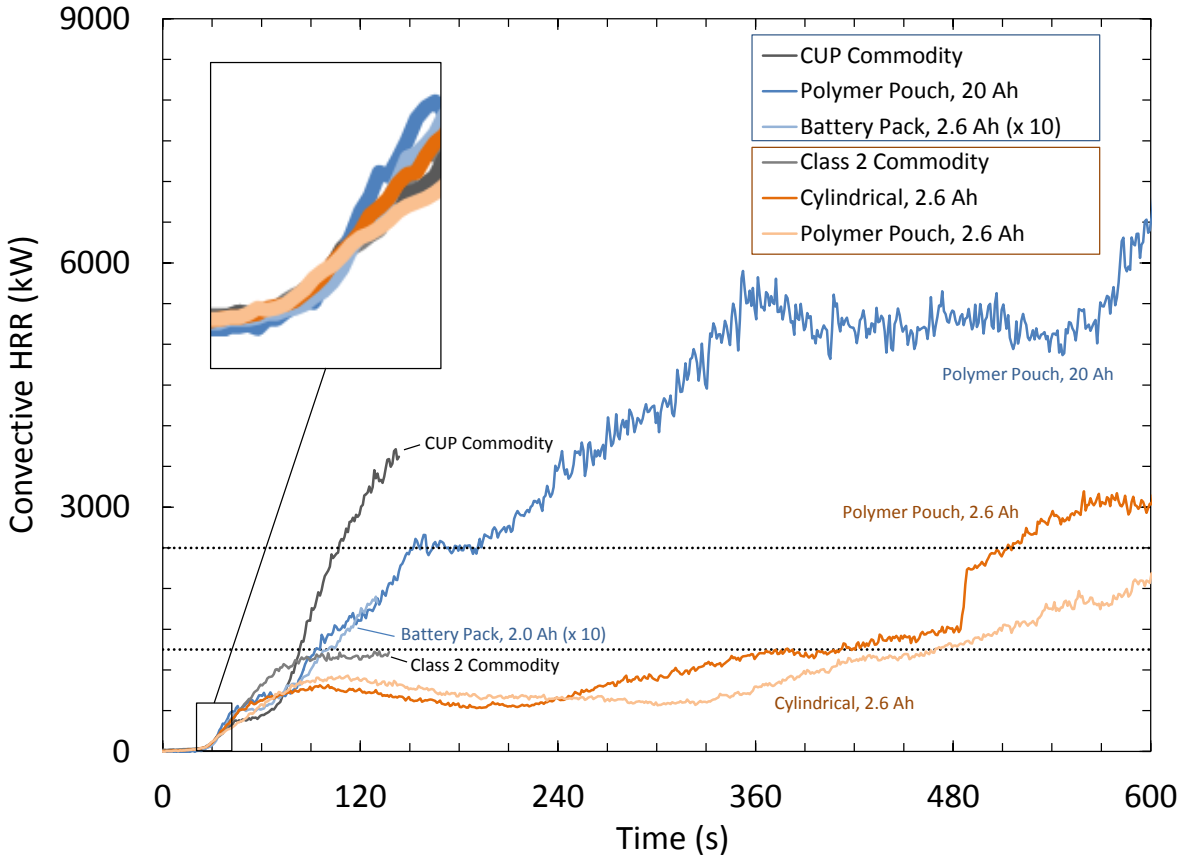

Figure 3-5: Convective heat release rates for 20 Ah polymer pouch battery and small-format Li-ion batteries and FM Global standard commodities. The time of each test has been slightly offset to align the initial fire growth period.

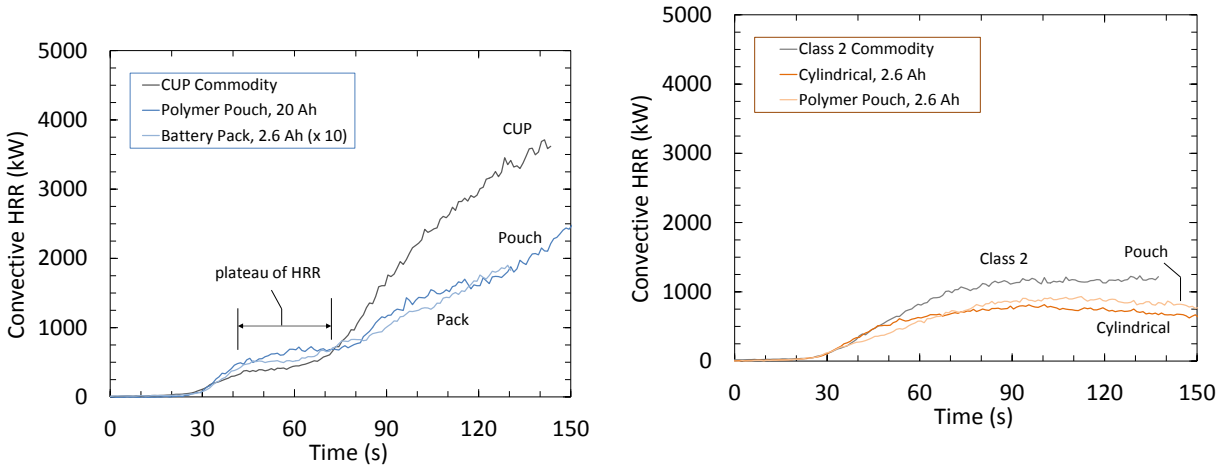

Figure 3-6: Close-up of convective heat release rates for FM Global standard commodities and Li-ion battery commodities; grouping based on similarity in growth curve.

3.3.2 Period of Flammability Characterization to Predict Sprinkler Response

Prediction of sprinkler operations resulting from the fire test should only occur during the period where fire damage was contained within the commodity of interest. For the purpose of this project, once the fire reached the extent of the combustible commodity the results could no longer be used to evaluate sprinkler response, since further fire propagation would not be possible.

It is important to note that additional information regarding the overall fire hazard of each commodity can be obtained after the period of flammability characterization. Evaluation of the time of significant battery involvement in the fire and the overall fire hazard from the quantity of commodity in each test are discussed in Section 3.3.4.

The three monitoring techniques for fire propagation are:

- Standard video cameras to monitor the location of flame attachment (Section 3.3.2.1)
- Thermocouples to monitor internal heating of the commodity (Section 3.3.2.2)
- Product collapse due to fire damage (Section 3.3.2.3)

Based on the combined techniques (*i.e.*, visual observation, internal heating, and commodity collapse), the period of flammability characterization to predict sprinkler operation times can extend to 2 min 30 s ± 5 s (150 ± 5 s) after ignition. This period extends beyond the 1 min 15 s ± 5 s (75 ± 5 s) established for previous results for FM Global standard cartoned commodities and small-format Li-ion batteries because of the additional quantity of test commodity used in the large-format battery test.

3.3.2.1 Flame Attachment (Standard Video Recording)

Figure 3-7 shows a photographic time evolution of the fire in 30 s increments after ignition of the propane burner. In can be seen that the fire was contained within the ignition flue at 30 s, with flames extending approximately 0.3 m (1 ft) above the array. At 1 min (60 s), flames had spread about one-third of the pallet width on the third tier. The fire then began to spread laterally on the third tier, reaching the

extents of the commodity by 2 min 20 s (150 s). Lateral spread along the second-tier commodity began at 3 min (180 s) after ignition.

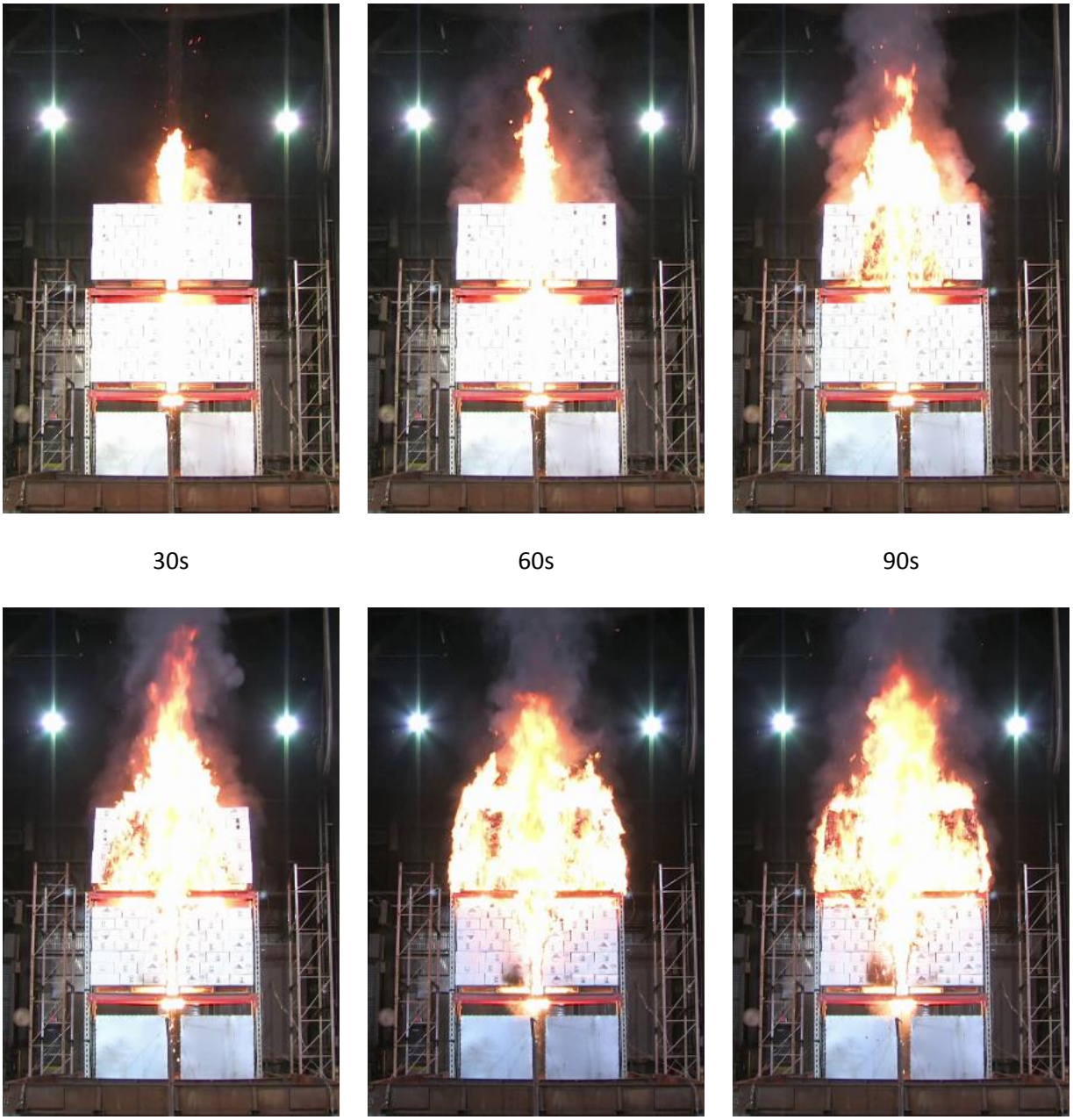

Figure 3-7: Test images shown in 30 s increments from ignition for the large-format polymer pouch batteries.

3.3.2.2 Internal Heat of Commodity (Thermocouples)

Internal heating of the commodity was measured with thermocouples located between battery cartons 150 mm (6 in.) in from the ignition flue. As detailed in Section 3.2, the thermocouples were located between the third and fourth level of cartons on both the second- and third-tier commodity. Horizontally, thermocouples were located at the midpoint of the pallet load and 150 mm (6 in.) from the outer edges.

Figure 3-8 presents the thermocouple measurements acquired during the fire test. The convective heat release rate is included for reference to the time evolvement of the fire. The threshold temperature of 180°C (356°F) was added based on the oxidation temperature of electrolyte that results in a high-rate runaway reaction (peak rates > 100°C/min) [9]. A legend is provided to describe the thermocouple location within the test array. Notable data series are additionally labeled using the following convention: tier 2 or tier 3 (T2/3), north or south pallet load (N/S), and horizontal position of West, center, or East (W/C/E). For example, T3-S-C references the thermocouple located at the center of the third-tier pallet load on the south side of the rack.

For this test, the threshold temperature was first exceeded by the thermocouple on tier 3, South pallet load, center location (T3-S-C) at 2 min 53 s (173 s) after ignition. Exceedance of the threshold temperature is only one measure of the potential for battery involvement. Since the thermocouples are located between the cartons, not directly connected to the batteries, high temperatures could also occur due to involvement of the cartons or plastic dividers.

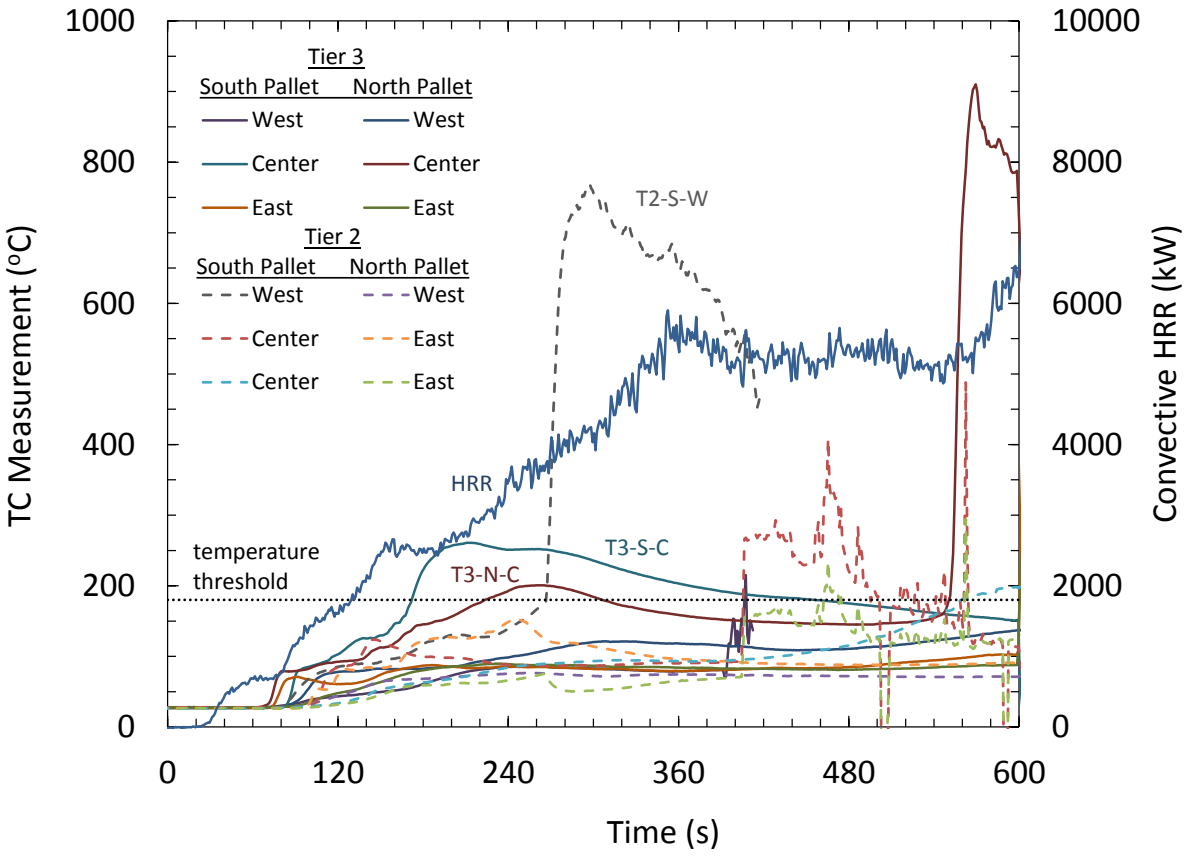

Figure 3-8: Internal heating of commodity using TCs located within the test commodity.

3.3.2.3 Commodity Collapse

Collapse of commodity due to fire damage is common in all rack storage tests and does not impact the validity of the test. In the previous reduced-commodity tests with small-format Li-ion batteries, collapse could significantly impact the fire development because the non-combustible portion of the pallet load might be exposed [15]. This concern does not exist in the present study, where the entire pallet load was comprised of Li-ion batteries. However, for comparison to the previous battery tests, collapse should not occur during the period where sprinkler predictions are made. It was assumed that major collapse, visually estimated as greater than 10% of the overall quantity of Li-ion batteries, was sufficient to impact the fire development. All other commodity collapse was considered minor.

During the 20 Ah polymer pouch battery test, individual batteries began falling from the third tier of the array sporadically at 3 min 48 s (228 s). A major collapse of commodity occurred at 7 min 15 s (435 s) after ignition, followed by sporadic minor collapses. A catastrophic failure of the rack beam supporting the third tier commodity occurred at 9 min 56 s (596 s), resulting in complete collapse of the commodity. Based on these observations, collapse impacting the fire development (*i.e.*, greater than 10% of available batteries) occurred at 9 min 56 s (596 s) after ignition.

3.3.3 Predicted Sprinkler Response

All sprinkler responses were calculated using the method described in Reference [15] and are based on the convective heat release rates from ignition, which are illustrated in Figure 3-5. Figure 3-9 provides the results of the predicted response of a quick-response sprinkler where the ceiling height was set to 9.1 m (30 ft) above the floor (*i.e.,* 4.9 m (16 ft) above the array). The fire growth rate was calculated as a 10 s linear trend of the convective fire size leading up to link operation.

Table 3-1 contains complete sprinkler response calculations for quick-response sprinklers, having an RTI of 27.6 $(m\text{-}s)^{1/2}$ (50 $(ft\text{-}s)^{1/2}$), with ceiling heights between 7.6 m and 12.2 m (25 ft and 40 ft) where the storage array was nominally 4.6 m (15 ft) high. Corresponding values for small-format Li-ion batteries and FM Global standard commodities are provided from Reference [15]. It should be noted that fire growth rates nominally within a factor of two and $\dot{Q}_{be}$ values nominally within 30% of the average are considered equivalent.

For a ceiling height of 7.6 m (25 ft), the predetermined sprinkler operation temperature of 74°C (165°F) was reached at 37 s after ignition for the 20 Ah polymer pouch test. The corresponding convective fire size at link operation, $\dot{Q}_{be}$, was 335 kW and the fire growth rate was 33 kW/s. Increasing the ceiling height to 9.1 m (30 ft) resulted in a predicted link operation time of 41 s, $\dot{Q}_{be}$ value of 480 kW, and a fire growth rate of 34 kW/s.

In comparison to previously tested small-format Li-ion batteries, the 20 Ah polymer pouch batteries exhibited similar flammability characteristics ($\dot{Q}_{be}$ and fire growth rate) at the time of sprinkler operation. When compared to FM Global standard commodities (both Class 2 and CUP), the 20 Ah polymer pouch batteries tended to display slightly higher flammability characteristics at the time of sprinkler operation.

Using full-pallet loads of batteries allowed for the prediction of sprinkler operations under greater ceiling heights than the previous testing, as discussed in Section 3.1. As a result, Table 3-1 includes sprinkler response calculations for 10.7 m and 12.2 m (35 ft and 40 ft) ceilings. The predicted link operation times were 48 s for a 10.7 m (35 ft) ceiling and 58 s for a 12.2 m (40 ft) ceiling. The corresponding $\dot{Q}_{be}$ values were 549 kW and 688 kW, and fire growth rates were 15 kW/s and 11 kW/s, respectively. The notable decrease in the fire growth rate (at sprinkler operation) compared to calculations at 7.6 m and 9.1 m (25 ft and 30 ft) ceilings is a result of the predicted sprinkler operation during the plateau portion of the heat release rate, which can be seen in Figure 3-9 around 1 min (60 s).

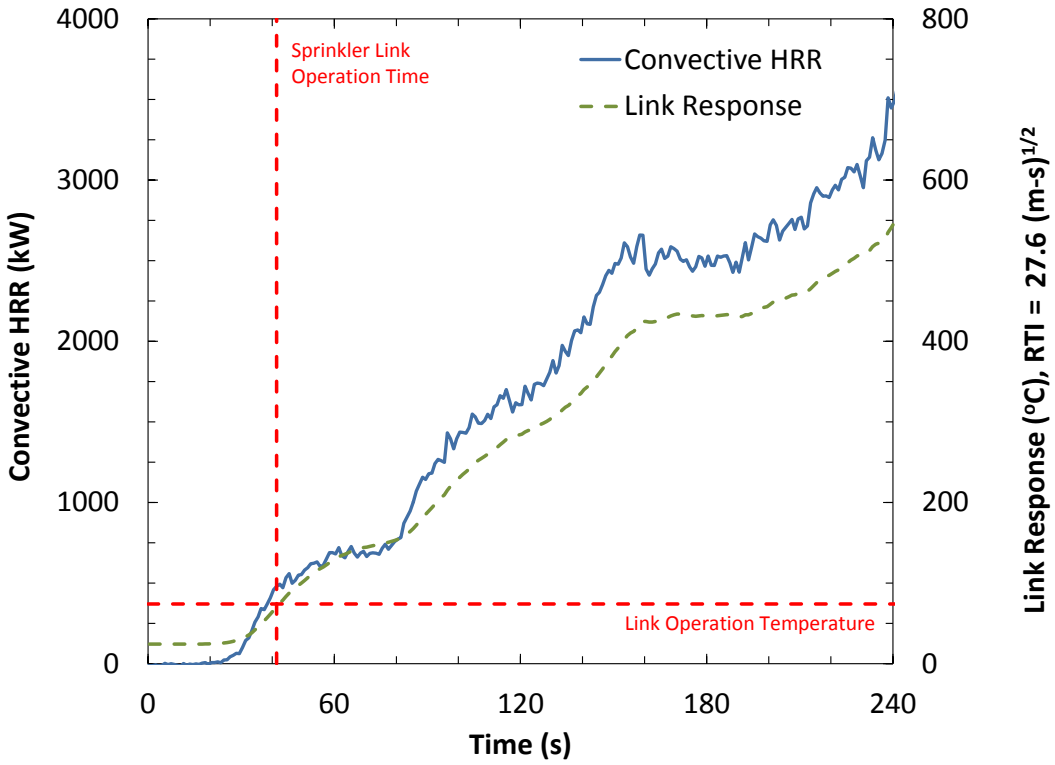

Figure 3-9: Example of sprinkler link response during 20 Ah polymer pouch test; quick-response sprinkler with a 74°C (165°F) temperature rating below a 9.1 m (30 ft) ceiling.

Table 3-1: Predicted operation times for quick-response sprinklers with a link temperature rating of 74°C (165°F) at multiple ceiling heights.

Predicted Sprinkler Response	Ceiling Height = 7.6 m (25 ft)		
	Link Operation (s)	Q_{be} kW	Fire Growth (kW/s)
Li-ion, 20 Ah Polymer Pouch	37	335	33
Li-ion, small-format†	43	270	20
Class 2	59	209	15
CUP	43	232	16
Ceiling Height = 9.1 (30 ft)			
Li-ion, 20 Ah Polymer Pouch	41	480	34
Li-ion, small-format†	77	388	18
Class 2	65	367	24
CUP	52	321	11
Ceiling Height = 10.7 m (35 ft)			
Li-ion, 20 Ah Polymer Pouch	48	549	15
Ceiling Height = 12.2 (40 ft)			
Li-ion, 20 Ah Polymer Pouch	58	688	11

† Represented as the average of the values from the small-format 2.6 Ah cylindrical and polymer battery tests found in Reference [15].

3.3.4 Time of Battery Involvement

For the purpose of this study, battery involvement references the time during the fire development when the batteries are observed to contribute significantly to the fire severity. In a warehouse storage fire scenario, the determination of battery involvement is complicated by the large quantities of combustible packaging components that comprise the test commodities, *i.e.*, wood pallets, plastic dividers, and cartons. By accounting for the contribution of the packaging, it is reasonable to attribute any excess energy release to the combustion of Li-ion batteries.

Figures 3-10 presents the convective heat release rate measured during the early growth portion of the fire. The convective heat release rates for FM Global standard Class 2 and CUP commodities are included for reference. Following the approach used for testing of small-format Li-ion batteries [15], lower and upper threshold values represent the range of time when the batteries became significantly involved in the fire.

The lower threshold value represents the steady-state heat release of FM Global standard Class 2 commodity of 1,250 kW. Exceedance of this threshold value provides a conservative estimate of the contribution to the overall fire severity from the contents stored within the cartons. Before this time, the heat release rate can be attributed solely to the combustion of carton material. As shown in Figure 3-10, the convective HRR for the Li-ion batteries exceeded the lower threshold value at approximately 1 min 30 s (90 s) after ignition.

The time of battery involvement can also be estimated at a later stage in the fire development. As discussed in Section 3-10, suppression tests have shown that the plastic dividers contribute to the fire before the batteries become involved. Thus the increase of the convective HRR that occurs before the plateau at approximately 2 min 30 s (150 s) can be (at least partially) attributed to the plastic dividers. Subsequent exceedance of the upper threshold value at 3 min (180 s) corresponds to the latest time after ignition that the Li-ion batteries are not significantly contributing to the fire severity.

Using the lower and upper threshold values, the time of significant involvement of the 20 Ah polymer pouch battery is estimated to occur between ~ 1 min 30 s (90 s) and ~ 3 min 15 s (195 s) after ignition. Taking the average of these values and rounding to the nearest 30 s increment results in a nominal time of battery involvement of 2 min 30 s (150 s), under free-burn conditions. Before this time, the heat release rate can be attributed to the combustion of packaging components. In comparison, the previously tested small-format Li-ion batteries became involved in the fire significantly later at an estimated 5 min (300 s) after ignition. Thus, the current battery represents a higher hazard commodity based on the flammability characteristics leading to first sprinkler operation and time of battery involvement in the fire.

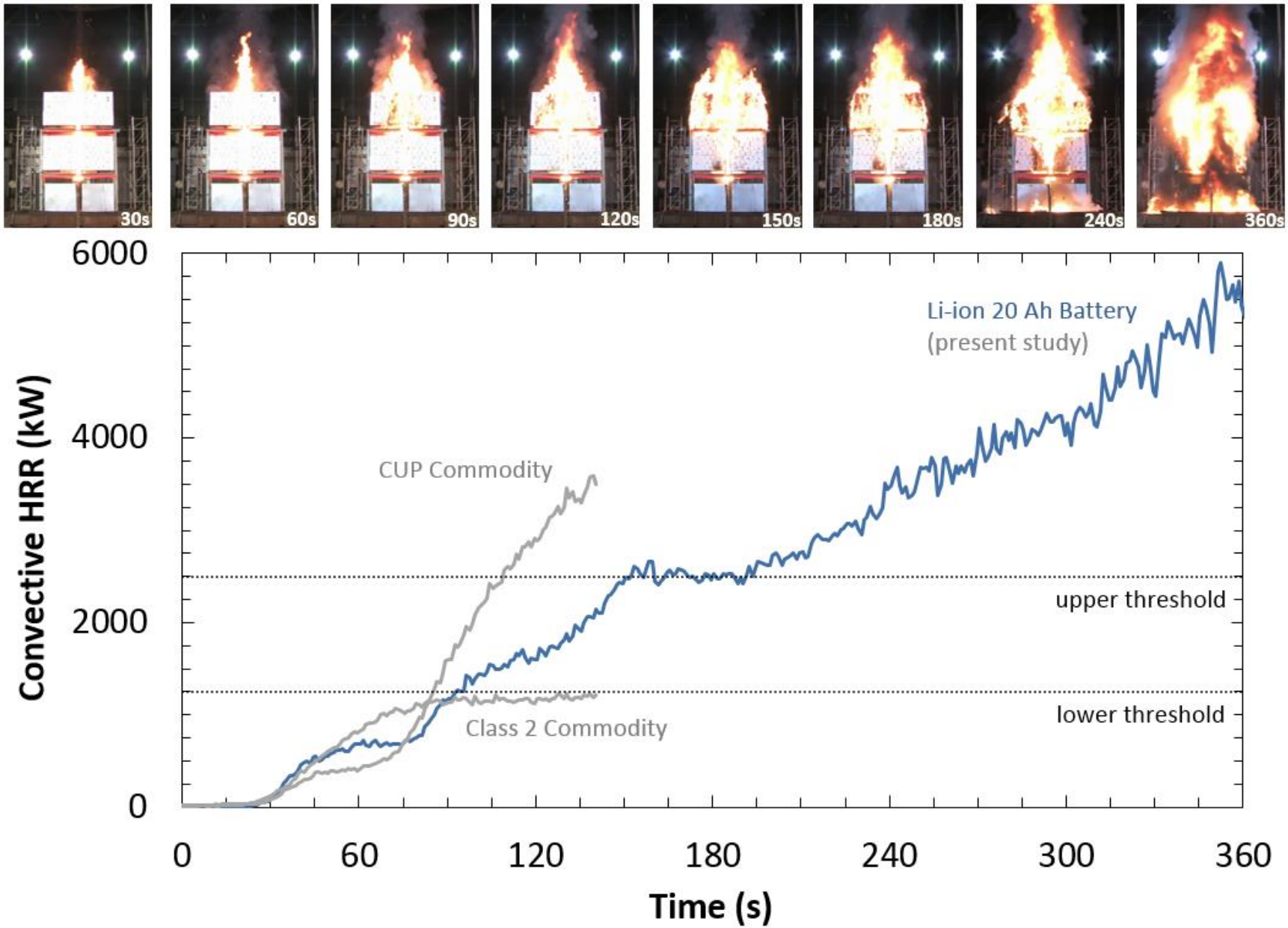

Figure 3-10: Determination of the time of battery involvement.

4. **Large-Scale Fire Test**

This section describes the large-scale sprinklered fire test conducted to determine automatic sprinkler fire protection guidance for warehouse storage of cartoned Li-ion batteries. As discussed in Section 3, the large-format 20 Ah Li-ion polymer pouch battery used in the present study represents a greater hazard than previously tested small-format Li-ion batteries in cartoned warehouse storage [15]. As a result, protection guidance established from the large-scale test can be applied to the small-format cylindrical and polymer Li-ion batteries evaluated during this multi-phase project.

4.1 Test Overview

Figure 4-1 presents a photo of the large-scale test array and Figure 4-2 presents an overview schematic of the array and sprinkler layout. The main fuel array consisted of a three-pallet-load-high open-frame, double-row steel rack under a 12.2 m (40 ft) ceiling. This array size represents rack storage up to 4.6 m (15 ft). The main array measured approximately 7.3 m long × 2.3 m (24 ft × 7.5 ft) wide in a 6 × 2 pallet load arrangement, and included 24 pallet loads of Li-ion battery commodity. The end pallet of each row consisted of FM Global standard cartoned unexpanded plastic (CUP) commodity [24]. A single-row target array containing four pallet loads of the CUP commodity was located across a 1.2 m (4 ft) aisle on either side of the main array. Overall, the target arrays measured approximately 4.9 m × 3.0 m (16 ft × 3 ft). Using the pallet load design, described in Section 2.2, this test included 26,880 batteries packaged in 1,344 cartons.

Figure 4-1: Photo of large-scale test main array, before constructing the target array.

Note that the 24 pallet loads of batteries available for this project were less than the 72 pallet loads of commodity used in a standard three-tier-high large-scale test. In a standard test, the main and target arrays consist of an 8 × 2 and 6 × 2 pallet load arrangement, respectively [25, 26]. As a result, the allowable extent of fire spread for the battery test is less than a standard test because the fire must be contained within the extent of the test commodity. Further details on the evaluation criteria can be found in Section 4.5.

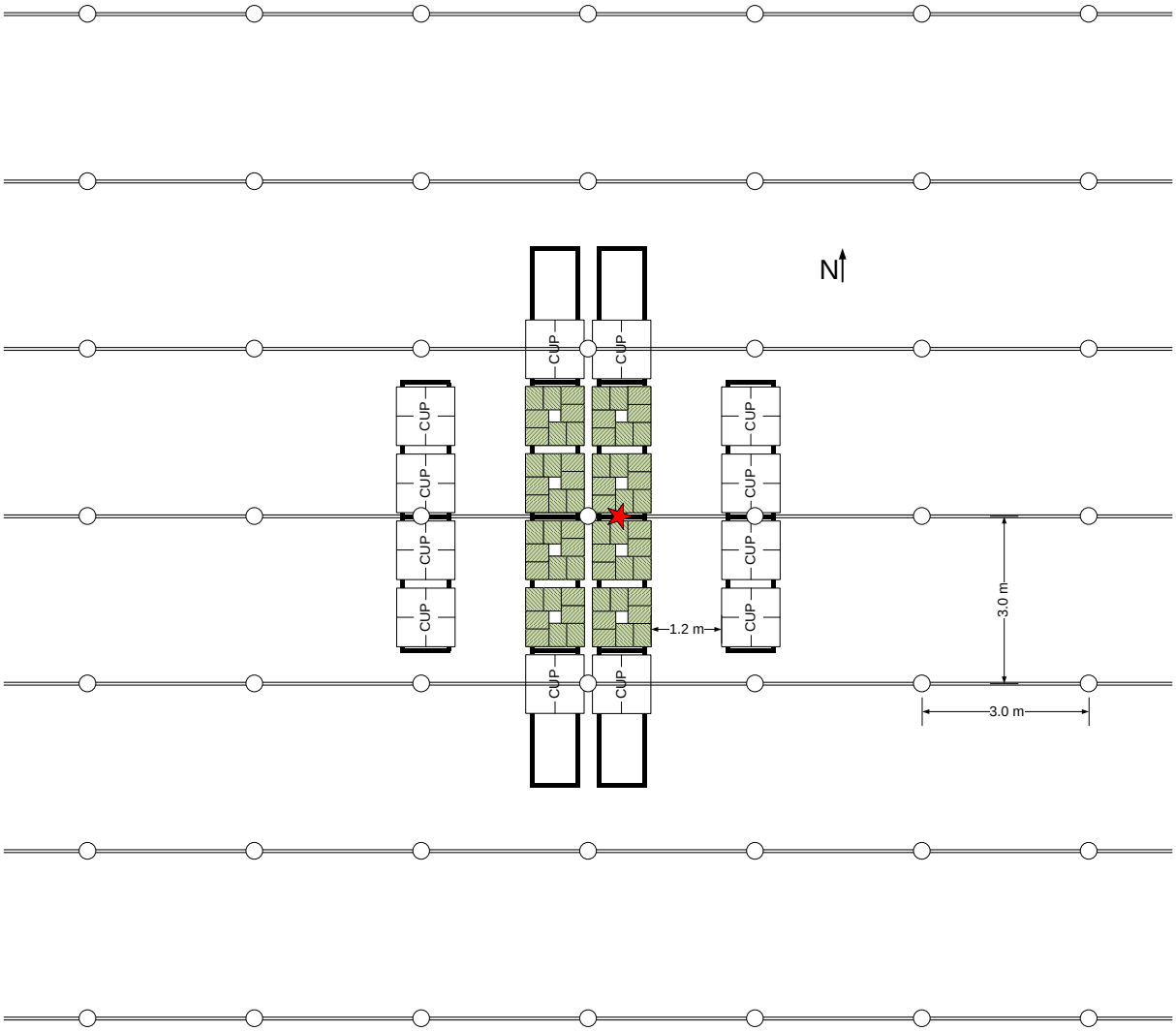

Figure 4-2: Plan view of large-scale test array. Li-ion battery commodity is shown as green cartons. Open circles represent the location of ceiling-level sprinklers. Ignition location at the base of the array is shown as a red star.

4.2 Automatic Sprinkler Protection

Ceiling-level sprinkler protection was provided by an FM Approved sprinkler with a K-factor of 320 L/min/bar^{½} (22.4 gpm/psi^{½}). The sprinkler was of pendent type, with a 74°C (165°F) temperature rating and a nominal RTI of 27.6 m^{½}s^{½} (50 ft^{½}s^{½}). A nominal operating pressure of 2.4 bar (35 psig) provided a discharge of 500 L/min (133 gpm) per sprinkler, resulting in a 53 mm/min (1.3 gpm/ft^2) water density.

Sprinklers were located on 3.0 m × 3.0 m (10 ft × 10 ft) spacing. In accordance with FM Global Property Loss Prevention Data Sheet 2-0, *Installation Guidelines for Automatic Sprinklers* [27], each sprinkler was installed with the heat-sensing link 0.43 m (17 in.) below the ceiling and was oriented with the sprinkler frame arms parallel to the sprinkler pipe. Consistent with FM Global standard procedures for a large-scale fire test, each the sprinkler's heat-sensing link was facing towards the north.

4.3 Ignition

Ignition was achieved with two FM Global standard half igniters, which are 76 mm x 76 mm (3 in. x 3 in.) cylinders of rolled cellu-cotton. Each igniter is soaked in 118 ml (4 oz.) of gasoline and sealed in a plastic bag, Figure 4-3. The igniters were placed in an offset ignition orientation, 0.6 m (2 ft) east of center, in the center transverse flue, between the uprights, of the eastern row of the main array. The igniters were lit with a flaming propane torch at the start of each test and the fires were allowed to develop naturally.

Figure 4-3: Igniter locations within the rack, located at the rack uprights. (representative image shown)

4.4 Documentation and Instrumentation

Documentation for each test included video, still photography, and pertinent measurements necessary to evaluate sprinkler performance. All instrumentation was calibrated in accordance with ISO 17025 [23].

Environmental conditions, including relative humidity, dry-bulb temperature, and wet-bulb temperature of the air inside and outside of the lab, were measured just prior to the test as well as continuously during the test. In addition, the following standard instrumentation was installed:

- Sprinkler protection was provided at 49 locations at the ceiling. Each sprinkler had its operating mechanism included in an electric circuit to determine operation times.
- Bare-bead, 0.8 mm (20-gage), chromel-alumel thermocouples, placed 165 mm (6-1/2 in.) below the ceiling at 125 locations. These thermocouples have been shown to have a response time index (RTI) of 8 ± 1 $m^{1/2}s^{1/2}$ (14.5 ± 1.8 $ft^{1/2}s^{1/2}$).

- Bi-directional probes to measure ceiling jet velocity immediately below the ceiling. Probes were located at four orthogonal locations with radial distances from the ceiling center of 2.1 m and 4.0 m (7 ft and 13 ft) [at 0.12 m (0.4 ft) below the ceiling], and 10.4 m (34 ft) [at 0.46 m (1.5 ft) below the ceiling]. These measurements are available for future analysis but are not discussed in this report.
- Thermocouples imbedded in a cross-shaped steel angle, made from two 51 mm wide x 610 mm long x 6 mm thick (2 in. x 24 in. x 0.25 in.) angle iron segments, attached to the center of the ceiling. Measurements from these thermocouples are referred to as steel temperatures.
- Flow meters and pressure controllers to monitor and control the sprinkler system.
- Combustion gases within the FPC duct were measured with non-dispersive infrared (NDIR) CO and CO_2 gas analyzers to measure the generation of carbon monoxide and carbon dioxide; a paramagnetic O_2 analyzer to measure depletion of oxygen; a flame ionization detector (FID) total hydrocarbon (THC) analyzer to measure the release of volatile organic compounds (VOC) as equivalent methane. THC measurements are available for future analysis but are not discussed in this report.

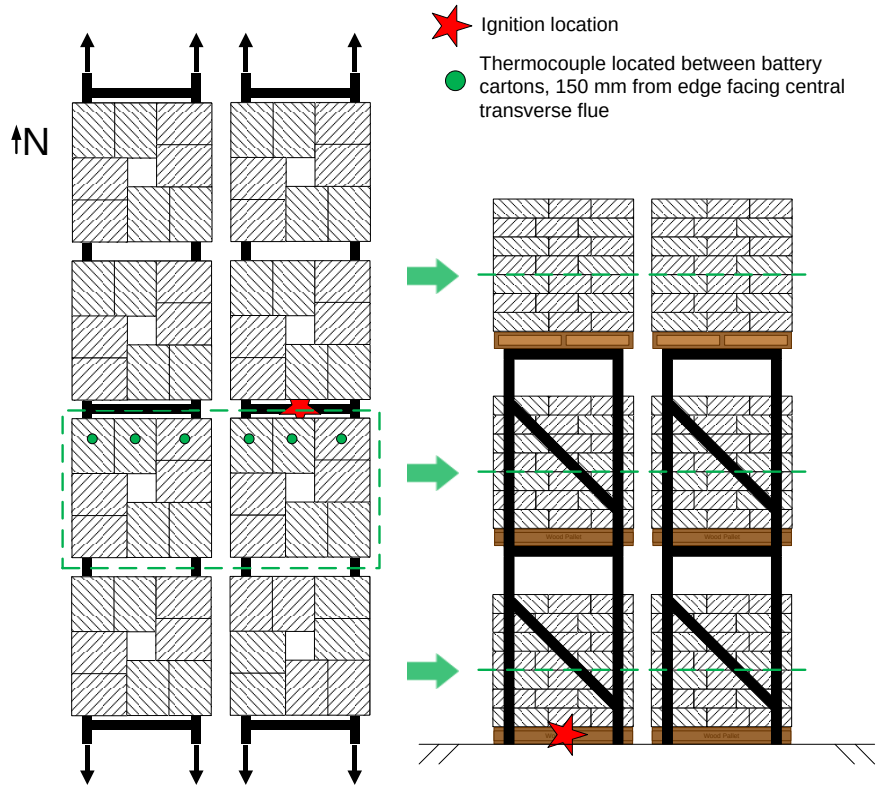

Figure 4-4: Thermocouple locations used during the large-scale test.

- Eighteen thermocouples were used to monitor internal heating of the commodity during the fire test. Each thermocouple was a Type K, grounded junction, 1.6 mm (0.625 in.) diameter, sheathed, chromel-alumel thermocouple. The thermocouples were located 150 mm (6 in.) in

from the ignition flue between the third and fourth level of cartons on all three tiers of the commodity. Horizontally, thermocouples were located at the midpoint of the pallet load and 150 mm (6 in.) from the outer edges. An illustration of the thermocouple placement can be found in Figure 4-4.

The video data included two high-definition video cameras located at the floor level, one high-definition camera elevated above the floor, and two infrared cameras (FLIR® T655 long-wave IR (LWIR) and Bullard® T4MAX) for observation of the fire. A schematic of each camera location is shown in Figure 4-5.

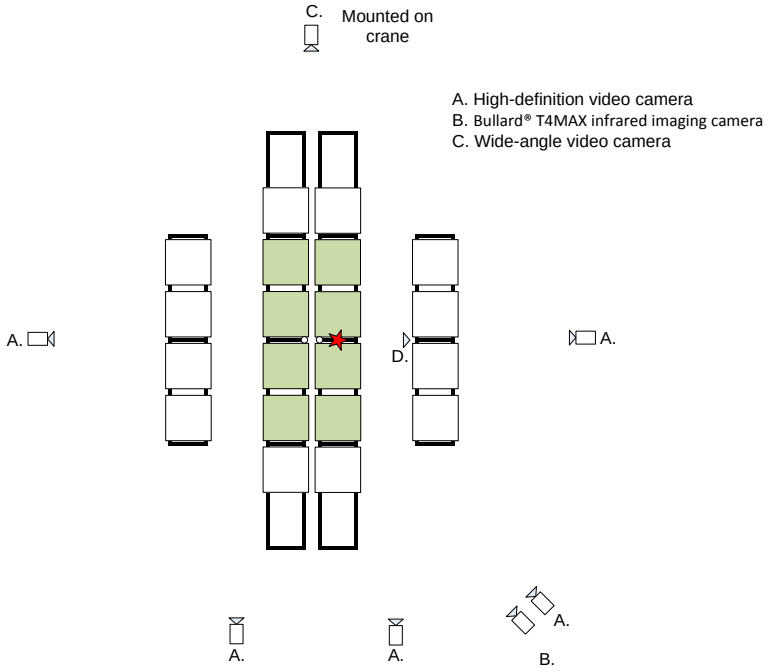

Figure 4-5: Plan view schematic of camera locations (not to scale).

4.5 Evaluation Criteria

Assessment of the sprinkler protection performance was based on its ability to efficiently suppress the test fire. The primary judgment criteria are the number of sprinkler operations, the extent of fire damage, and the magnitude and duration of ceiling steel temperatures.

1) Sprinkler operations. Since this is a unique test configuration, there is no specified number of acceptable sprinkler operations. However, excessive sprinklers along the perimeter of the test ceiling would constitute a failure. Sprinklers operating at the ceiling perimeter would indicate the presence of high-temperature gases at the edge of the ceiling that could have traveled further along the ceiling, operating additional sprinklers, had they been present.

2) Extent of fire spread. Fire damage should be largely confined to the commodity surrounding the central transverse flue (*i.e.*, ignition flue), the fire should not propagate into the CUP commodity capping the array, and there should be no fire spread across the aisle to the target array.

3) Steel TC measurements. The maximum allowable ceiling steel temperature measurement is 538°C (1,000°F). This criterion is based on the assessment that structural steel loses 50-60

percent of its load-bearing strength upon reaching the 538°C (1,000°F) threshold [28, 29]. The loss of strength could cause failure of the ceiling structure resulting in collapse of the roof. Values in excess of these thresholds during a test are taken as an indication of ineffective fire protection.

4.6 Test Results and Data Analysis

A summary of the test conditions and results is shown in Table 4-1. A single sprinkler operated at 1 min 30 s (90 s) after ignition and suppressed the fire. Fire damage remained within the confines of the array and there was no jump to the target commodity. The results in terms of fire damage, steel temperatures, and number of sprinkler operations were within levels specified in Section 4.5 indicating that the sprinkler system provided adequate protection.

Table 4-1: Large-scale fire test setup summary

Test Configuration and Results	**Value**
Test Configuration	
Commodity	Cartoned 20 Ah Li-ion batteries
Main array dimensions [pallet loads]	6 x 2 x 3
Target array dimensions [pallet loads]	4 x 1 x 3
Flue width, nominal [m (ft)]	0.15 (0.5)
Aisle width [m (ft)]	1.2 (4)
Storage height [m (ft)]	4.6 (15)
Ceiling height [m (ft)]	12.2 (40)
Main array located below - number of sprinklers	1
Ignition location relative to rack	offset
Sprinkler response, nominal [RTI, $m^{1/2}s^{1/2}$ ($ft^{1/2}s^{1/2}$)]	27.6 (50)
Sprinkler rating [°C (°F)]	74 (165)
Sprinkler K-factor [L/min/$bar^{1/2}$ (gpm/$psi^{1/2}$)]	53 (22.4)
Sprinkler discharge pressure [bar (psi)]	2.4 (35)
Sprinkler spacing [m × m (ft × ft)]	3 × 3 (10 × 10)
Test Results	
Sprinkler Operations	1
Total Chemical Energy Released [MJ (BTU x 10^3)]	100 ± 5 (90 ± 5)
Consumed Commodity [pallet load equivalent]	< 1
Target Jump (west only) @ Time [min:s]	No
Maximum Steel Temperature [°C (°F)] @ Time [min:s]	32°C (90°F) @ 1 min 30 s
Test Termination [min:s]	40:00

4.6.1 Test Images

From the fire test images shown in Figures 4-6 and 4-7 it can be seen that the fire within the central transverse flue reached the top of the array by 30 s after ignition. The fire continued to grow and at 1 min (60 s) flames extended approximately 1.5 m (5 ft) above the array. The sprinkler centered over the main array operated at 1 min 30 s (90 s) as flames were spreading across the aisle face of the commodity on the second and third tier, as well as across the longitudinal flue. By 2 min (120 s) the fire was contained within the array, though involvement of the commodity on either side of the central transverse flue on the first and second tiers persisted until approximately 2 min 30 s (150 s). The test was conducted for 40 min (2,400 s) and required only minimal manual firefighter intervention to extinguish a few lingering deep-seated flames.

The extent of damage to the test array is shown in Figure 4-8. All three tiers of commodity surrounding ignition in the central transverse flues were heavily damaged. The top left image shows the damage sustained to the east (aisle) face of the main array. The top right image shows the corresponding damage to the commodity across the longitudinal flue after the east commodity was removed. In both images, a portion of the cartons was charred or consumed allowing involvement of the internal plastic dividers and batteries in the fire. Examples of the damage sustained by the commodity on either side of the central transverse flue, adjacent to ignition, are shown in the bottom right image for the first tier and bottom left image for the second tier.

0 min 30 s (30 s)

1 min 0 s (60 s)

1 min 30 s (90 s)

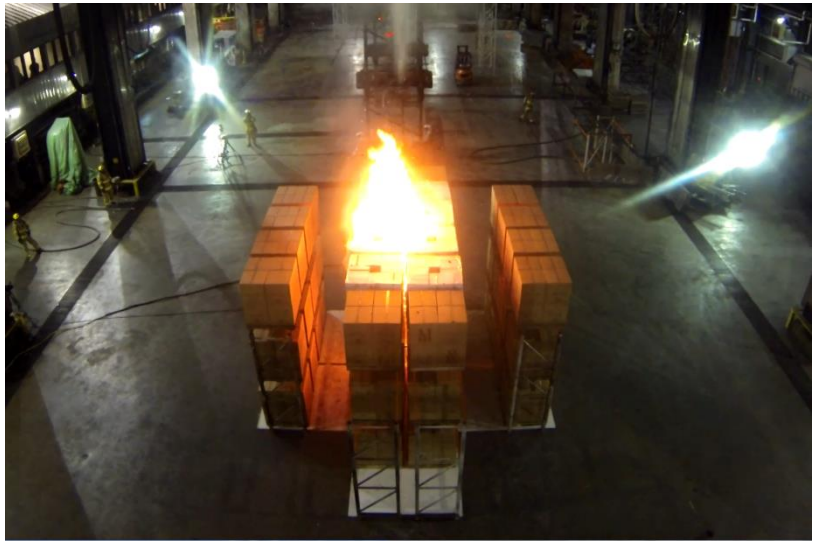

1 min 30 s (90 s)

Figure 4-6: Images of large-scale fire test.

~ 2 min (120 s)

~ 2 min 30 s (150 s)

> 6 min (360 s)

Figure 4-7: Images of large-scale fire test (continued).

East (aisle) face of main array

Commodity across longitudinal flue

First tier ignition flue

Pallet load from second tier ignition flue

Figure 4-8: Post-test images showing extent of damage to test commodity.

4.6.2 Sprinkler Operations and Area of Commodity Damage

A plan view of the sprinkler operation pattern is presented in Figure 4-9. A single sprinkler, centered over the main array, operated at 1 min 30 s (90 s) and suppressed the fire. The approximate extent of commodity damage is shown in the figure by the shaded areas. Damage was primarily limited to the ignition flue with some lateral fire spread along the sides of the pallet loads facing the longitudinal flue and the aisle space. Charring of the cartons facing the open inner core of the pallet loads on the second and third tiers was also observed.

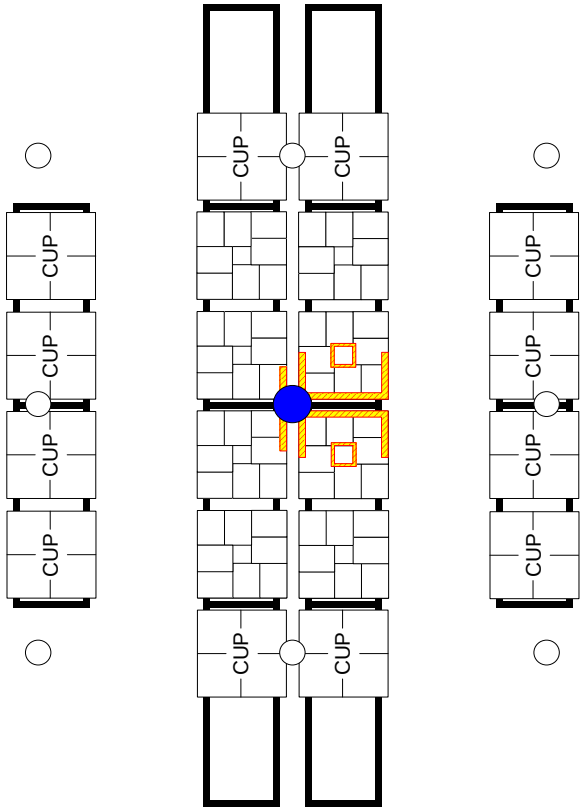

Figure 4-9: Sprinkler operation pattern and commodity damage.

4.6.3 Energy Release

Figure 4-10 presents the convective heat release rate and total integrated chemical energy produced during the large-scale test. The convective heat release rate was estimated by applying the ceiling gas temperature measurements made immediately below the fire test ceiling to fire plume and ceiling layer correlations [30]. While not as accurate as the measurements made with the FPC for the Reduced-Commodity test (Section 3.3.1), the estimated convective HRR provides a reasonable approximation of the real-time fire development up to sprinkler operation. Convective measurements can be significantly impacted by cooling from a sprinkler discharge and therefore may not reflect the heating condition within the test array. For example, cooling of the fire plume gases above the test array or wetting of thermocouples used to measure ceiling gas temperatures can occur even though the fire is still present

within the array. Total energy was calculated from the generation rates of carbon dioxide and carbon monoxide[12] during the test and the measurement was therefore not affected by sprinkler operation. Also, since the majority of consumed materials in this test were ordinary combustibles, the errors associated with burning Li-ion batteries in Section 3.3.1 are not a significant factor in this case. It should be noted that chemical energy was measured within the exhaust duct located well above the movable fire test ceiling and is therefore significantly delayed and smeared compared to the actual fire development. For error analysis, it was assumed that the total energy up to test termination has ± 10% error. The estimated total energy released was 100 ± 5 MJ (90 ± 5 BTU x 10^3) or the equivalent of less than one pallet load of batteries, as listed in Section 2.2 Data were acquired for the 40-minute duration of the test.

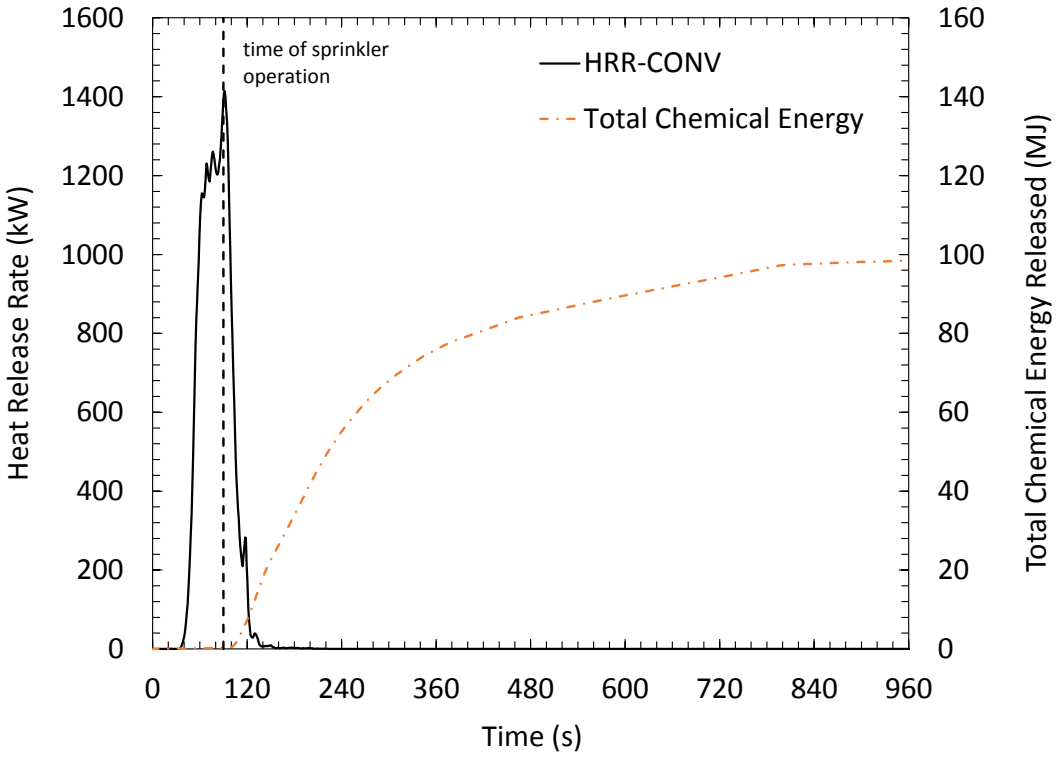

Figure 4-10: Total integrated energy.

4.6.4 Ceiling Thermocouple (TC) Measurements

Figure 4-11 presents the steel TC measurements for the large-scale test. The maximum steel TC measurement was 32°C (90°F) at 1 min 30 s (90 s). This value represents the average of all nine thermocouples extending out to 0.3 m (12 in.) in all four directions from the center of the ceiling. The adjacent ceiling TC measurement, located above ignition, was 109°C (228°F).

[12] Energy calculations use the following average values for the net heat for complete combustion per unit mass of fuel: ΔH_{CO2} = 11.4 kJ/g (4,900 BTU/lb) and ΔH_{CO} = 7.9 kJ/g (3,400 BTU/lb).

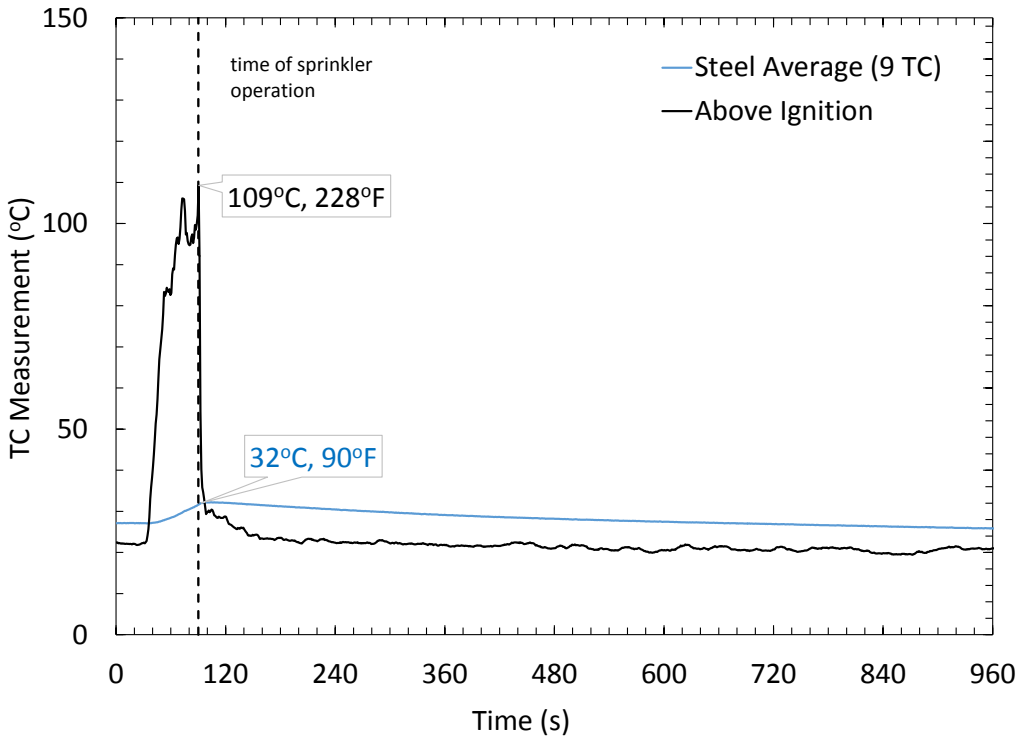

Figure 4-11: Ceiling level TC measurements.

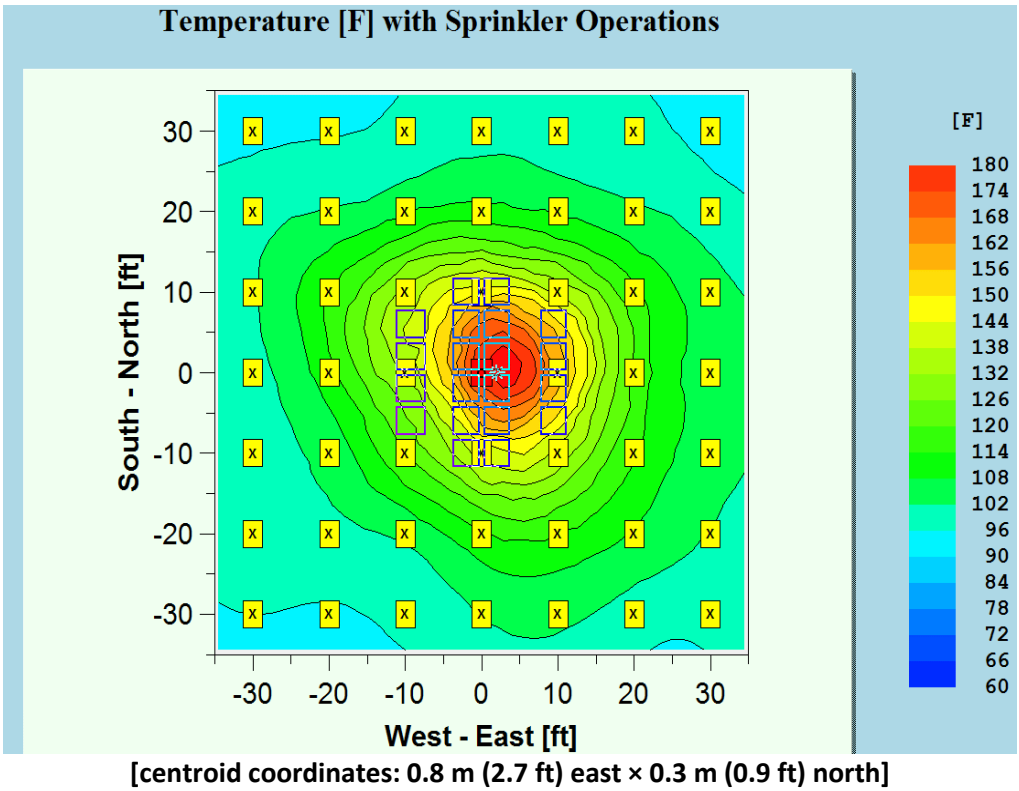

[centroid coordinates: 0.8 m (2.7 ft) east × 0.3 m (0.9 ft) north]

Figure 4-12: Contour plot of ceiling TC measurements at first sprinkler operation 90 s after ignition.

Figure 4-12 presents the ceiling TC measurement contours at first sprinkler operation. The corresponding location of the ceiling gas centroid was 0.8 m (2.7 ft) east × 0.3 m (0.9 ft) north, which coincides with the ignition location. The alignment of the centroid with the ignition location indicates the fire plume was centered over ignition.

4.6.5 Evaluation of Internal Heating

Internal heating of the commodity was measured on all three tiers. As illustrated in Figure 4-4, thermocouples were located in the pallet loads on the south side of the central transverse flue on both the east and west side of the longitudinal flue.

Figure 4-13 presents the thermocouple measurements acquired during the large-scale fire test. A legend is provided to describe the thermocouple locations within the test array. Notable data series are additionally labeled using the following convention: tier number (T#), east or west pallet load (EP/WP), and horizontal position of west, center, or east (W/C/E). For example, T1-EP-W references the first tier, east row, west horizontal thermocouple location.

Unlike the Reduced-Commodity test, which was a free-burn fire, the convective heat release rate is not included in Figure 4-13 for reference to the time evolvement of the fire. In a sprinklered test, convective measurements can be significantly impacted by cooling from the discharged water and therefore may not reflect the heating condition within the test array.

The peak TC measurement of 83°C (180°F) was recorded on tier 1, east pallet load, center location (T1-EP-C) at 2 min 40 s (160 s) after ignition. This location was adjacent to ignition and shows the prolonged heating of the commodity due to the sustained fire within the ignition flue after the sprinkler operated at 1 min 30 s (90 s). Elevated measurements were also observed in the commodity in the east row surrounding ignition at T2-EP-W, T2-EP-C, and T1-EP-W.

It is notable that wetting of the TCs can be observed from the reduction of the measurement from a nominal ambient value of 25°C (77°F) to 19°C (66°F). Wetting was more prevalent on the upper two tiers, which is consistent with post-test observations where significant water infiltration into the cartons was noted during test cleanup.

No TC measurements were observed to exceed the threshold temperature of 180°C (356°F), which was used for the Reduced-Commodity test to represent the oxidation temperature of electrolyte that results in a high-rate runaway reaction (peak rates > 100°C/min) [9]. However, since these thermocouples are located between cartons, not directly attached to the batteries, the actual temperature of the batteries could have been significantly higher. Visual observations of batteries damaged during the test were made during cleanup suggesting that the carton packaging was insulating the thermocouples from the heat released by the batteries.

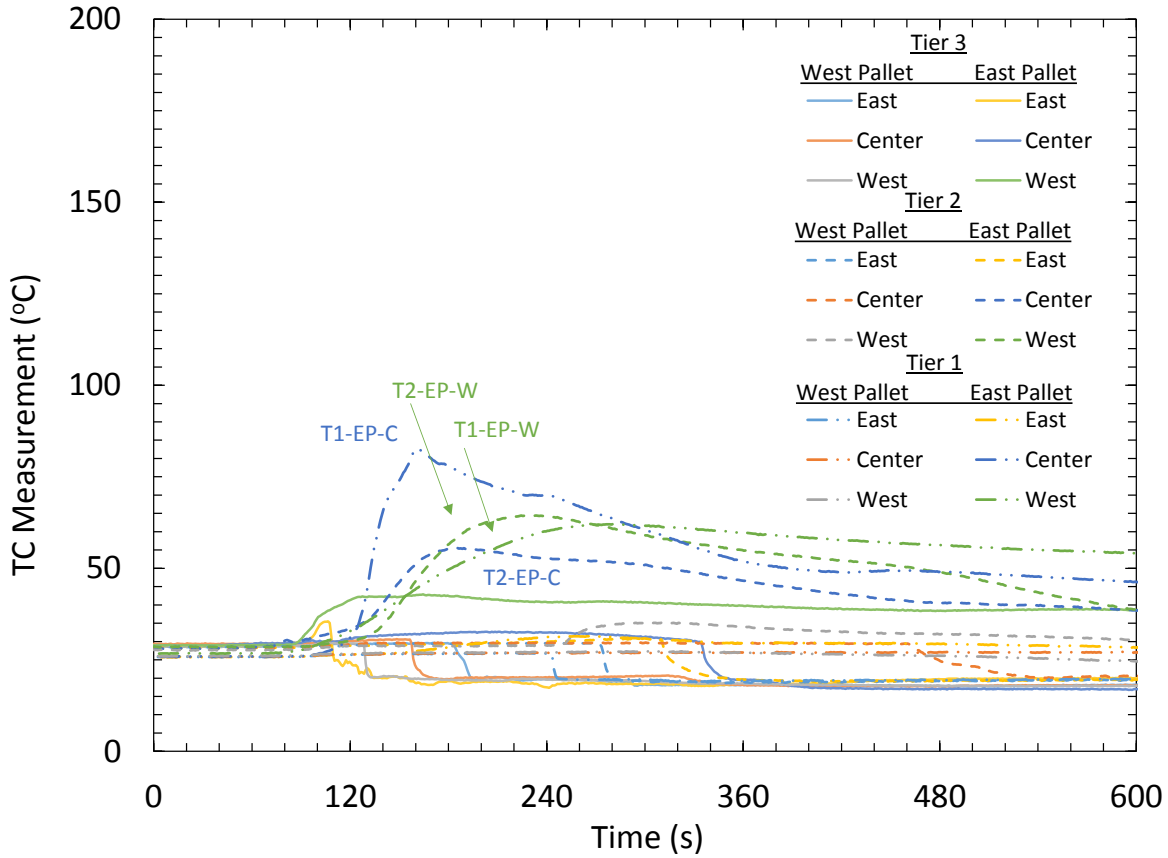

Figure 4-13: Internal heating of commodity using TCs located within the test commodity.

5. **Supplemental Experimental Evaluations**

Two supplemental experimental evaluations were conducted to address the potential for battery-to-battery fire spread. Section 5.1 considers an internal ignition scenario, where thermal runaway of a battery propagates to adjacent batteries. Section 5.2 evaluates the effectiveness of the sprinkler protection at suppressing a fire at a later stage of battery involvement than was achieved in the large-scale test.

5.1 Internal Ignition

Four fire tests have been conducted to establish a reliable and consistent method for assessing the potential to induce internal ignition of a pallet load of batteries. For this purpose, internal ignition refers to a cascading effect where thermal runaway of one or more batteries propagates to the batteries within adjacent cartons, without causing an external fire. Images of each test are shown in Figure 5-1 and descriptions of each test are as follows:

- For the first test, a single battery was placed on top of a metal surface that was heated from below with a propane burner. Thermal runaway of the battery was observed as an expansion of the pouch battery due to conductive heating. The severity of the heating resulted in rupture of the seams along the edges of the battery and an errant propane flame (from the heating source) ignited the escaped electrolyte.
- The second test consisted of a single battery heated to 343°C (650°F) via a foil heater affixed to both sides of the battery. Thermal runaway began within five minutes of exposure. The battery pouch expanded; however, the seams did not rupture and no fire occurred.
- For the third test, foil heaters were again used to overheat one battery within a carton (which contained 20 batteries). Limiting the space for the battery pouch to expand resulted in breach of the seams and leaked electrolyte was observed as a discoloration of the carton. At the completion of a 2-hour heating period, thermal runaway occurred in only three batteries: the battery with the heaters was heavily damaged, while the adjacent batteries above and below were partially expanded. The polystyrene plastic dividers were softened but not charred.
- The fourth test was a repeat of the third test, except ignition of the flammable gases outside of the carton was achieved with a propane pilot flame after a 1-hour heating period. The carton of batteries burned to completion with a peak heat convective HRR of ~ 30 kW.

From these tests it can be concluded that thermal runaway of the polymer pouch battery used in this project does not result in battery-to-battery propagation within a carton. It is therefore reasonable to assume that thermal runaway of one or more batteries within a single carton will not propagate to batteries within an adjacent carton. Thus an external fire, possibly initiated by ignition of escaping electrolyte, is necessary to spread the fire beyond the carton where a thermal runaway occurs. Once an external fire is present, flame propagation along the carton results in a similar fire development to the external ignition scenario.

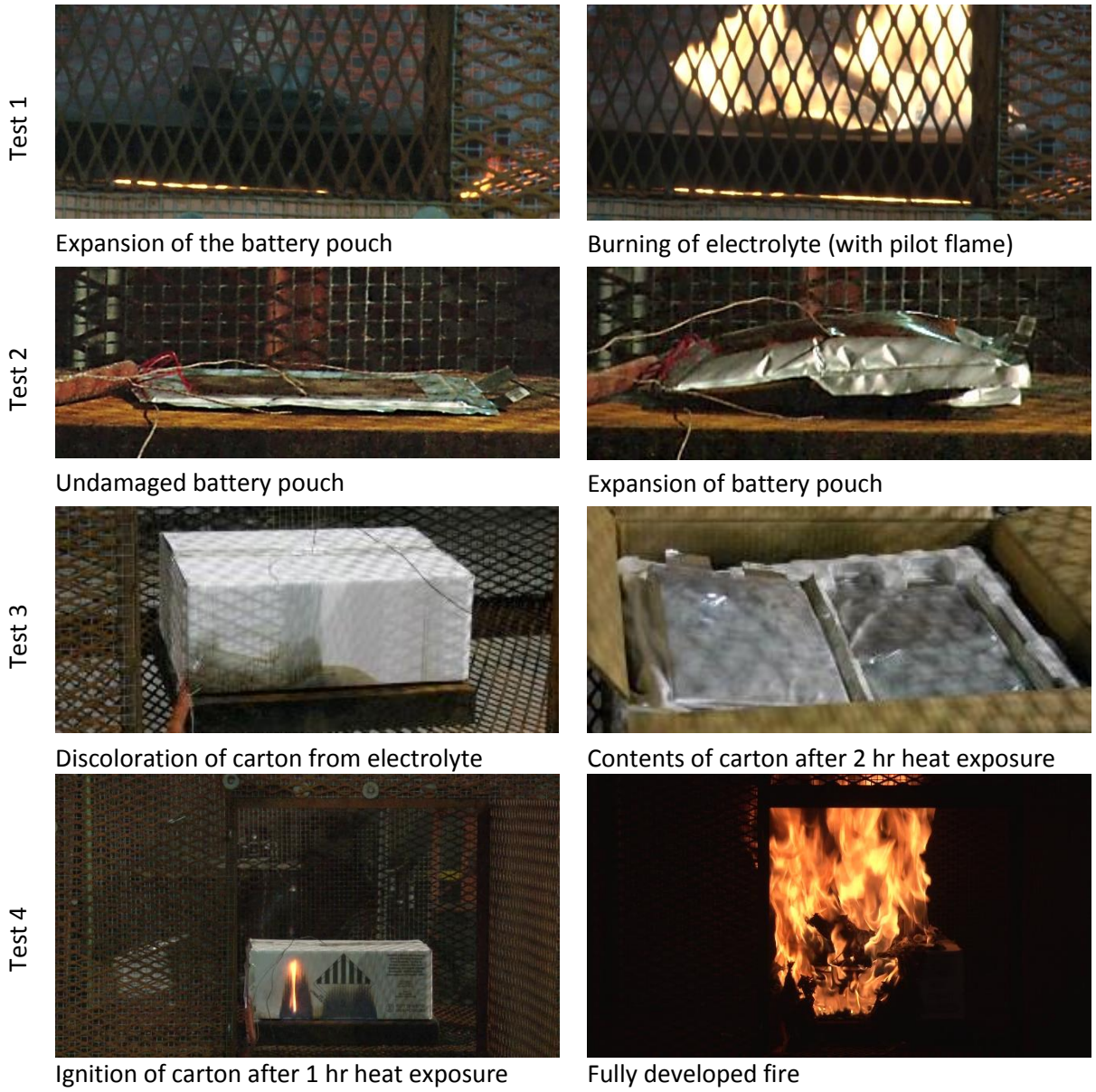

Figure 5-1: Photos of internal ignition evaluation tests.

It is also worth noting that there is not enough air within a carton to burn a single battery. Each battery (used in this project) contains 34 g (0.07 lb) of electrolyte. Using diethyl carbonate as a representative electrolyte component, the stoichiometric equation and air-to-fuel ratio can be quantified as shown in Eqs. 1 and 2. Assuming an air density of 1.2 kg/m^3 (0.075 lb/ft^3) combustion of each battery requires 0.2 m^3 (7.1 ft^3) of air. Each carton has dimensions of 0.43 m × 0.33 m × 0.15 m (16.75 in. × 12.8 in. × 5.75 in.), or an empty volume of 0.02 m^3 (0.7 ft^3), which provides an order of magnitude less air than needed to burn a single battery.

$$C_5H_{10}O_3 + 6\,(O_2 + 3.76\,N_2) \rightarrow 5\,CO_2 + 5\,H_2O + 22.6\,N_2 \qquad \text{Eq. 1}$$

$$AF = \frac{m_{air}}{m_{fuel}} = \frac{6\ mol\ (32\ g/mol + 3.76 \times 28\ g/mol)}{1\ mol \times 118\ g/mol} = 7\ \frac{g}{g} \quad \text{Eq. 2}$$

The conclusion that an external fire is necessary to propagate battery involvement to adjacent cartons can also be reasonably applied to hard-cased Li-ion batteries, where rupture can be accompanied by spattered molten aluminum and other ignition sources. In 2010, Webster studied the process of battery-to-battery propagation in a carton containing one hundred 18650 cylindrical Li-ion batteries [31]. A single battery was removed from the carton and replaced with an electric cartridge heater. During that test, it was noted that the carton caught fire before the batteries adjacent to the heater experienced thermal runaway. Webster conducted a larger version of this test in 2012, involving 50 cartons (5,000 batteries) stacked in a 2 × 4 × 6 arrangement [32]. Overheating of the adjacent batteries resulted in thermal runaway and ignition of the released flammable gas outside of the carton. Subsequent spread of the fire to adjacent cartons occurred due to the external fire.

5.2 Later Stage Suppression Test

An intermediate-scale suppression evaluation using the water application apparatus was conducted to determine the effectiveness of applied water at suppressing a battery fire. Since this test does not rely on sprinkler response, water application can be delayed to a later stage of battery involvement than can be achieved during the large-scale fire test. The combination of the intermediate- and large-scale tests confirms that sprinklers can protect a growing rack storage fire, as well as a developed battery fire.

Test Design and Method

The pallet design for the intermediate-scale suppression test is shown in Figure 5-2. The design consists of 21 cartons, arranged 3 wide x 1 deep x 7 high, resulting in dimensions of 0.97 m × 0.43 m. × 1.0 m (38.3 in. × 16.75 in. × 40.25 in.). A metal liner was fabricated to fill the remaining portion of the pallet, with dimensions of 1.1 m × 0.64 m × 1.0 m (42 in. × 25.25 in. × 40.25 in.).

The later stage suppression evaluation consisted of two tests, as shown in Figure 5-3. Test 1 involved a single pallet load to represent thermal runaway of a carton facing the aisle of a rack storage arrangement. Test 2 involved two pallet loads to represent thermal runaway of a carton facing the flue of a rack storage arrangement. In both cases, thermal runaway was induced in a battery centrally located within a carton using foil heaters as shown in Figure 5-4. The 'ignition carton' was located at the middle of the bottom stack of the pallet load. A propane pilot flame was offset ~25.4 mm (1 in.) from the face of the carton to ignite flammable gas that escaped from the carton.

Water application began after carton surfaces on the ignition side of the pallet were consumed. This approach improved the potential that the batteries are contributing to the overall severity of the fire. Water was applied using the water application apparatus (WAA), which provides a uniform water flux to the top surface of an object [33], at a density[13] of 12 mm/min (0.3 gpm/ft^2). While water applied from

[13] Note that the critical delivered flux to 3.0 m (10 ft) high rack storage of cartoned commodities ranges from 7.3 mm/min (0.18 gpm/ft^2) for CUP to 11 mm/min (0.26 gpm/ft^2) for CEP.

the WAA is not equivalent to sprinkler density, it should be noted that the 52 mm/min (1.3 gpm/ft^2) discharge density used in the sprinklered test was a factor of four higher. The actual quantity of sprinkler water reaching the test commodity is impacted by the non-uniformity of the spray pattern, as well as evaporation and displacement due to the fire plume gases. As a result, suppression in the intermediate-scale test suggests a safety factor in the sprinklered test, in terms of discharge density needed to protect the battery portion of the fire.

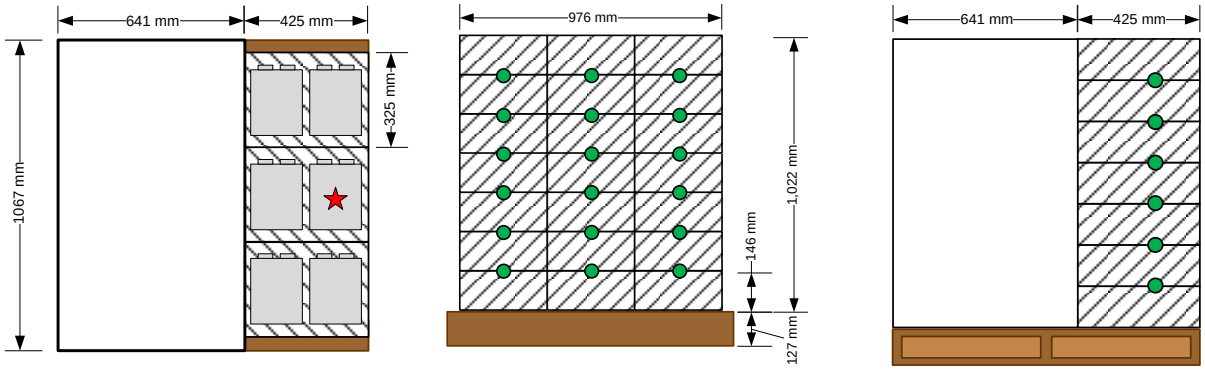

Plan view (illustrating battery location with the cartons) | Front elevation view | Side elevation view

Figure 5-2: Intermediate-scale suppression test pallet design. The location of the ignition battery is identified with a red star and TC locations are shown with green circles.

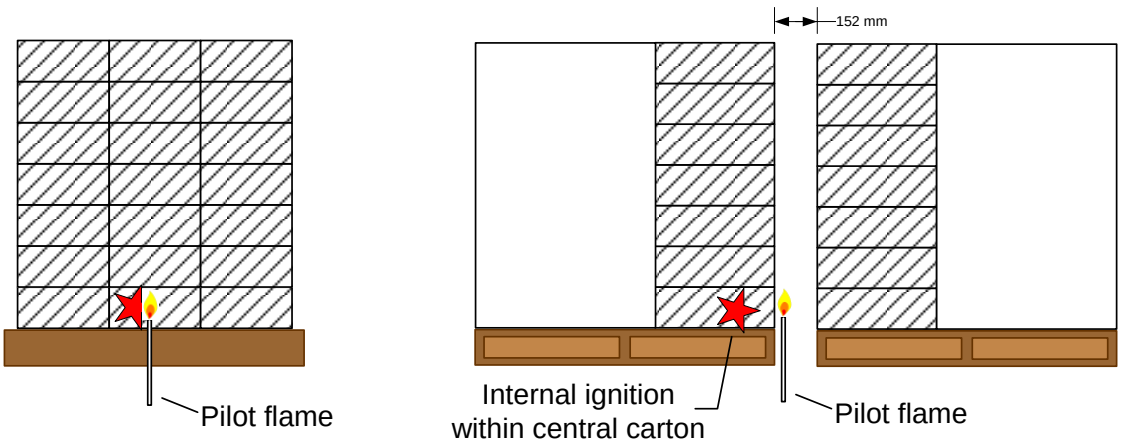

Test 1: Aisle face ignition | Test 2: Flue ignition.

Figure 5-3: Intermediate-scale suppression test ignition location. The location of the carton containing the ignition battery is identified with a red star.

Figure 5-4: Photos of heater placement within ignition carton. Left photo shows a foil heater affixed to a battery on the fifth level (of ten levels) within the carton. Right photo shows the heater wiring exiting the carton.

5.2.1 Suppression Test 1: Aisle Face Ignition

The first suppression test was conducted using a single pallet load to represent ignition of an aisle-facing carton. Photos of the test are shown in Figure 5-5. The foil heaters were set to 340°C (650°F) and the pilot flame was ignited at 0 min. Thermal runaway, observed as wetting of the ignition carton due to leaked electrolyte, occurred by 10 min 30 s (630 s). No ignition of the flammable contents within the carton occurred and at 31 min 37 s (1,897 s) the pilot ignition flame was pushed against the cartons. The cartons ignited and by 34 min (2,040 s) flames had traveled along a narrow vertical path to the top of the pallet load. Since the base of the pilot flame was located at the vertical midpoint of the carton, the lower portion of the carton saturated with electrolyte did not ignite. At 46 min (2,760), a propane torch was used to ignite the lower portion of the carton. Fire spread across the entire face of the pallet load leading to collapse of the center stack of cartons at 49 min (2,940 s). Water application, at a rate of 12 mm/min (0.3 gpm/ft^2) began at 50 min 27 s (3,027 s) and the fire was suppressed within 5 min (300 s). The test was terminated at 60 min (3,600 s) using a garden hose to extinguish a few lingering flames shielded by the collapsed cartons.

During post-test inspection, it was estimated that 30% of the batteries showed signs of damage. The majority of damaged batteries was located in the area adjacent to ignition, *i.e.*, bottom of the center stack of cartons. Minimal damage was observed on the batteries located in the outer stacks of cartons. In addition, the fire was generally contained to the outside portion of the cartons (towards ignition), including all the carton surfaces on the ignition side of the pallet load, with minimal penetration to the inside portion of the cartons (towards the metal liner).

Figure 5-6 shows the convective heat release rate as well as the predicted response of a quick-response sprinkler located 3.0 m (10 ft) above the array (following the method described in Section 3.3.3). Water was applied to the fire 25 s after the predicted operation time of a quick-response sprinkler, 50 min 27 s (3,027 s) versus 50 min 2 s (3,002 s). Additional delay in the time of water application was not possible due to collapse of the commodity. The convective HRR peaked at ~300 kW, before water application, and a total of 25.5 MJ of convective energy was released during the test. The carton surfaces on the ignition side of the pallet load account for 65%, *i.e.*, 16.5 MJ, of the total energy released[14]. Since the

[14] Using the carton dimensions and heat of combustion listed in Section 2.2 and 2.3, respectively.

wood pallet was not involved in the fire, the remaining energy was contributed from the plastic dividers and batteries.

31 min 37 s – pilot flame pushed against cartons

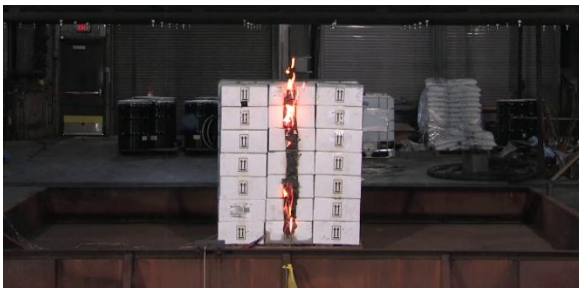

34 min 0 s – flame spread

46 min 0 s – secondary ignition

49 min 0 s – collapse of center stack

50 min 27 s – start of water application

55 min 27 s – suppressed fire

1 hr – test termination
(before fire fighter intervention)

Figure 5-5: Photos of suppression Test 1.

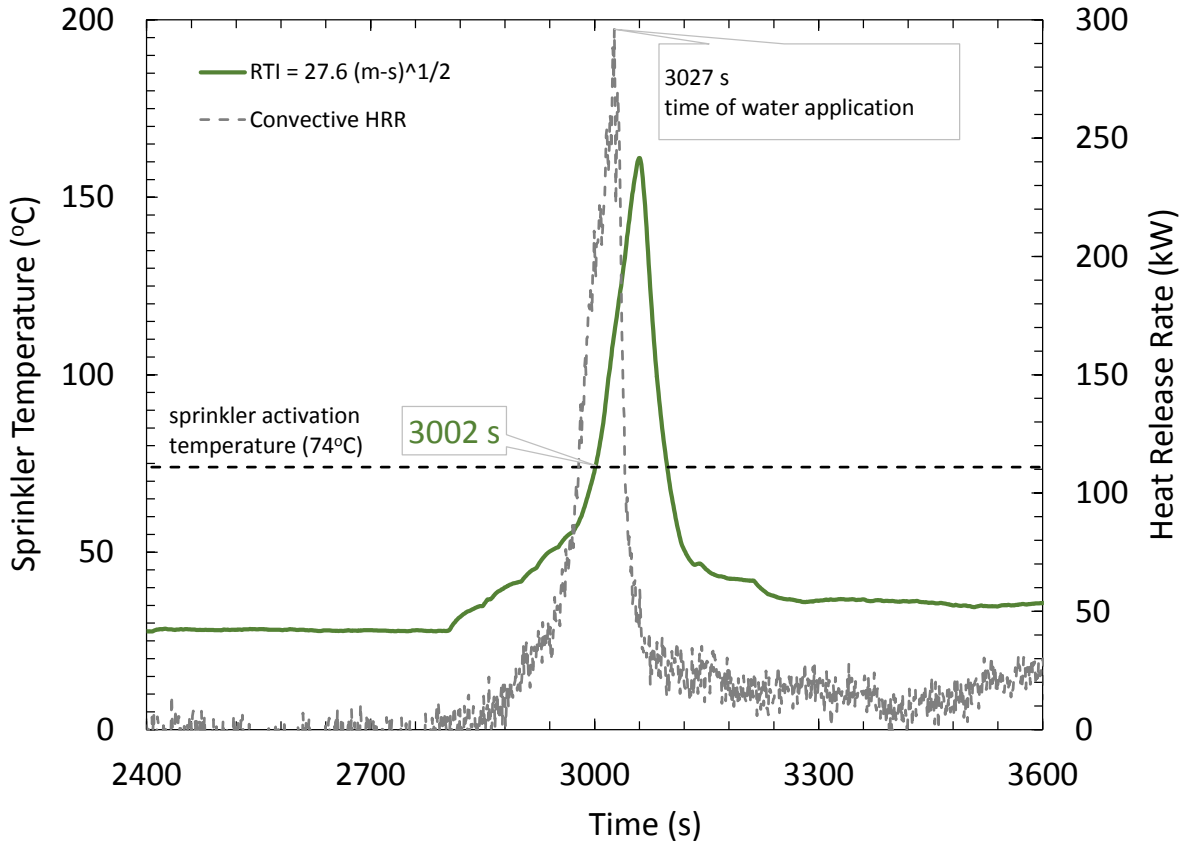

Figure 5-6: Suppression Test 1 convective heat release rate and predicted sprinkler response.

5.2.2 Suppression Test 2: Flue Face Ignition

The second suppression test was conducted using two pallet loads separated by 150 mm (6 in.) to represent ignition of a flue-facing carton. Photos of the test are shown in Figure 5-7. The foil heaters were set to 340°C (650°F) and the pilot flame was ignited at 0 min. Smoke was observed exiting the carton at the penetration for the heater cables at 10 min (600 s). Thermal runaway, observed as wetting of the ignition carton due to leaked electrolyte, occurred by 19 min (1,140 s). There was no ignition of the flammable contents within the carton and at approximately 32 min (1,920 s) the pilot ignition flame was pushed against the cartons. The cartons ignited and by 38 min (2,280 s) the entire flue area was involved in the fire and flames had traveled across the tops of the cartons. Water application, at a rate of 12 mm/min (0.3 gpm/ft^2) began at 41 min 10 s (2,470 s) and the fire was largely suppressed within 5 min (300 s). The combination of fire damage and wetting of the cartons caused the stacks to lean towards each other, which impeded the water flow to the remaining burning surfaces and resulted in a small deep-seated fire that was not extinguished.

At 60 min (3,600 s) the water flow was turned off to evaluate the potential for reignition. As shown in Figure 5-8, the fire slowly redeveloped and began to spread along exposed combustible material. The test was terminated at 75 min (4,500 s) with a fire hose stream.

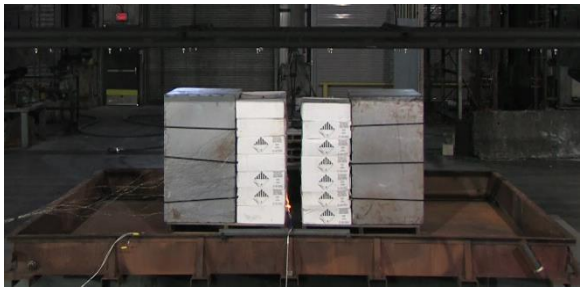

32 min - pilot flame pushed against cartons

36 min 20 s – fire spread across ignition flue

37 min 30 s – fire spread across of cartons

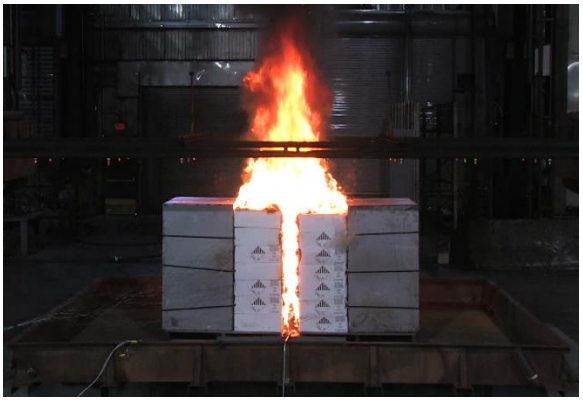

38 min – full involvement of ignition flue

41 min 10 s – start of water application

44 min 10 s – suppressed fire

60 min – water off

Figure 5-7: Photos of suppression Test 2.

During post-test inspection, it was estimated that at least 70% of the batteries showed signs of damage. The most heavily damaged batteries were located in the area facing the ignition flue, though damaged batteries were also observed on the backside of the cartons facing the non-combustible liners.

Figure 5-9 shows an example of a battery rupture that occurred well after the local fire was extinguished. The fire had been suppressed for over 10 min before thermal runaway of a battery resulting in a fire within the flue. The fire could not ignite the combustible material wetted by the water discharge and the fire extinguished when the battery was consumed.

Front of array

Back of array

Figure 5-8: Photos of Test 2 reignition after shutdown of water application.

54 min 30 s – suppressed fire

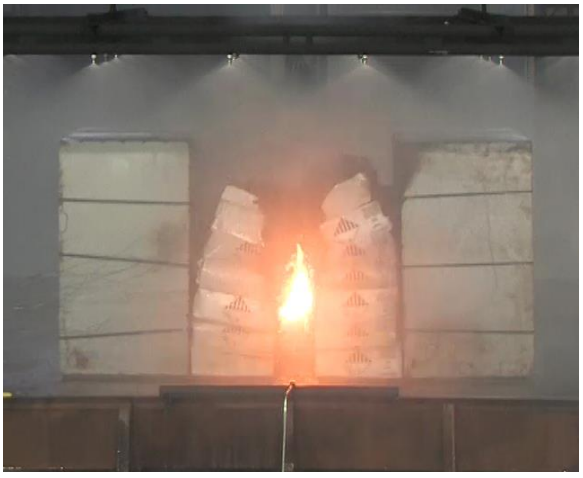

56 min 10 s – battery rupture

Figure 5-9: Example photos of thermal runaway leading to battery rupture.

Figure 5-10 shows the convective heat release rate as well as the predicted response of a quick-response sprinkler (following the method described in Section 3.3.3). Water was applied to the fire 2 min 48 s (168 s) after the predicted operation time of a quick-response sprinkler, 41 min 10 s (2,470 s) versus 38 min 22 s (2,302 s). The convective HRR peaked at ~ 675 kW, before water application, and a total of

110 MJ convective energy was released during the test. The carton surfaces on the ignition side of the pallet load account for 45%, *i.e.*, 49 MJ, of the total energy released. Since the wood pallet was not involved in the fire, the remaining energy was the contribution of the plastic dividers and batteries.

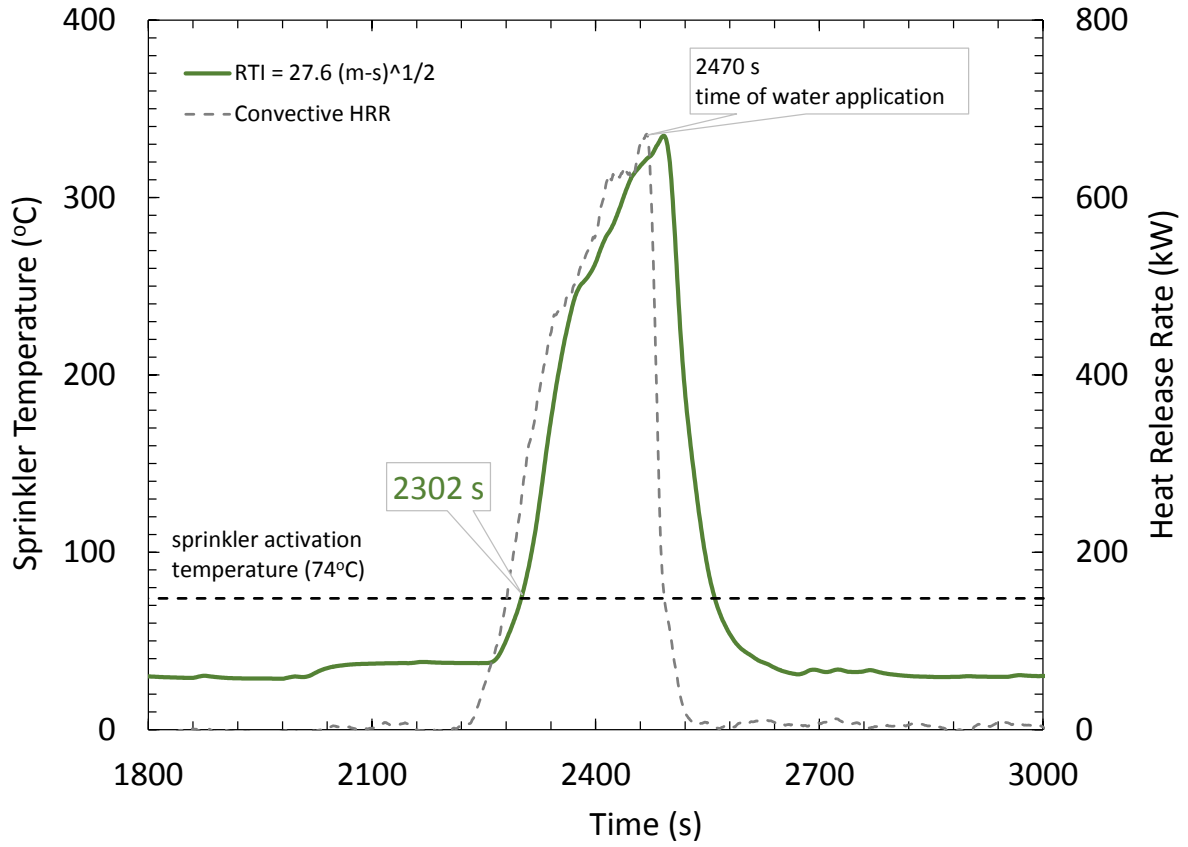

Figure 5-10: Suppression Test 2 convective heat release rate and predicted sprinkler responses.

5.2.3 Comparison of Internal Heating

Internal heating of the commodity was measured with thermocouples located between each level of battery cartons in the pallet load containing the internal ignition heater. As shown in Figure 5-2, 18 thermocouples were located 150 mm (6 in.) in from the ignition face of the pallet load. Horizontally, thermocouples were located at the midpoint of the pallet load and 150 mm (6 in.) from the outer edges. Additional description of the thermocouple type can be found in Section 3.2.

Figure 5-11 presents the thermocouple measurements acquired during Suppression Tests 1 and 2. A legend is provided to describe the thermocouple location within the test array. Notable data series are additionally labeled using the following convention: Level (1 through 6) and horizontal position of west, center, or east (W/C/E). For example, L6C references the thermocouple located between the sixth and seventh carton of center of the pallet load.

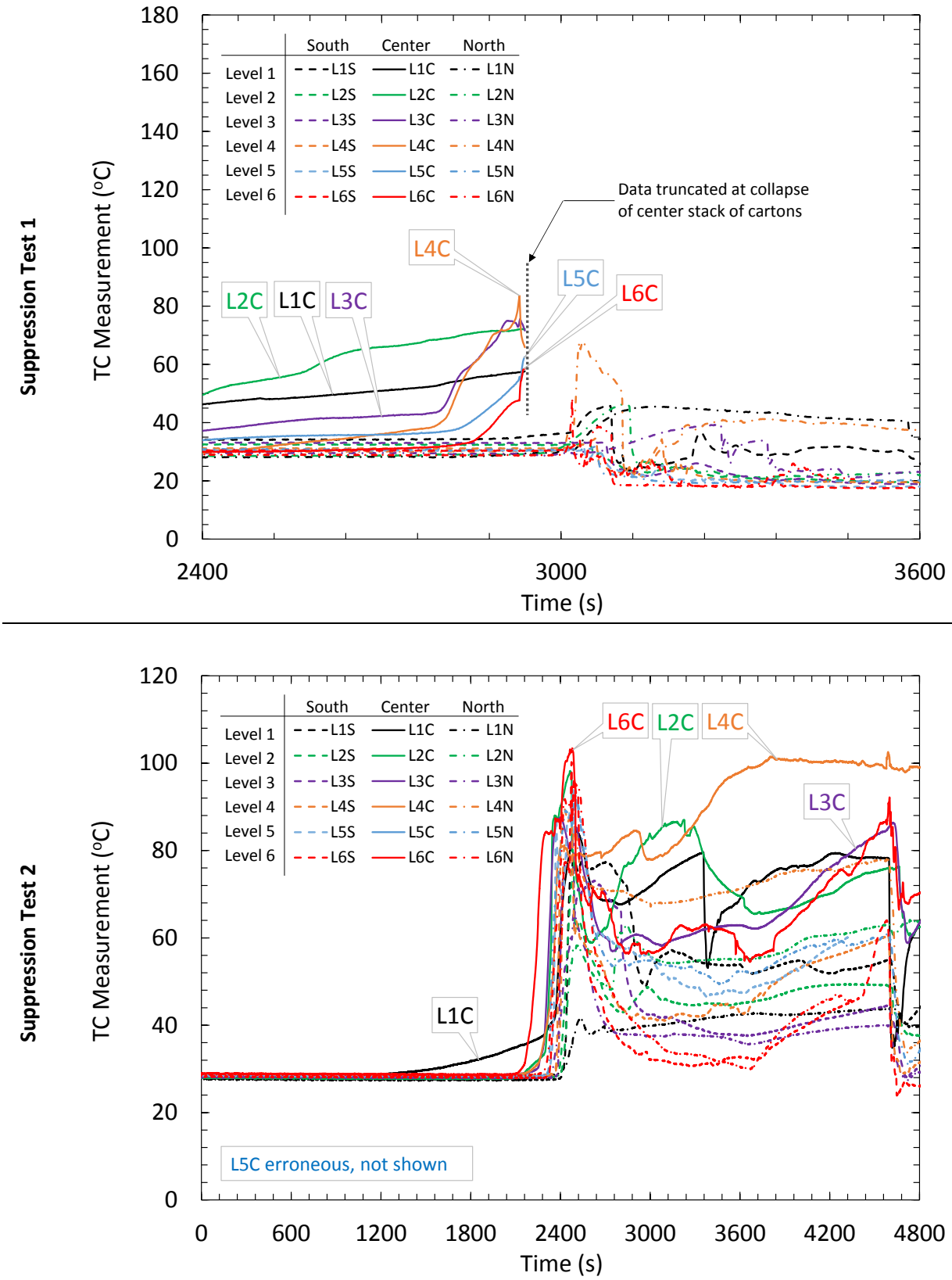

Figure 5-11: Internal heating of commodity using thermocouples located between the cartons of the test commodity.

For Suppression Test 1, a maximum temperature of 756°C (1,390°F) was recorded by L4C at 50 min 25 s (3,025 s) after ignition. A similar response was seen for other thermocouples located within the center stack of cartons. This spike in temperature coincided with collapse of the center stack, which exposed the thermocouple to combustion gases, and was likely not related to widespread thermal runaway of the batteries within the cartons. Since these measurements no longer represent the heating condition within the cartons, the data series for the thermocouples within the center stack have been truncated at the time of collapse, *i.e.*, 49 min (2,940 s). The remainder of thermocouples located at the outer stack of cartons recorded peak temperature that were nominally consistent with ambient temperature.

For Suppression Test 2, a maximum temperature of 103°C (217°F) was recorded by L6C at 41 min 04 s (2,464 s) after ignition. In general, higher temperatures were recorded at center stack of cartons compared to the outer stacks. However, all thermocouples measured peak temperatures that were elevated above ambient temperature. The reduced peak temperatures measured in Suppression Test 2 compared to Suppression Test 1, 103°C (217°F) versus 756°C (1,390°F), is due to the increased stability of the cartons. Without collapse of the cartons, the thermocouples were not directly exposed to combustion gases.

The combined results of Suppression Test 1 and 2 indicate that heat transfer between cartons is slow, even in the presence of a large fire. The insulating properties of the cartons and the plastic dividers effectively inhibit the fire development and delay battery involvement in the fire.

6. **Discussion**

6.1 Pre-wetting of Adjacent Combustibles

Automatic sprinkler protection can prevent fire spread by pre-wetting adjacent combustibles. This mechanism is particularly important for deep-seated fires where sprinkler water may not able to reach burning materials. In the case of cartoned Li-ion batteries, battery-to-battery thermal propagation can occur inside a carton even after the fire has been extinguished. The obvious questions is then, how much pre-wetting is needed to prevent fire spread after the fire has been initially suppressed? The discussion below addresses this question.

Thumuluru and Xin studied the effect of pre-wetting on fire propagation along corrugated board surfaces [34]. Experiments were conducted using a 2.4 m (8 ft) tall parallel panel apparatus to represent conditions of a rack storage fire, Figure 6-1 (left). The fuel load consisted of three layers of double-wall corrugated board attached to non-combustible panel walls that were located on either side of a 0.3 m (12 in.) wide propane sand burner.

Using a range of ignition sizes and water flow rates, a critical water flow rate beyond which the fire would no longer spread along the corrugated board was identified. Figure 6-1 (right) shows the total heat released over a 450 s period for ignition fire sizes of 48, 66, and 99 kW. It was found that a critical water flow rate of 12 g/m/s (0.005 gpm/in.) was sufficient to prevent flame spread for all fire sizes tested.

While not a parameter of the study, the critical water flow rate applied to the top of the fuel array is also a function of the wall height exposed to the ignition fire. As the wall height increases, the quantity of water reaching the base of the ignition fire will decrease due to evaporation. In the context of pre-wetting, the height of the exposed wall used by Thumuluru and Xin [34] is greater than the height of a single carton, or pallet load, of batteries. Thus the critical water flow rates of their work can be reasonably applied to the battery reignition scenario.

Pre-wetting water flow rates expressed as mass flow rate per lateral width (g/m/s [gpm/in.]) can be roughly compared to volumetric flow rate per unit area (mm/min [gpm/ft^2]), *i.e.*, sprinkler density, by assuming that water applied to the top of a pallet load does not accumulate and flows uniformly to the sides of the pallet load [35]. Using the dimensions of an FM Global standard pallet load, 1 g/m/s (4.05 x 10^{-4} gpm/in.) converts to 0.2 mm/min (0.005 gpm/ft^2). As noted in Section 5.2, direct comparison between sprinkler density and flow rate per unit area is not possible due to the non-uniformity of a typical sprinkler discharge pattern, evaporation and displacement of discharged water due to the fire plume gases, and evaporation of water flow along the commodity surfaces.

Following the commodity classification protocol, Xin and Tamanini [33] reported critical delivered water flux (CDF) values for 3.0 m (10 ft) high rack storage of cartoned commodities ranging from 7.3 mm/min (0.18 gpm/ft^2) for cartoned unexpanded plastic (CUP) to 11 mm/min (0.26 gpm/ft^2) for cartoned expanded plastic (CEP) [33]. Discounting differences in the test configurations, the critical pre-wetting

flow rate of 12 g/m/s (0.005 gpm/in.) noted above, *i.e.*, 2.4 mm/min (0.06 gpm/ft^2), is on the order of one third of the CDF values. This result is consistent with the conclusions of Thumuluru and Xin [34] who argued that less water is needed to prevent fire spread than to control or suppress a growing fire.

With respect to the present project, adequate protection of a large-scale battery fire was accomplished with a 53 mm/min (1.3 gpm/ft^2) sprinkler density. Reducing the water density delivered to the top of the commodity by half to account for the non-uniformity of the sprinkler discharge pattern, the corresponding pre-wetting flow rate of 130 g/m/s (0.05 gpm/in) is a factor of 10 larger than the critical pre-wetting flow rate determined by Thumuluru and Xin [34]. While there is no direct comparison between pre-wetting flow and sprinkler density, it is reasonable to assume that reignition of the batteries within a carton will not lead to fire spread over adjacent cartons once sprinklers are discharging water.

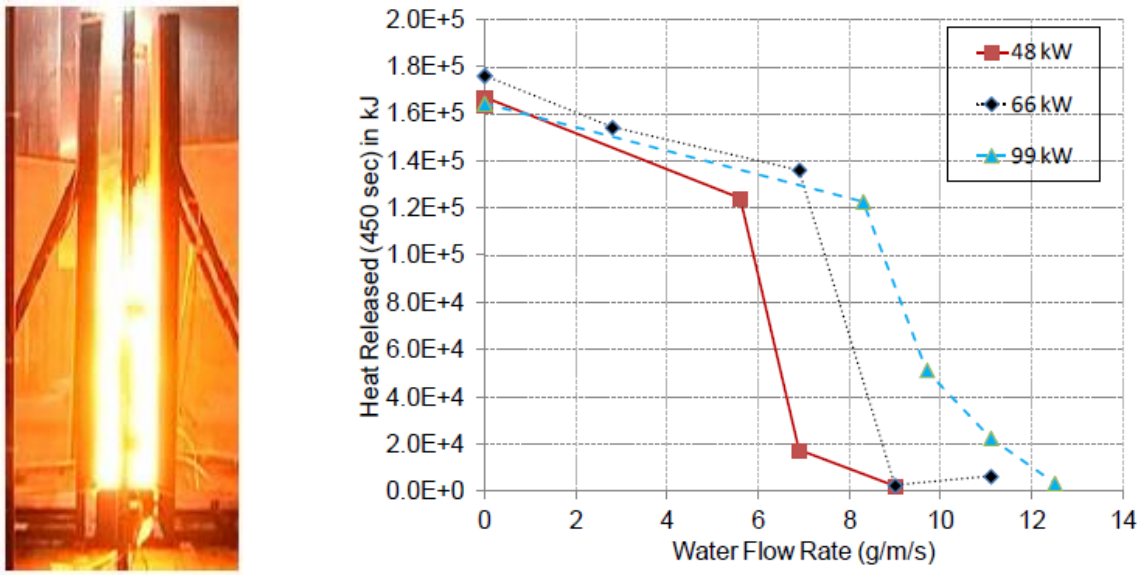

Figure 6-1: Photo demonstrating the fire spread in a parallel panel configuration (left) and plot of overall heat released as a function of the water flow rate for various ignition sizes (right). *Courtesy of Thumuluru and Xin.*

6.2 Application of Test Results to Protection Recommendations

Protection recommendations for warehouse storage of cartoned Li-ion batteries have been developed through fire testing and comparison to commodities with similar hazard characteristics. In consultation with the FM Global Engineering Standards group, which is responsible for the *FM Global Property Loss Prevention Data Sheets,* protection recommendations have been established based on current knowledge and may be amended if additional research specific to the hazard of Li-ion batteries is conducted. The bases for the protection recommendations, which can be found in Section 8, are described below and are specific to warehouse storage of cartoned Li-ion batteries and should not be generally applied to other commodities or storage configurations.

Based on the results of the testing presented in this report, and building upon Reference [15], cartoned Li-ion batteries exhibit a fire hazard similar to CUP commodity (Section 3.3). For limited storage heights,

this conclusion aligns with Hazard Class HC-3 of FM Global Property Loss Prevention Data Sheet 3-26, *Fire Protection Water Demand for Nonstorage Sprinklered Properties* [36], which defines protection for nonstorage facilities where the fire hazard could approach the equivalent of nominal 1.5 m (5 ft) high in-process storage of CUP commodity. In addition, power tool packs exhibited no observable energy contribution from the Li-ion batteries when stored up to 4.6 m (15 ft) high [15]. Therefore, for the storage configuration tested in this project, *i.e.*, 4.6 m (15 ft) high, power tool packs can be protected as CUP commodity per FM Global Property Loss Prevention Data Sheet 8-9, *Storage of Class 1, 2, 3, 4 and Plastic Commodities* [37] for ceiling heights up to 12.2 m (40 ft).

Storage beyond those included in this project or listed above, including battery characteristics (e.g., SOC, quantity of electrolyte, and format) and packaging components (e.g., cartons and dividers) requires a more robust protection scheme to account for several unknowns that can negatively affect protection effectiveness. Fire Protection Scheme A combines in-rack automatic sprinklers (IRAS) and horizontal barriers for protection of high-hazard commodities, such as rack storage of ignitable liquids or level 3 aerosols. Complete specifications and drawings can be found in Section D.2.2.1 of DS 7-29, *Ignitable Liquid Storage in Portable Containers*, July 2014 [38]. Similar specifications can be found in Section E.2 of FM Global Property Loss Prevention Data Sheet 7-31, *Storage of Aerosol Products*, January 2012 [39]. This system design is expected to provide the highest level of protection required for storage of the Li-ion batteries tested in this project and can be applied to array configurations beyond the scope of this project.

The previous phase of this project discussed how the low-flash point hydrocarbons commonly used within the electrolyte for Li-ion batteries are prone to reignition [15]. While that discussion related to testing with small-format batteries, a similar result has been observed for large-format batteries (Section 5.2). Reignition is a concern for any battery chemistry using low-flash point hydrocarbons and has been observed for multiple Li-ion battery chemistries. The impact of burning projectiles is expected to be minimal where commodity is segregated away from other combustibles or where Scheme A protection utilizing quick-response sprinklers is provided. The segregation distance recommendation should reflect the propensity for projectiles based on the Li-ion battery design. For instance, hard-cased cylindrical batteries are more prone to be ejected far distances than soft-cased polymer batteries and therefore require a greater segregation distance.

7. Conclusions

A project was conducted to determine fire protection guidance for warehouse storage of cartoned Li-ion batteries. Testing was conducted at multiple scales with the intent of expanding the application of a large-scale sprinklered fire test to other Li-ion battery types. All evaluations were conducted at the FM Global Research Campus in West Glocester, R.I., USA.

This project represents a unique approach to determining protection guidance due to the inordinate cost and limitations of availability associated with testing of Li-ion batteries. The combined effects of different storage height, ceiling height, protection system design, commodity type and composition are yet to be well understood and should not be inferred from these test results alone. Additionally, significant changes in the Li-ion battery design and chemistry may require additional research.

The applicable storage conditions are:

- Rack storage heights up to 4.6 m (15 ft).
- Ceiling heights up to 12.2 m (40 ft).
- Bulk-packaged 20 Ah polymer pouch batteries in corrugated board cartons with heavy plastic dividers at nominally 50% state-of-charge (SOC).

The methodology for this project consisted of bench-scale through large-scale evaluations using a 20 Ah polymer pouch Li-ion battery, comprised of iron phosphate chemistry, at a nominal 50% SOC. The first test evaluated the flammability characteristics of the selected Li-ion battery compared to FM Global's standard commodities and previously tested small-format Li-ion batteries. This was an intermediate-scale free-burn fire test focused on measurement of the heat release rate and the time of significant battery involvement. Subsequent predictions established the fire hazard present in a sprinklered fire scenario and provided the basis for protection system guidance. Based on the result of the intermediate-scale test, and building upon Reference [15], the following conclusions can be made:

- The cartoned 20 Ah large-format battery used in the present study represent a higher hazard than the previously tested 2.6 Ah small-format batteries (cylindrical and polymer pouch). This conclusion is based on the following test results, which indicate that the large-format battery contributed to the overall fire severity closer to the predicted time of sprinkler operation than the small-format batteries:
    - The predicted time of sprinkler operation was similar for all cartoned Li-ion batteries and FM Global standard commodities included in this project. This result supports the assumption that, for three-tier-high, open-frame racks, the carton packaging dominates the fire development leading to first sprinkler operation.
    - Under free-burn conditions, the 20 Ah Li-ion polymer pouch battery used in this project contributed to the overall severity of the rack storage fire 2 min 30 s (150 s) after igntion, versus 5 minutes (300 s) for the 2.6 Ah cylindrical and polymer pouch batteries previously tested in Phase 2 [15].

- The product packaging, e.g., corrugated board containers and dividers, was identified as a key factor driving the hazard in Li-ion batteries in storage. While the corrugated board cartons were shown to dominate the initial fire growth, the plastic content within the cartons was shown to be a driving factor in the overall commodity hazard, in particular:
    - Cartoned batteries containing significant quantities of plastics exhibited a similar rapid increase in the released energy due to plastics involvement early in the fire development.
        - For the large-format 20 Ah Li-ion polymer pouch batteries used in this project, the heavy plastic dividers contributed to the overall severity of the fire before involvement of the batteries.
        - For the power tool packs, tested in Phase 2 [15], the heavy plastic case of the battery pack dominated the fire hazard and there was no observable contribution from the batteries.
    - Cartoned batteries containing minimal plastics (*e.g.,* the small-format Li-ion cylindrical and polymer batteries tested in Phase 2 [15]) exhibited a slower increase in energy release and a delay in the battery involvement due to heating of the batteries. In this case the plastic dividers represented a lesser combustible load than the heavy plastic dividers used for the 20 Ah polymer pouch battery.

Caution should be taken when extending the results of the testing presented in this report beyond the specific combination of packaging and battery listed. Changes in the components of the packaging can significantly impact the flammability characteristics of cartoned Li-ion batteries. One key aspect of the packaging driving the fire hazard is the divider used to separate the batteries within the cartons. Potential divider materials represent a wide range of fire properties and include liner board, fiber board, thin or heavy plastic, and expanded foam. Even for the same battery, changing the liner material can significantly impact the fire hazard. Changes in the Li-ion battery can also have a similar effect on the overall hazard of the cartoned product. For instance, high SOC has been shown to increase the likelihood and severity of thermal runaway. The quantity of electrolyte, which is the main combustible source, is a function of the battery capacity and can also vary with the battery format (e.g., cylindrical or polymer pouch). Thus, even for the same packaging, changes in the battery can impact the fire hazard. A new flammability assessment should be conducted when potentially significant changes to the cartoned product are encountered.

The performance of ceiling-level sprinkler protection was then assessed with a large-scale sprinklered fire test of the cartoned large-format 20 Ah polymer pouch batteries. The test was conducted using a three-tier-high rack-storage array, which represents storage up to 4.6 m (15 ft) high. Protection was provided by quick-response, pendent sprinklers, having a 74°C (165°F) rated link with a K-factor of 320 L/min/bar$^{1/2}$ (22.4 gpm/psi$^{1/2}$) under a 12.2 m (40 ft) ceiling. In accordance with the evaluation criteria established in Section 4.5, and building upon Reference [15], the following conclusions can be made:

- Storage up to 4.6 m (15 ft) under ceiling heights up to 12.2 m (40 ft) is adequately protected by a fire protection system comprised of pendent sprinklers having a K-factor of 320 L/min/bar^{½} (22.4 gpm/psi^{½}), with a nominal 74°C (165°F) temperature rating and a nominal RTI of 27.6 m^{½}s^{½} (50 ft^{½}s^{½}), installed on 3.0 m × 3.0 m (10 ft × 10 ft) spacing at an operating pressure of 2.4 bar (35 psig). This conclusion is based on one sprinkler operation extinguishing a large-scale test fire without manual intervention.

- Protection guidance established from the large-scale fire test can be reasonably applied to the small-format Li-ion batteries previously tested for this project. This conclusion is based on the results of the reduced-commodity test indicating that the cartoned large-format battery used in this project represented a higher hazard than the previously tested small-format batteries.

Three supplemental evaluations were then carried out to reinforce the sprinkler protection guidance resulting from the successful large-scale fire test. The first evaluation assessed the likelihood and impact of ignition resulting from thermal runaway of one or more batteries within a carton. The effectiveness of sprinkler water at suppressing a fire at a later stage of battery involvement than was achieved in the large-scale test was then assessed. Finally, literature data were reviewed to compare the minimum water application rate needed to prevent flame spread along the carton packaging versus the sprinkler protection used in the large-scale test. Based on the results of these supplemental tests the following conclusions can be made:

- For all small- and large-format Li-ion batteries used in this project, the development of a rack storage fire leading to sprinkler operation should be similar for both ignition scenarios where the fire initiates inside or outside of the carton. This conclusion is based on the following test results:

    - Thermal runaway of the 20 Ah polymer pouch battery used in this project did not result in battery-to-battery propagation within the carton. Experimental data have shown that thermal runaway of up to three batteries simultaneously within a single carton did not propagate to the adjacent batteries within the same carton.

    - There is not sufficient air within a carton to support combustion of a single 20 Ah polymer pouch battery. Thus, fire propagation primarily occurs outside of the carton. In addition, review of literature data has shown that battery-to-battery propagation following thermal runaway of small-format cylindrical batteries occurs only after the carton has breached [32].

    - Once an external fire is present, flame propagation along the carton material will dominate the fire development leading to sprinkler operation and will occur before the batteries contribute to the overall fire severity.

- The sprinkler system used in the large-scale fire test is sufficient to protect against a fire where the Li-ion batteries are contributing more to the overall fire severity than occurred in the large-scale test. This conclusion is based on the following analysis:

- Intermediate-scale testing, designed to delay the application of protection water until the batteries were contributing to the overall fire, confirmed the adequacy of sprinkler protection guidance resulting from the successful large-scale fire test.
- In addition, review of literature data provided in Reference [34] has shown that a lower sprinkler discharge rate than used in the large-scale fire test can also control or suppress fire development along corrugated board cartons.

An experimental methodology to develop sprinkler protection guidance for warehouse storage of Li-ion batteries using a reduced quantity of commodity has been established. This methodology provides a unique means of extending the application of a successful large-scale fire test to other Li-ion batteries by a combination of small- to intermediate-scale fire tests. However, lacking complete large-scale sprinklered fire test experience for each Li-ion battery, a conservative approach to establishing sprinkler protection guidance should be taken.

8. **Recommendations**

Protection recommendations for warehouse storage of cartoned Li-ion batteries have been developed through fire testing and comparison to commodities with similar hazard characteristics. In consultation with the FM Global Engineering Standards group, which is responsible for the *FM Global Property Loss Prevention Data Sheets,* protection recommendations have been established based on current knowledge and may be amended if additional research specific to the hazard of Li-ion batteries is conducted.

The best protection recommendations based on current knowledge, for each Li-ion battery included in this project and Reference [15], are summarized below:

- Li-ion polymer pouch batteries (capacity up to 20 Ah at ≤ 50% SOC) and Li-ion cylindrical batteries (capacity up to 2.6 Ah at ≤ 50% SOC):
    - For a single unconfined pallet load of batteries stored on the floor to a maximum of 1.5 m (5 ft) high, protect as an HC-3 occupancy per FM Global Property Loss Prevention Data Sheet 3-26, *Fire Protection Water Demand for Nonstorage Sprinklered Properties*, July 2011. Additionally, maintain a minimum of 3.0 m (10 ft) separation between adjacent combustibles.
    - For batteries stored solid pile, palletized, or in racks up to 4.6 m (15 ft) under a ceiling up to 12.2 m (40 ft) high, protect with quick-response, pendent, sprinklers with a 165°F (74°C) nominal temperature rating. Protection options include:
        - K320 L/min/bar$^{1/2}$ sprinklers @ 2.4 bar (K22.4 @ 35 psi). The water flow demand should allow for 12 sprinkler operations.
        - K360 L/min/bar$^{1/2}$ sprinklers @ 2.4 bar (K25.2 @ 35 psi). The water flow demand should allow for 12 sprinkler operations.
    - For batteries stored higher than 4.6 m (15 ft) or ceiling heights greater than 12.2 m (40 ft), store batteries in racks and protect with Scheme A per Section D.2.2.1 of FM Global Property Loss Prevention Data Sheet 7-29, *Ignitable Liquid Storage in Portable Containers*, April 2012 (DS 7-29)
- Li-ion power tool packs (*i.e.,* comprised of 18650-format cylindrical batteries with a total pack capacity up to 26 Ah at ≤ 50% SOC):
    - Protect in-process storage of power tool packs as an HC-3 occupancy per FM Global Property Loss Prevention Data Sheet 3-26, *Fire Protection Water Demand for Nonstorage Sprinklered Properties*, July 2011. Limit in-process storage area to 19 m^2 (200 ft^2) and one pallet high. Additionally, maintain a minimum of 2.4 m (8 ft) separation between adjacent combustibles.
    - For power tool packs stored up to 4.6 m (15 ft) high under a ceiling up to 12.2 m (40 ft), protect as FM Global standard cartoned unexpanded plastic (CUP) commodity per

FM Global Property Loss Prevention Data Sheet 8-9, *Storage of Class 1, 2, 3, 4 and Plastic Commodities*, FM Global, July 2011.

- For power tool packs stored higher than 4.6 m (15 ft) or ceiling heights greater than 12.2 m (40 ft), store batteries in racks and protect with Scheme A per Section D.2.2.1 of DS 7-29.

All ceiling sprinklers should be installed in accordance with FM Global Property Loss Prevention Data Sheet 2-0, *Installation Guidelines for Automatic Sprinklers*, January 2014.

Storage beyond the above listed conditions, including battery characteristics (*e.g.*, SOC, quantity of electrolyte, and format) and packaging components (e.g., cartons and dividers), requires a more robust protection scheme to account for several unknowns that can negatively affect protection effectiveness. Fire Protection Scheme A combines in-rack automatic sprinklers (IRAS) and horizontal barriers for protection of high-hazard commodities, such as rack storage of ignitable liquids or level 3 aerosols. Complete specifications and drawings can be found in Section D.2.2.1 of DS 7-29. Similar specifications can be found in Section E.2 of FM Global Property Loss Prevention Data Sheet 7-31, *Storage of Aerosol Products*, January 2012. This system design is expected to provide the highest level of protection required for storage of the Li-ion batteries tested in this project and can be applied to array configurations beyond the scope of this project.

References

1. Transparency Market Research, "Global Lithium Ion Battery Market - Industry Analysis, Size, Share, Growth, Trends, and Forecast 2013 - 2019," Transparency Market Research, 2013.

2. M. Buser, "Lithium Batteries: Hazards and Loss Prevention," *S+S Report International*, pp. 10-17, February 2011.

3. R. T. Long, M. Kahn, and C. Mikolajczak, "Lithium-Ion Battery Hazards," *Fire Protection Engineering*, pp. 22-36, 4th Quarter 2012.

4. D. Lisbona and T. Snee, "A Review of Hazards Associated with Primary Lithium and Lithium-Ion Batteries," *Process Safety and Environmental Protection*, vol. 89, no. 6, pp. 434-442, November 2011.

5. National Highway Traffic Administration (NHTSA), "Chevrolet Volt Battery Incident Overview Report," Washington DC, DOT HS 811 573, January 20, 2012.

6. C. Arbizanni, G. Gabrielli, and M. Mastragostino, "Thermal Stability and Flammability of Electrolytes for Lithium-ion Batteries," *Journal of Power Sources*, vol. 196, no. 10, pp. 4801-4805, May 2011.

7. S.M. Summer, "Flammability Assessment of Lithium-Ion and Lithium-Ion Polymer Battery Cells Designed for Airfcraft Power Usage," U.S. Department of Transportation Federal Aviation Administration, Springfield VA, DOT/FAA/AR-09/55, 2010.

8. E.P. Roth, C. Crafts, D.H. Doughty, and J. McBreen, "Advanced Technology Development Program for Lithium-Ion Batteries: Thermal Abuse Performance of 18650 Li-Ion Cells," Unlimited Release SANDIA REPORT SAND2004-0584, March 2004.

9. D.P. Abraham, E.P. Roth, R. Kostecki, and D.H. Doughty, "Diagnostic Examination of Thermally Abused High-Power Lithium-ion Cells," *Journal of Power Sources*, vol. 161, pp. 648-657, 2006.

10. P. Ribiere, S. Grugeon, M. Morcrette, S. Boyanov, S. Laruelle, and G. Marlair, "Investigation on the Fire-Induced Hazards of Li-ion Battery Cells by Fire Calorimetry," *Energy and Environmental Science*, vol. 5, pp. 5271-5280, 2012. DOI: 10.1039/clee02218k

11. F. Larsson, P. Andersson, and B.-E. Mellander, "Lithium-Ion Batter Aspects on Fires in Electrified Vehicles on the Basis of Experimental Abuse Tests," *Batteries*, vol. 2, no. 9, 2016. DOI: 10.3390/batteries2020009

12. F. Larsson, P. Andersson, P. Blomqvist, A. Loren, and B.-E. Mellander, "Characteristics of Lithium-Ion Batteries During Fire Tests," *J. Power Sources*, no. 271, pp. 414-420, 2014.

13. Y. Fu, S. Lu, X. Cheng, and H. Zhang, "An Experimental Study on the Burning Behaviours of 18650 Lithium Ion Batteries Using a Cone Calorimeter," *J. Power Sources*, no. 273, pp. 216-222, 2015.

14. National Fire Protection Association Standard 13 (NFPA 13), Standard for the Installation of Sprinkler Systems, 2010.

15. B. Ditch and J. de Vries, "Flammability Characterization of Lithium-ion Batteries in Bulk Storage," FM Global, Technical Report J.I. 0003045375, March 2013.

16. C. Mikolajczak, M. Kahn, K. White, and R. T. Long Jr., "Lithium-Ion Batteries Hazard and Use Assessment," Fire Protection Research Foundation, June, 2011.

17. R. Thomas Long Jr., R. T. Long Jr., J. Sutula, and M. Kahn, "Li-ion Batteries Hazard and Use Assessment Phase IIB: Flammability Characterization of Li-ion Batteries for Storage Protection," Fire Protection Research Foundation, 2013.

18. R. T. Long, "Title TBD," Exponent, Inc., September, 2016.

19. M.M. Khan, A. Tewarson, and M. Chaos, "Combustion Characteristics of Materials and Generation of Fire Products," in *SFPE Handbook of Fire Protection Engineering*, P. DiNenno, Ed. Quincy, Massachusetts, New York: Springer, 2016, ch. Section 3, Chapter 4, pp. 1143-1232.

20. S. J. Harris, A. Timmons, and W. J. Pitz, "A Combustion Chemistry Analysis of Carbonate Solvents in Li-Ion Batteries," *Journal of Power Sources*, vol. 193, pp. 855-858, 2009.

21. ASTM E 2058-09, Standard Test Method for Measurement of Synthetic Polymer Material Flammability Using a Fire Propagation Apparatus (FPA), 2009.

22. A. Tewarson, "Flammability Parameters for Materials: Ignition, Combustion, and Fire Propagation," *Journal of Fire Science*, vol. 10, pp. 188-241, 1994.

23. International Standards Organization (ISO/IEC) 17025:2005, General Requirements for the Competence of Testing and Calibration Laboratories, 2005.

24. FM Global Property Loss Prevention Data Sheet 8-1, Commodity Classification, April April 2014.

25. FM Approvals Standard Class 2000, Approval Standard for Automatic Control Mode Sprinklers for Fire Protection, March 2006.

26. FM Approvals Standard Class 2008, Approval Standard for Suppression Mode [Early Suppression - Fast Response (ESFR)] Automatic Sprinklers, October 2006.

27. FM Global Property Loss Prevention Data Sheet 2-0, Installation Guidelines for Automatic Sprinklers, January 2014.

28. American Institute of Steel Construction, *Specifications for the Design, Fabrication, and Erection of Structural Steel for Building*. New York, 1978.

29. J. Milke, "Analytical Method for Determining Fire Resistance of Steel Members," in *SFPE Handbook of Fire Protection Engineering*, P. DiNenno, Ed., 2002, ch. 4-9, pp. 4-212 to 4-238.

30. H-C Kung, H-Z You, and R. D. Spaulding, "Ceiling Flows of Growing Rack Storage Fires," in *Twenty-first Symposium (International) on Combustion*, 1986, pp. 121-128.

31. H. Webster, "Fire Protection for the Shipment of Lithium Batteries in Aircraft Cargo Compartments," U.S. Department of Transportation Federal Aviation Administration, DOT/FAA/AR-10/31, November 2010.

32. H. Webster, "Preliminary Full-Scale Tests with Bulk Shipments of Lithium Batteries," FAA Fire Safety Highlights 2012.

33. Y. Xin and F. Tamanini, "Assessment of Commodity Classification for Sprinkler Protection," *Fire Safety Science*, vol. 9, pp. 527-538, 2008. doi: 10.3801/IAFSS.FSS.9-527

34. S. Thumuluru and Y. Xin, "An Experimental Study of Pre-Wetting on Fire Propagation in Parallel Panels," in *Proceedings of the 13th International Fire Science and Engineering Conference (INTERFLAM 2015)*, Windsor, UK, 2013, pp. 317-326.

35. K. Meredith, J. de Vries, Y. Wang, and Y. Xin, "A Comprehensive Model for Simulating the Interaction of Water with Solid Surfaces in Fire Suppression Environments," in *Proceedings of the Combustion Institute*, 2013, pp. 2719-2726. 34(2)

36. FM Global Property Loss Preventation Data Sheet 3-26, Fire Protection Water Demand for Nonstorage Sprinklered Properties, April 2014.

37. FM Global Property Loss Prevention Data Sheet 8-9, Storage of Class 1, 2, 3, 4 and Plastic Commodities, July 2011.

38. FM Global Property Loss Prevention Data Sheet 7-29, Ignitable Liquids Storage in Portable Containers, July, 2014.

39. FM Global Property Loss Prevention Data Sheet 7-31, Storage of Aerosol Products, January 2012.

fmglobal.com/researchreports

FM Insurance Company Limited
1 Windsor Dials, Windsor, Berkshire, SL4 1RS
Authorized by the Prudential Regulation Authority and regulated by the Financial Conduct Authority and the Prudential Regulation Authority.

March 30, 2021
Medway Planning & Economic Development Board Meeting

Appointments to Master Plan Committee

- Memo from Susy Affleck-Childs recommending two more appointments to the Master Plan Committee

Susan E. Affleck-Childs
Planning and Economic
Development Coordinator

Medway Town Hall
155 Village Street
Medway, MA 02053
Phone (508) 533-3291
Fax (508) 321-4987
Email: sachilds@
townofmedway.org
www.townofmedway.org

TOWN OF MEDWAY
COMMONWEALTH OF MASSACHUSETTS

PLANNING AND ECONOMIC DEVELOPMENT OFFICE

MEMORANDUM

March 25, 2021

TO: Planning and Economic Development Board
FROM: Susy Affleck-Childs
RE: Appointments to Medway Master Plan Committee

I would recommend the PEDB make the following appointments to the Medway Master Plan Committee.

Medway Lions Club:	Linda Reynolds
Medway Business Council	Faina Shapiro

Representatives from the following Town boards and committees have been requested and are under consideration.

- Board of Selectmen
- Affordable Housing Trust/Committee
- Energy and Sustainability Committee